JYVÄSKYLÄ STUDIES IN BIOLOGICAL AND ENVIRONMENTAL SCIENCE
315

Elina Mäntylä

Import and Impact

Characterization of parvovirus-nucleus interactions

JYVÄSKYLÄN YLIOPISTO

JYVÄSKYLÄ STUDIES IN BIOLOGICAL AND ENVIRONMENTAL SCIENCE 315

Elina Mäntylä

Import and Impact

Characterization of parvovirus-nucleus interactions

Esitetään Jyväskylän yliopiston matemaattis-luonnontieteellisen tiedekunnan suostumuksella
julkisesti tarkastettavaksi yliopiston vanhassa juhlasalissa S212,
toukokuun 27. päivänä 2016 kello 12.

Academic dissertation to be publicly discussed, by permission of
the Faculty of Mathematics and Science of the University of Jyväskylä,
in building Seminarium, auditorium S212, on May 27, 2016 at 12 o'clock noon.

UNIVERSITY OF JYVÄSKYLÄ

JYVÄSKYLÄ 2016

Import and Impact

Characterization of parvovirus-nucleus interactions

JYVÄSKYLÄ STUDIES IN BIOLOGICAL AND ENVIRONMENTAL SCIENCE 315

Elina Mäntylä

Import and Impact

Characterization of parvovirus-nucleus interactions

UNIVERSITY OF JYVÄSKYLÄ

JYVÄSKYLÄ 2016

Editors
Varpu Marjomäki
Department of Biological and Environmental Science, University of Jyväskylä
Pekka Olsbo, Ville Korkiakangas
Publishing Unit, University Library of Jyväskylä

Jyväskylä Studies in Biological and Environmental Science

URN:ISBN:978-951-39-6656-0
ISBN 978-951-39-6656-0 (PDF)

ISBN 978-951-39-6655-3 (nid.)
ISSN 1456-9701

Jyväskylä University Printing House, Jyväskylä 2016

ABSTRACT

Mäntylä, Elina
Import and Impact – Characterization of parvovirus-nucleus interactions
Jyväskylä: University of Jyväskylä, 2016, 91 p.
(Jyväskylä Studies in Biological and Environmental Science
ISSN 1456-9701, 315)
ISBN 978-951-39-6655-3 (nid.)
ISBN 978-951-39-6656-0 (PDF)
Yhteenveto: Parvoviruksen ja tuman väliset vuorovaikutukset
Diss.

Parvoviruses (PVs) interact with the host nucleus throughout their life cycle. During nuclear import, the nuclear envelope (NE) acts as a selective barrier limiting access to the nucleus. Inside the nucleus, the expression of viral genes has to be initiated while subjected to recognition by the host. Nuclear functions are modified to benefit viral replication, assembly, maturation and egress. However, the related mechanisms are not well known. PV´s natural oncotropism and oncolytic properties are applicable to virotherapy. Novel information on the mechanisms regulating nuclear import and viral gene expression allows for the development of parvovirus-based tools. The aims of this thesis were to characterize the nuclear import of PV, to analyze the chromatinization of the viral genome, and to elucidate the effects of the infection on the structural organization of the nucleus. Confocal microscopy with fluorescence correlation spectroscopy analyses, *in situ* hybridization, atomic force microscopy, biochemical assays and chromatin immunoprecipitation combined with high-throughput sequencing were used to shed light on these processes in a canine parvovirus (CPV) infection. Firstly, we found that the nuclear tethering of CPV is an active process mediated by importin β. At the NE, CPV capsids were transported into the nucleoplasm across the nuclear pore complex (NPC). Secondly, in the nucleus the CPV genome was chromatinized and the acetylation of histones (H3K27ac) at the viral promoter areas was required for the infection to proceed. Finally, a CPV infection leads to the apical enrichment of NPCs and lamin B1 with a concomitant structural modification of Nup 153. As an outcome, this thesis unravels the previously unknown dynamics of the nuclear import of PV. It describes the chromatinization of the viral genome and demonstrates the importance of its epigenetic regulation. This thesis provides insight into how PV reorganizes the nuclear architecture.

Keywords: Canine parvovirus, nuclear transport, nuclear pore complex, modification of nuclear architecture, chromatinization, promoters.

Elina Mäntylä, University of Jyväskylä, Department of Biological and Environmental Science, P.O. Box 35, FI-40014 University of Jyväskylä, Finland

Author's address Elina Mäntylä
Department of Biological and Environmental Science
Survontie 9C
P.O. Box 35
FI-40014 University of Jyväskylä
Finland
elina.h.mantyla@jyu.fi

Supervisors Docent Maija Vihinen-Ranta
Department of Biological and Environmental Science
Survontie 9C
P.O. Box 35
FI-40014 University of Jyväskylä
Finland

Professor Michael Kann
UMR-CNRS 5234 MFP
Université Bordeaux
Bordeaux
France

Reviewers Professor Veijo Hukkanen
Department of Virology
University of Turku
Kiinamyllynkatu 13
20520 Turku
Finland

Doctor Johanna Laakkonen
Department of Biotechnology and Molecular Medicine
A. I. V. Institute for Molecular Sciences
University of Eastern Finland
Neulaniementie 2
P.O.Box 1627
FI-70211 Kuopio
Finland

Opponent Professor José María Almendral
Centro de Biología Molecular "Severo Ochoa"
Consejo Superior de Investigaciones Científicas-
Universidad Autónoma de Madrid
Cantoblanco
28049 Madrid
Spain

CONTENTS

LIST OF ORIGINAL PUBLICATIONS

The thesis is based on the following original papers, which will be referred to in the text by their Roman numerals I-III.

I Mäntylä E., Chacko J., Di Rienzo C., Parrish C., Kann M., Shahin V., Digman M., Gratton E. & Vihinen-Ranta M. 2016. Single–particle analysis unveils dynamics of parvovirus capsid passage through nuclear pore complex. Manuscript.

II Mäntylä E.*, Salokas K.*, Oittinen M., Aho V., Mäntysaari P., Palmujoki L., Kalliolinna O., Ihalainen T.O., Niskanen E.A., Timonen J., Viiri K. & Vihinen-Ranta M. 2016. Promoter targeted histone acetylation of chromatinized parvoviral genome is essential for infection progress. *Journal of Virology* 90(8): 4059-66.

III Mäntylä E., Niskanen E., Ihalainen T. & Vihinen-Ranta M. 2015. Reorganization of nuclear pore complexes and the lamina in late-stage parvovirus infection. *Journal of Virology* 89(22): 11706-11710.

* Equal contribution

RESPONSIBILITIES IN THE ARTICLES

Article I I was responsible for the planning of the study, conducted and analyzed most of the experiments including the confocal imaging for the fluorescence correlation spectroscopy analysis, *in situ* proximity ligation analysis, and immunoprecipitations. Jenu Chacko, Michelle Digmann and Enrico Gratton analyzed the spectroscopy data including Number and Brightness and velocity trajectories. Carmine DiRienzo assisted in performing the correlation analysis. Ian Liashkovich and Victor Shahin conducted the AFM experiments. I wrote the article and produced the figures together with Jenu Chacko and Maija Vihinen-Ranta.

Article II I took part in the planning of the study, took part in analysing all of the experiments and conducted the drug experiments together with Olli Kalliolinna, Lassi Palmujoki and Pekka Mäntysaari. Mikko Oittinen and Keijo Viiri were responsible for the main analysis of the ChIP-seq results, and conducted the qPCR experiments and high-throughput sequencing. Kari Salokas and Vesa Aho were responsible for the correlation and distance analyses, respectively. I produced most of the figures. I wrote the article with Maija Vihinen-Ranta and took part in finalizing it together with Teemu Ihalainen, Einari Niskanen and Jussi Timonen.

Article III I took part in the planning of the study and also conducted all of the experiments. Teemu Ihalainen and Einari Niskanen assisted in analyzing the data. I produced the figures and wrote the article together with Maija Vihinen-Ranta.

Studies for articles I, II and III were carried out under the supervision of Docent Maija Vihinen-Ranta and Professor Michael Kann. Article I was produced in collaboration with Professor Victor Shahin, Professor Colin Parrish, Professor Michael Kann (second supervisor) and Professor Enrico Gratton.

ABBREVIATIONS

AAV	Adeno-associated virus
APAR	Autonomous parvovirus replication
ATP	Adenosine-5´-triphosphate
BAF	Barrier-to-autointegration-factor
CMV	Cytomegalovirus
CPV	Canine parvovirus
CRM1	Chromosome region maintenance 1
DMEM	Dulbecco´s modified eagle medium
DNA	Deoxyribonucleic acid
dsDNA	Double stranded DNA
EBV	Epstein-Barr virus
EGFP	Enhanced green fluorescent protein
ER	Endoplasmic reticulum
FCS	Fluorescence correlation spectroscopy
GTP	Guanosine triphosphate
H3	Histone H3
HAT	Histone acetyl transferase
HBV	Hepatitis B virus
HIV1	Human immunodeficiency virus type 1
HPV	Human papillomavirus
HSV	Herpes simplex virus
IFI16	Interferon gamma inducible protein 16
INM	Inner nuclear membrane
KASH	Klarsicht/ANC-1/Syne-1 homology –domain
LAD	Lamina-associated domains
LAP1	Lamin-associated protein 1
LBR	Lamin B receptor
LEM	LAP2-emerin-MAN1 –domain
LINC	Linker of nucleoskeleton and cytoskeleton
MLV	Murine leukemia virus
MVM	Minute virus of mice
mRNA	Messenger RNA
NAD	Nucleolar-associated domains
NE	Nuclear envelope
NES	Nuclear export signal
NLFK	Norden laboratory feline kidney cells
NLS	Nuclear localization signal
NPC	Nuclear pore complex
NS	Non-structural protein
Nup	Nucleoporin
ONM	Outer nuclear membrane
ORF	Open reading frame

ORI	Origin of recognition complex
PFA	Paraformaldehyde
PCNA	Proliferating cell nuclear antigen
PLA_2	Phospholipase A_2
PV	Parvovirus
REST	RE-1 silencing transcription factor
RF DNA	Double stranded replicating DNA
RNA	Ribonucleic acid
ssDNA	Single stranded DNA
SIV	Simian immunodeficiency virus
SUN	Sad1/UNC-84 -domain
SV40	Simian virus 40
TAD	Topologically-associating domains
VP	Viral protein

1 INTRODUCTION

Billions of years before the appearance of multicellular entities, unicellular microorganisms and their obligate parasites, viruses, occupied even the harshest habitats. Via communication and the exchange of material, cells acquired diverse structures and functions to adapt to the changing environment. At the same time, viruses evolved developing competent strategies to invade and reproduce in their hosts. Therefore, viruses can be considered as a driving force of evolution and an important source of selective pressure.

The development of the eukaryotic cell nucleus was a milestone in evolutionary history. The nucleus enabled a more sophisticated regulatory control over the interpretation of deoxyribonucleic acid (DNA) genome, and the production of ribonucleic acid (RNA) intermediates. The highly selective nuclear envelope (NE) also protected the cell's genome from cytoplasmic interference. However, it posed a major challenge and a physical barrier for viruses, which depended on the nuclear replication and transcription machinery.

Most DNA viruses but also a few RNA viruses need nuclear proteins for replication thus needing mechanisms to pass the NE. The mechanisms of nuclear entry depend on the structure of the virus and are limited to a large degree by the size of the virus or the subviral structure. For retroviruses with the exception of the genus lentivirus, entry into the nucleus is achieved by translocation into the nucleoplasm during cell division and the temporal disintegration of the NE. Their target cells are thus limited to those cells undergoing frequent cell division such as epithelial and undifferentiated cells. Most viruses exploit the nuclear transport machinery, which includes an interaction between the virus capsid and nuclear transport receptors (importins), which is mediated by a nuclear localization signal (NLS). This is followed by the transport of either intact (herpesvirus) or partially disassembled capsids (human immunodeficiency virus type 1 (HIV1) and influenza A virus) into the nuclear pore complexes (NPCs). Docking of their capsids to the NPC has been shown to be an important and rate limiting step

for several viruses, including hepatitis B virus (HBV), baculovirus and parvoviruses, which all translocate into the nucleus as intact particles. For parvoviruses, the viral protein 1 (VP1)-NLS, which is exposed during the endosomal entry pathway, serves as a trigger for nuclear import.

The nuclear targeting, in addition to host tissue specificity and oncotropism, has made parvoviruses potential vectors for the nuclear delivery of therapeutic agents. A dependoparvovirus adeno-associated virus (AAV) has been successfully applied in virus vector design. Currently, AAV is seen as a promising tool for the treatment of human diseases due to its inability to self-replicate, low immunogenicity, and because it can mediate long-term and robust expression of therapeutic genes while being non-pathogenic for humans. Recombinant AAV vectors for liver-directed gene therapy have proceeded from preclinical and human trials to a commercially available gene therapy drug. The European Commission granted marketing authorization for Glybera® as a treatment for patients suffering from familial lipoprotein lipase deficiency in October 2012. Furthermore, parvoviruses are naturally oncolytic. Their ability to malignant cell killing without inducing premature cytopathic effects is being therapeutically exploited in cancer therapy. Administration of these oncolytic viruses as anti-cancer agents has successfully led to regression of tumors. Currently, autonomous parvovirus H-1-based ParvOryx developed in 2011 has reached phase I/IIa clinical trials designed to treat patients with glioblastoma multiforme.

For viruses that replicate in the nucleus an interaction with the NE and associated components is required throughout the infection cycle. The interaction is involved in the invasion of the host's metabolism, viral gene expression, and the production and maturation of progeny viruses. Accumulating evidence shows that during these processes viruses, including parvoviruses, completely alter the architecture and molecular dynamics of the nucleus. Therefore, viral infections can be applied as models to study nuclear function under stress.

In this thesis, the interactions and dynamics of canine parvovirus (CPV) in the NE were studied. CPV is a small (~2μnm), nonenveloped virus encasing a single-stranded negative-sense DNA-genome. It is an important pathogen of dogs causing damage to the gastrointestinal tract and coronal disease. This thesis gives insights into the nuclear infection mechanisms of parvoviruses. It describes the nuclear import dynamics, virus-induced modification of nuclear structures and viral gene activation, extending our knowledge about the interactions between DNA-viruses and the nucleus.

2 REVIEW OF THE LITERATURE

2.1 Canine parvovirus

Parvoviruses of the family *Parvoviridae* are small (18-28 nm in diameter), non-enveloped, spherical or icosahedral DNA viruses that infect both invertebrate (*Densovirinae*) and vertebrate hosts (*Parvovirinae*). Canine parvovirus (CPV) is a member of the *Protoparvovirus* genus and carnivore protoparvovirus 1 species of the *Parvovirinae* subfamily (Cotmore *et al.* 2014). CPV is an important pathogen of dogs. This was first discovered in 1978 and soon after the virus was found to be highly contagious and pandemic (Parrish *et al.* 1985). Presently, the adapted CPV and its variants are known to cause severe outbreaks and self –sustaining epidemics worldwide (Parrish and Kawaoka 2005, Allison *et al.* 2014, Organtini *et al.* 2015).

CPV causes severe damage to the gastro-intestinal tract (typically gastroenteritis) and coronal disease (myocarditis) especially in young puppies infected in the uterus of a non-immunized female dog. Without vaccination, the mortality is ~10 % in adult dogs and ~91% in puppies (Nandi and Kumar 2010). Transmission occurs commonly via the fecal-oral route upon contact with infected feces or contaminated surfaces. During acute stage of the disease, the infection begins from lymph nodes and tonsils where the virus targets lymphocytes. Infection proceeds to thymus, bone marrow, and epithelial cells of the small intestine. Viremia is detected 1-5 days post infection (p.i.), and fecal shedding of viral particles occurs as early as three days p.i., lasting for ~10 days (Decaro and Buonavoglia 2012). The symptoms include bloody diarrhea, vomiting, fever and loss of appetite (anorexia) leading to anemia, septic shock, respiratory and cardiac failure (Nandi and Kumar 2010). Currently, there is no effective therapy for a CPV infection. Therefore, active immunization against CPV via vaccination is important and part of the vaccination regime for dogs internationally.

The capsid of CPV (~26 nm or 255 Å in diameter) protects the viral genome and is involved in cellular recognition and uptake, cytoplasmic

trafficking, nuclear entry and genome release. The capsid follows the T=1 icosahedral symmetry and is composed of three viral proteins, VP1-3, which are shorter splice variants of the VP1 gene (Agbandje-McKenna and Chapman 2006). The largest protein, VP1 is a minor capsid protein (~10 % of capsid proteins). It has a classical NLS and an additional unique phospholipase-A2 (PLA_2) enzymatic domain in its N-terminus (Vihinen-Ranta 1997, Vihinen-Ranta *et al.* 2001, Zádori *et al.* 2001). The N-terminus of VP1 also contains a classical NLS (). The major capsid protein is VP2, which is known to participate in the nuclear assembly of capsids (Lombardo et al 2000, Sánchez-Martínez *et al.* 2012). VP3 is the smallest capsid protein found only in intact capsids, where its ratio with VP2 defines the virus species and maturity (Chapman and Agbandje-McKenna 2006). The capsid has a traditional 5-3-2 point group symmetry where six 5-folds, ten 3-folds and fifteen 2-folds form the 31 rotational symmetry elements intersecting at the center. The capsid surface has three distinct topologies: an elevated region at the 3-fold axis, a depression between this and the 2-fold axis, and another depression encircling the 5-fold axis creating a "3-fold spike" centered at each 3-fold axes (Chapman and Agbandje-McKenna 2006).

The CPV capsid encloses a single-stranded, linear, non-segmented and negative sense DNA-genome of ~5.3 kb, which is unique in our biosphere (Xie *et al.* 1996, Reed *et al.* 1988). Inverted terminal repeats (ITRs) or hairpins known to be required for replication and transcription are located in both the left-hand (3´-) and the right-hand (5´-) ends of the genome (Reed *et al.* 1988). The CPV genome has only two genes transcribed from two major open reading frames (ORFs) running from the P4 and P38 promoters (Hanson and Rhode 1991, Tullis *et al.* 1994). The first ORF on the left-hand side encodes the non-structural (NS1-2) proteins, whereas the second on the right-hand side encodes the VPs, which are also the main antigens of the virus (Tullis *et al.* 1994, Nelson *et al.* 2007).

NS1 is a multifunctional adenosine-5-triphosphate (ATP)-dependent protein, which exhibits site-specific DNA-binding, ATPase, helicase and nickase activities. It is required for productive virus replication, where it serves as an initiator, and in the maintenance and establishment of the replication fork (Nüesch, *et al.* 1995, Christensen *et al.* 1997, Christensen *et al.* 2002, Cotmore *et al.* 2007, Niskanen *et al.* 2010). NS1 has also been suggested to function as a transactivator of viral promoters, and in parvovirus-induced cell cycle regulation and cytotoxicity during an infection (Chistensen *et al.* 1995, Ohshima *et al.* 2001, Morita *et al.* 2003, Nüesch and Rommelaere 2006, Niskanen *et al.* 2013). NS1 is known to interact with various cellular proteins necessary for viral replication and transcription regulation (Lorson *et al.* 1998, Christensen and Tattersall 2002). NS1 might also be subjected to cellular regulation by post-translational modifications. For parvovirus H1, phosphorylation and acetylation have been shown to play important roles in modulating the cellular activities of NS1. Importantly its ability to bind to DNA, to transactivate the P38 promoter, and to regulate replication have been suggested to be affected (Li *et al.* 2013).

The function of the parvoviral NS2 is required for the effective assembly of capsids and for the production of progeny viruses (Naeger *et al.* 1990, Cotmore *et al.* 1997, Engelsma *et al.* 2008). It plays an essential role in the maturation of the MVM capsid and nuclear egress, where its supraphysiological nuclear export signals (NES), which display increased affinity for nuclear export receptor chromosome region maintenance 1 (CRM1), have been shown to mediate CRM1-dependent NPC tethering and the nuclear export of mature viral particles, at least in mice (Eichwald *et al.* 2002, Engelsma *et al.* 2008). However, the function of NS2 in a CPV infection is uncharacterized.

2.1.1 Canine parvovirus life cycle

Regardless of the species, the life cycle of a virus is tightly connected to that of the host cell. Parvoviruses are remarkable examples of viruses with exquisite cell-cycle dependence reflected by their tropism for highly proliferating cells.

A CPV infection begins when the virus recognizes and binds to the transferrin receptors and enters the cells by dynamin-dependent endocytosis in clathrin-coated vesicles (Parker *et al.* 2001). From the cell surface, CPV is trafficked from the early to the recycling-like and finally to the late endosomes located in the nuclear periphery (Suikkanen *et al.* 2002). Vesicular escape has been suggested to occur when the low pH in the endosomal compartment induces conformational changes in the capsid structure revealing the N-terminus of VP1 and the PLA_2 domain. The PLA_2 activity of VP1 is potentially required to penetrate the endosomal membrane, and to release the virus into the cytoplasm, however, other factors may also be involved (Suikkanen *et al.* 2003a). After endosomal release, CPV capsids tether to the NE in a microtubule and dynein mediated manner (Suikkanen *et al.* 2003b). In early infection, CPV has been suggested to associate with mitochondrial membranes inducing transient depolarization of the transmembrane potential, increased ROS levels and ERK1/2 signalling (Nykky *et al.* 2014).

As an autonomous parvovirus, CPV needs, but is not able, to induce an active S-phase of the cell cycle for efficient replication. However, nuclear entry seems to occur independently from the cell cycle controls. The nuclear targeting of CPV is thought to be an active process that exploits the interactions of the NLSs located in the N-terminus of the capsid VP1 (Vihinen-Ranta *et al.* 1997, Vihinen-Ranta *et al.* 2000). CPV translocates over the NE in relatively intact form in a NPC-dependent manner (Vihinen-Ranta *et al.* 2000). Transcription of the viral genome takes place in the nucleoplasm upon the formation of double-stranded replicative intermediates. The two transcriptional units are read in a temporal order, where products of the P4 promoters precede those of the P38 promoter (Clemens and Pintel 1988, Tullis *et al.* 1994). Concomitantly, replication of the genome is initiated.

Parvoviruses have been shown to induce a pseudo S-phase in infected cells creating a pre-mitotic nuclear environment for sustained viral replication (Adeyemi and Pintel 2014). In addition to replication, the cell cycle dependence of parvoviruses is emphasized in later phases of the infection, where nuclear

translocation of capsid proteins in trimeric assembly intermediates, capsid assembly, maturation and egress are closely coupled to the progression of the cell cycle (Riolobos *et al.* 2006, Gil-Ranedo *et al.* 2015). While the nuclear transport of capsid proteins and capsid assembly are S-phase dependent processes, replication of the viral genome and the maturation of the virus occur in cells arrested in late S/G2 -phase (Gil-Ranedo *et al.* 2015).

Mature parvoviral capsids are targeted for nuclear escape via a CRM1 and NS2-mediated export pathway (Miller and Pintel 2002, Eichwald *et al.* 2002, Maroto *et al.* 2004, Engelsma *et al.* 2008). At the nucleoplasmic side of the NPC, the Nup 358 is required for CRM1-mediated nuclear transport (Bernard *et al.* 2004). In addition to the CRM1-dependence, parvoviral capsids have been shown to localize in close vicinity of Nup 358 (Engelsma *et al.* 2008). Currently, the nuclear export of parvoviruses is thought to occur via the NPCs. The process of nuclear export has been shown to be associated with the remodeling of the actin cytoskeleton by an enzyme called gelsolin, which is modified by the viral NS1 protein (Bär *et al.* 2008). In addition, after their nuclear maturation and egress the newly synthesized cytoplasmic parvoviral capsids seem to be associated with NS1 linking the viral genome to the capsid. It might be that this connection is required for genome packaging or capsid maturation (Cotmore and Tattersall 1989).

2.1.2 Canine parvovirus transcription and replication

Parvoviral replication in the nucleus takes place in well-defined autonomous parvovirus replication (APAR) bodies (Czieplüch *et al.* 2000). These virus-induced structures recruit several cellular factors including replication protein A (RPA), proliferating cell nuclear antigen (PCNA), DNA polymerase α and δ and cyclin A and are later filled with viral proteins, especially NS1 (Czieplüch *et al.* 2000, Bashir *et al.* 2000, Christensen and Tattersall 2002). In CPV infection, APAR bodies first emerge as small NS1-containing foci in the interchromatin space at 10-12 h p.i. and fill most of the nucleus at 24 h p.i. (Ihalainen *et al.* 2007).

The inverted terminal repeats at both ends of the parvoviral single stranded DNA (ssDNA) fold onto themselves forming hairpin duplexes to create the viral origins of replication (ORIs). Upon infection, the hairpin at the left-hand end (3´-end) with a free hydroxyl group serves as a primer for complementary strand synthesis. The production of a replicative form (RF) of double-stranded DNA (dsDNA) is essential for the initiation of transcription and replication (Wolter *et al.* 1980). Its formation relies on the cellular DNA replication machinery, such as polymerase-δ, which is most available in the S-phase of the cell cycle (Bashir *et al.* 2000, Christensen and Tattersall 2002). In addition, genome synthesis has been shown to require Cyclin A and its associated kinase activity known to promote the G1/S transition and the establishment of a replicative environment (Bashir *et al.* 2000). The amplification of the RF DNA is proceeded subsequently by leading strand synthesis and the formation of multimeric intermediates, which requires the function of NS1 (Cotmore and Tattersall 2006).

Viral transcription from the P4 promoter produces the NS1-protein, which functions in an ATP-dependent manner and binds viral DNA in the $(ACCA)_{2-3}$ sequence at the OriR site near the right-hand end (5´-end), produces a nick and becomes covalently attached allowing replication to continue accordingly (Cotmore *et al.* 1995, Cotmore and Tattersall 1998, Cotmore *et al.* 2000). Parvoviral replication proceeds by a rolling hairpin synthesis, where the hairpins can reverse the direction of the DNA synthesis allowing continuous amplification (Cotmore and Tattersall 2006). This process is followed by RPA binding, presumably to stabilize the ssDNA produced due to nicking (Christensen and Tattersall 2002). Additionally, the PCNA complex is recruited to the viral DNA to load polymerase-δ. Here, NS1 functions as a helicase unfolding the DNA for the polymerase complex (Christensen and Tattersall 2002). The production of NS1 and its binding to the transactivation region, called *tar*, presumably leads to the trans-activation of the P38 promoter (Christensen *et al.* 1995, Lorson *et al.* 1996). Additionally, the formation of the dsDNA RFs reveals an additional NS1 binding site at the left-hand side (Cotmore and Tattersall 2006). Here, at the OriL, NS1 nicks the dsDNA and unidirectional strand elongation proceeds creating positive-sense ssDNA genomes. The viral DNA contains several potential binding sites for NS1 suggesting that the function of NS1 could be required for the maintenance of the viral chromatin structure (Cotmore and Tattersall 2006). Moreover, the interaction between NS1 and DNA in viral replication compartments was shown to be ATP dependent, and mutations in the transactivation domains resulted in reduced binding dynamics (Niskanen *et al.* 2013). The formation of the replicative intermediates is temporally regulated (Clemens and Pintel 1988). In the late phases of an infection, the formation of dsDNA RF decreases, while the production of ssDNA genomes continues seemingly coupled to capsid assembly (Cotmore and Tattersall 2006).

Although the importance of NS1 in the replication and transcription of parvoviruses is known, the function and the acetylation status of CPV NS1 in gene expression and in interaction with viral promoters are not well understood. NS1 of MVM has been shown to modify host gene expression through histone acetylation by recruiting cellular proteins with HAT activity. Until date, evidence for the involvement of NS1 in the regulation of histone acetylation on parvoviral promoters has not been reported.

2.2 Overview of the eukaryotic cell nucleus

The nucleus is a defining feature of a eukaryotic cell. It is surrounded by a double bilipid membrane called the NE, which allows molecular crosstalk between the cytoplasm and the nucleoplasm (Wilson and Berk 2010). The NE partitions and protects the genetic material enabling a highly intricate regulatory control over the synthesis of DNA, its interpretation and the production of RNA intermediates.

The nucleus has a complex internal architecture. Its structural scaffold, the nucleoskeleton, is composed of networking intermediate filaments including A- and B-type lamins and vimentin, as well as actin, titin, spectrins, and nuclear myosin and kinesins (Simon and Wilson 2011, Burke and Stewart 2013). Also referred to as the nuclear matrix, this filamentous network is thought to be responsible for the compartmentalization of the nucleus meaning that nuclear macromolecules are segregated into distinct compartments (Hancock 2004, Meng *et al.* 2015). The genetic material, chromatin, is spatially organized into subnuclear domains promoting the movement and temporal regulation of gene expression (Meldi and Brickner 2011, Alexander and Lomvardas 2014, Bouwman and de Laat 2015). These domains are chromatin higher order structures classified in active or repressive states. These include topologically-associating domains (TADs) rich in interchromatin interactions associated with high transcriptional activity, and lamina-associated domains (LADs) that are generally in a transcriptionally repressed state, and less-well characterized nucleolar-associated domains (NADs) (Guelen *et al.* 2008, van Koningsbruggen 2010, Bianchi and Lanzuolo 2015). In the interchromatin space, nuclear tasks are organized in proteinaceous structures including nuclear speckles, paraspeckles, PML nuclear bodies, nuclear stress bodies, orphan nuclear bodies, nucleoli, perinuclear compartments, Cajal bodies, and histone locus bodies, which can respond to changes in the cell cycle or environmental conditions (Biamonti and Vourc´h 2010, Carmo-Fonseca *et al.* 2010, Dundr and Misterli 2010, Lallemand-Breitenbach and de Thé 2010, Nizami *et al.* 2010, Pederson 2011, Spector and Lamond 2011, Zhu and Brangwynne 2015). Macromolecular crowding in the nucleus (~100 mg/ml) has been suggested to both influence the nuclear architecture as well as stabilize nuclear processes (Hancock 2004, Richter at al. 2007). It is thus evident that the nucleus is a dynamic compartmentalized entity, which houses a variety of functional substructures.

2.2.1 Nuclear envelope

The NE consists of the inner and outer nuclear membranes (INM and ONM), the latter of which is connected to the endoplasmic reticulum (ER) (Hetzer 2010). The INM and the ONM are separated by the perinuclear space that is 30-50 nm thick (Burke and Stewart 2013, Cain and Starr 2015). These two phospholipid bilayers are fused at nuclear pore complexes (NPCs), which are responsible for nucleocytoplasmic communication and the exchange of material

between the nucleus and the cytoplasm (Ficthman *et al.* 2010, Grossman *et al.* 2012). The nuclear surface is also known to harbor distinct ion channels, which provide routes for at least calcium, potassium and chloride ion exchange influencing nuclear signaling processes (Matzke *et al.* 2010, Jang *et al.* 2015).

Nuclear membranes are biochemically distinct and characterized by a diverse array of tissue specific transmembrane proteins (Figure 1) (Schirmer and Gerace 2005, Wilson and Foisner 2010, Korfali *et al.* 2012). The ONM is comprised of proteins, such as ribosomes characteristic of the ER, and Klarsicht/ANC-1/Syne-1 homology (KASH) -domain proteins including mammalian nuclear envelope spectrin-repeat proteins (nesprins). At the INM, the majority of the integral proteins bind the underlying lamins and the structure is therefore referred to as "the peripheral lamina". The proteins of the peripheral lamina include lamin B receptor (LBR), lamin-associated protein 1 (LAP1), and LAP2-emerin-MAN1 (LEM) -domain containing proteins including LAP2, MAN1, and emerin. The INM also contains a few non-integral proteins such as LEM-binding protein barrier-to-autointegration-factor (BAF) and SLAP75 (Wilson and Foisner 2010, Roux *et al.* 2012). Like nuclear lamins, LAP2, emerin and LBR interact with chromatin and/or its associated proteins including histones, BAF and HP1 (Wilson and Foisner 2010). These proteins enable the INM to control the dynamics of chromatin anchoring and organization, and regulate gene expression (Reddy *et al.* 2008, Wilson and Foisner 2010).

Nuclear transmembrane proteins also interlink the NE and the nucleoskeleton to the cytoskeleton (Figure 1). These proteins are a part of the LINC (linker of nucleoskeleton and cytoskeleton) –complex, which forms a physical connection between the nuclear lamina and the cytoskeleton (Crisp *et al.* 2006). These complexes consist of Sad1/UNC-84 (SUN) -domain proteins interacting with KASH-domain proteins in the perinuclear space (Chang *et al.* 2015a). The SUN-KASH bridges are required for maintaining the perinuclear space of the NE under extensive mechanical stress (Cain *et al.* 2014). LINC complexes transmit physical forces from the cytoskeleton to the NE and thus affect nuclear geometry, function and movement (Méjat and Misteli 2010, Tapley and Starr 2013). Via KASH-domain, nesprins allow cross-linking between cellular filaments and dynamic remodelling of the cellular cytoskeleton and nucleoskeleton essential for the movement of the entire nucleus along cytoskeletal filaments in response to mechanical stress (Hetzer *et al.* 2005, Starr and Fisher 2005, Rajgor and Shanahan 2013). In addition, LINC complexes stabilize the NE, and facilitate the alignment of chromosomes along the NE (Chang *et al.* 2015b).

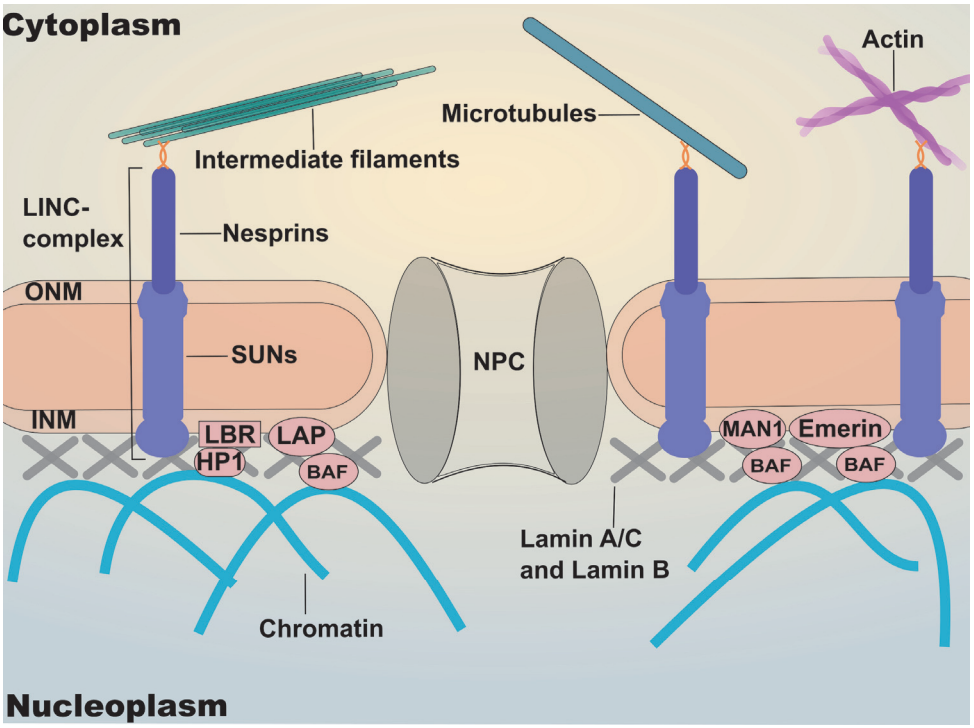

FIGURE 1 Molecular composition of the NE. The NPCs responsible for molecular transport are embedded in the NE at the sites where the INM and the ONM fuse. Nuclear membranes are interlinked with the nucleoskeleton (lamins) and the cytoskeleton via the LINC-complex. The NE is also connected to the chromatin through proteins of the INM.

During the last few decades, studies on the structural and functional complexity of the NE have contributed to a better understanding of the behavior and function of the nucleus. The NE is no longer viewed as a passive transport barrier. Instead, the interactions of the NE are now known to be more complex and its responses to physical cues are suggested to affect the stability and functional organization of the nucleus.

2.2.2 Nuclear pore complex

The nuclear pore complexes (NPCs) are supramolecular assemblies with molecular weights of ~125 MDa in higher eukaryotes. NPCs are responsible for nucleocytoplasmic exchange and are important regulators of chromatin architecture and gene expression (Strambio-De-Castillia *et al.* 2010). NPCs consist of approximately 30 protein species called nucleoporins (Nups) essential for cell viability. Each Nup is present in 8-48 copies due to the eight fold symmetry of the NPC resulting in ~400 polypeptides forming distinct subcomplexes present in multiple copies per NPC (Wente and Rout 2010, Kabachinski and Schwartz 2015). On its cytoplasmic side, the NPC has eight proteinaceous fibers protruding from a ring-like central pore. The central pore

is approximately 90 nm in length and 45-50 nm in diameter at the midplane of the NE. On the nucleoplasmic side, an additional eight protein fibers extrude from the pore forming the cage-like distal ring of the nuclear basket (Brohawn *et al.* 2009, Fahrenkrog et al 2004). The central ring forms an aqueous opening in NE allowing the transport of cargos with a maximum diameter of ~39 nm (Panté and Kann 2002). The structure of the NPC seems to be well conserved from yeast to higher eukaryotes with certain differences in linear dimensions reflecting the larger size of vertebrate NPCs (Adam 2001, Fahrenkrog *et al.* 2004).

NPCs function as highly selective gateways for the bidirectional nucleocytoplasmic transport of a wide range of cargoes with a mass flow of ~100 MDa/s and rates of 10^3 translocation events per second (Ribbeck and Görlich 2001). NPCs allow the free diffusion of water, sugars, ions and small molecules with less than ~9 nm in diameter, although dependent upon their form and surface charge (Paine, et al. 1975, Mohr *et al.* 2009, Goryaynov and Yang 2014). Concomitantly, these complexes need to restrict the passage of nonspecific or inert macromolecules, while facilitating the translocation of other macromolecules such as proteins, RNAs and ribonucleoprotein particles.

The principles of the classical NPC mediated active nuclear import are well known. The traffic of size-excluded macromolecules is mediated by dedicated soluble transport receptors called karyopherins or importins and exportins, recognizing nuclear localization and export signals, respectively, on their cargoes (Fried and Kutay 2003). Karyopherins have also binding sites for NPCs and the small Ras-like GTPase Ran, which serves as a driving force for nucleocytoplasmic transport. The regulated binding of Ran-GTP in the nucleoplasm and Ran-GDP in the cytoplasm determines the association or disassociation of the karyopherin-cargo complexes. The gradient of Ran over the NE is maintained by the cytoplasmic Ran-GTPase activating protein (RanGAP) and the nucleoplasmic Ran guanine nucleotide exchange factor (Ran-GEF). The actual mechanism of transport along the central channel of the NPC has remained relatively unknown despite extensive studies. In all models of transport, however, the interactions of phenylalanine-glycine (FG) repeated Nups in the NPC core have been shown to be essential (Wente and Rout 2010, Fahrenkrog, et al., 2004). Growing evidence suggests that other NE associated proteins, such as ER proteins of the reticulon family, might be required for maintaining the integrity and function of the NPCs (Dawson *et al.* 2009, Casey *et al.* 2015).

The NPCs are dynamic structures capable of assembly, disassembly and redistribution with the cell cycle (Maeshima *et al.* 2006, Dultz and Ellenberg 2010, Imamoto and Funakoshi 2012). New NPCs are assembled in the G1 phase and de novo synthesis takes place during the interphase of the cell cycle and disassembly prior to mitosis (Winey *et al.* 1997, D´Angelo *et al.* 2006, Dultz and Ellenberg 2010). Anchoring to the nuclear lamina orchestrates the distribution of the NPCs on the NE (Walther *et al.* 2001, Guo *et al.* 2014). Commonly, B-type lamins have been shown to concentrate in pore-rich regions, whereas A-type

lamins are found in pore-free islands (Maeshima *et al.* 2006). Accordingly, changes in the distribution of NPCs correlate with the reorganization of the nuclear lamina (Fiserova and Goldberg 2010, Maeshima *et al.* 2010). The net of NPC-lamin interactions might be more extensive than expected, since evidence for direct interactions with A-type lamin has been presented recently (Lussi *et al.* 2011).

In addition to their well-established roles in molecular transport, NPCs and individual Nups have been found to play a part in cell differentiation, gene regulation and chromatin organization (Liang and Hetzer 2011, Gomez-Cavazos and Hetzer 2015). Several Nups acquire direct binding sites for chromatin and the tethering of chromatin to the periphery of the nucleus is considered an important regulator of the gene expression (Sood *et al.* 2014). Studies on the activation of gene expression have shown that Nups can associate with the promoter areas of genes (Schmid *et al.* 2006, Akhtar and Gasser 2007). NPCs also seem to actively participate in chromatin silencing and the formation of peripheral heterochromatin (Wozniak 2014, Breuer and Ohkura 2015). Today, NPCs are conceived as dynamic effectors of the genetic landscape and DNA metabolism. The high structural and mechanical flexibility of NPCs allows the nucleus to respond to changes in cellular metabolism such as stress induced by pathogenic viruses (Cohen *et al.* 2012, D´Angelo *et al.* 2012, Comez-Cavazos *et al.* 2015, Flat and Greber 2015, Lord *et al.* 2015).

2.2.3 Nuclear lamina

The nuclear lamina is a mechanotransductive structural scaffold underlining the INM. It is composed of dynamic type V intermediate filaments called lamins (Dechat *et al.* 2010, Osmanagic-Myers 2015). Lamin proteins come in two subtypes, type A (lamin A, A10, C and C2) and type B (B1, B2 and B3). Type A lamins are alternative splice products of the *LMNA* gene, and B type lamins are encoded by the *LMNB1* (B1) and *LMNB2* (B2 and germ line specific B3) genes (Dittmer and Misteli 2011). Both subtypes contain a typical tripartite structure of intermediate filaments including a central alpha-helical rod with globular head (N-) and tail (C-) domains. *In vitro*, lamins dimerize in a parallel fashion followed by filament assembly (Gruenbaum and Medalia 2015, Köster *et al.* 2015). The expression of lamins is developmentally regulated. B-type lamin is expressed in all cell types in all stages of development. However, A and C lamins are commonly expressed only in differentiated cells (Burke and Stewart 2002, Dechat *et al.* 2010).

Nuclear lamins bind several structural proteins including lamin associated proteins (LAPs), which interact with transcriptional and epigenetic regulators, LEM-domain proteins including MAN1 and emerin, which are involved in organization nuclear architecture and chromatin, and proteins of the LINC-complex, which sense mechanical forces (Somech *et al.* 2005, Gruenbaum *et al.* 2005, Crisp *et al.* 2006, Wagner and Khrone 2007). A-type lamins are known to impact the local chromatin organization via direct genome contacts (Lund *et al.*

2013). Via these interactions nuclear lamins maintain the structure and mechanical stability of the nucleus, and mediate signals that influence chromatin organization, gene expression, cell cycle regulation, and intranuclear functional compartmentalization (Gruenbaum *et al.* 2005, Shumaker *et al.* 2008, Ho and Lammerding 2012, Lund *et al.* 2013, Ward and Kirschner 2014). The loss of any type of lamin impairs nuclear positioning and cytoskeletal organization (Lammerding *et al.* 2004, Ji *et al.* 2007). In addition to cell-type specific roles, lamins have also tissue-specific functions. In tissues, lamins orchestrate differentiation by regulation of NPC assembly, DNA replication, transcription, spindle morphogenesis and cell survival (Goldman *et al.* 2002, Verna and Parnaik 2015). Additionally, a plethora of genetic disease called laminopathies, of which symptoms vary from muscular dystrophy to neuropathy to premature aging, is caused by mutations in the proteins of the nuclear lamina. Underlying mechanisms causing these diseases are commonly defects in cell mechanics, polarization and migration (Hutchison 2002, Lee *et al.* 2007, Schreiber and Kennedy 2013).

Nuclear lamins anchor NPCs to the NE creating relatively immobile networks (Daigle *et al.* 2001). The organization of the nuclear lamina has been shown to affect the assembly and distribution of NPCs (Hawryluk-Gara *et al.* 2005, Maeshima *et al.* 2010). The mechanisms for how lamins regulate the density of NPCs are largely unknown. However, recent studies have suggested that alterations in nuclear functions due to mechanical cues, such as reorganization of the cytoskeleton, might be involved. The regulation of microtubule-based motor forces has been shown to affect the distribution of NPCs via lamins (Guo and Zheng 2015). The tight coupling of NPCs to the lamina seems to be important for counterbalancing the exerted mechanical force from the cytoplasm (Splinter *et al.* 2010, Guo and Zheng 2015).

2.2.4 Chromatin architecture

The architecture of chromatin encompasses a complex and a highly dynamic hierarchy. The first level of chromatin organization is achieved when histone proteins bind DNA to form nucleosomes (Figure 2). The nucleosome core particle is an octamer composed of two copies of H2A, H2B, H3 and H4 histones. On the next level chromatin is condensed into tight 30 nm fibers composed of particular nucleosome patterns mediated by partly charge-dependent internucleosomal interactions and linker DNA (Mariño-Ramírez *et al.* 2005). Chromatin can exist in specific states of compaction, which correlate with an activated or repressed transcriptional status, euchromatin and heterochromatin, respectively. Heterochromatin has a compact architecture while euchromatin is less condensed. Heterochromatin is further classified into facultative and constitutive heterochromatin. Facultative heterochromatin can reversibly undergo structural modifications from a transcriptionally inactive to a more transcriptionally active state. In contrast, constitutive heterochromatin is enriched with repetitive, transcriptionally repressed DNA sequences (Woodcock and Gosh 2010).

The different forms of chromatin are modified by epigenetic regulation that modulates information of the DNA affecting the activity and expression of the genes without altering the nucleotide sequences. In recent years, the development of single-cell analysis methods based on microfluidics, DNA barcoding and next-generation sequencing coupled methods such as chromatin immunoprecipitation (ChIP-seq) has enabled investigation of epigenetic regulation and chromatin states, which allows evaluation of the cellular epigenetic heterogeneity (Swami 2015). Epigenetic regulation includes modification of chromatin via spatial organization of physical or topological chromatin domains, interaction of small and non-coding RNAs that induce RNA interference pathways, DNA methylation especially by cytosine-5 methyltransferases, and modification of histones (Lee 2012, Tanay and Cavalli 2013, Holoc and Moazed 2015, Zhang *et al.* 2015). The core histone tails are reversibly modified by post-translational acetylation, methylation, ubiquitination and phosphorylation, sumoylation etc. Among these, acetylation and methylation are the best characterized. Generally, active chromatin is hyperacetylated, whereas hypoacetylation is detected in repressed chromatin (Figure 2). The acetylation status of chromatin is governed by a balance in the activity of histone acetyl transferases (HATs) and histone deacetylases (HDACs). Epigenetic markers that generally correlate with euchromatin and gene activation include the acetylation of histone H3 lysine 27 (H3K27) and the acetylation of histone H4 lysine 16 (H4K16) (Woodcock and Gosh 2010, Saksouk *et al.* 2015). Additionally, the methylation of histone H3 lysine 4 (H3K4), H3 lysine 36 (H3K36) and H3 lysine 39 (H3K39) are characteristic of active chromatin (Kouzarides 2007, Saksouk *et al.* 2015). In contrast, the trimethylation of histone H3 on lysine 9 (H3K9) and histone H4 on lysine 20 (H4K20) are typical markers for constitutive heterochromatin, while the trimethylation of the H3 lysine 27 (H3K27) is found on facultative heterochromatin (Grewal and Jia 2007).

The epigenetic modification of histones affects access to hereditary information and gene expression by altering the spatial organization of chromatin architecture and the binding of transcription factors. Related to this, chromatin is distributed in the nucleus in a non-random manner, where TADs are commonly defined into linear units of chromatin or in linear clusters of co-expressed genes tending to favor internal, rather than external, chromatin interactions (Ciabrelli and Cavalli 2015). However, relatively little is known about the actual mechanisms that underlie epigenetic regulation. Recently it was shown that lysine acetylation unfolds chromatin by decreasing the availability of histone tails, which is required for compacting internucleosome interactions (Collepardo-Guevara *et al.* 2015).

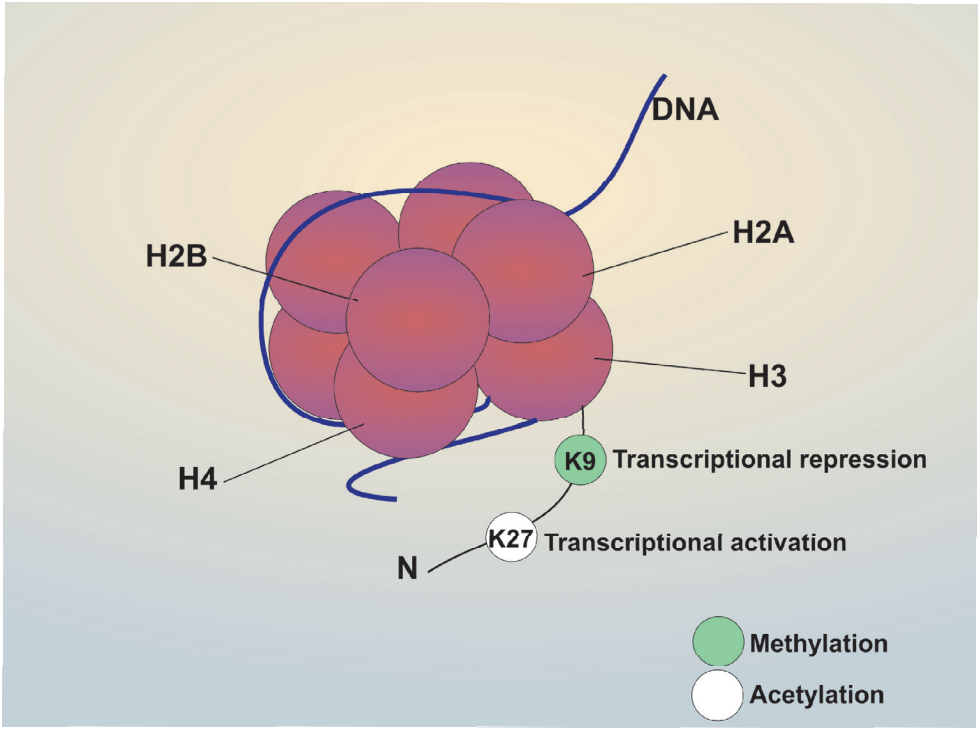

FIGURE 2 Nucleosome structure. Histone proteins bind DNA forming nucleosomes. Two copies of H2A, H2B, H3 and H4 histones form the nucleosome core particle. Epigenetic regulation refers to the post-translational modification of histone tails. In this thesis, the acetylation of histone H3 lysine 27 (H3K27) is used as an epigenetic marker for transcriptionally active euchromatin. The trimethylation of histone H3 lysine 9 (H3K9me3) is used as a marker for transcriptionally repressed or silenced heterochromatin.

The structure of chromatin is constantly rearranged and chromatin is now viewed as highly dynamic (Soutoglou and Misteli 2007).Intranuclear movement and the spatial organization of chromatin are crucial for transcription, for the coordinated expression of genes and for genome stability. In the nucleus, chromatin is spatially organized in a non-random manner. A conventional distribution of chromatin, with heterochromatin in the periphery and euchromatin in the interior of the nucleus, is found in several cell types (Kalverda *et al.* 2008, Pombo and Dillon 2015). Attachment to the NE is important for preserving the three dimensional architecture of chromatin. Interactions with components of the NE such as the nuclear lamina and NPCs in particular, are a conserved feature of chromatin organization. Lamin proteins are involved in tethering the heterochromatin to the nuclear periphery and in interacting with transcription factors. These interactions are mediated by LBR and heterochromatin protein 1 (HP1) and lamin-associated sequences in the DNA. Finally, NPCs seem to be associated with active chromatin and certain Nups have been suggested to function as insulators between active and repressive chromatin (Capelson *et al.* 2010, Talamas and Capelson 2015).

Therefore, the expression of biological information within chromatin is mediated by DNA-binding proteins that regulate the conformation of DNA and the activity of its genes.

2.3 Nuclear import of macromolecules

The bidirectional active nucleo-cytoplasmic transport of macromolecules, such as proteins and genetic material, functions via nuclear transport receptors, such as importins and exportins of the karyopherin β superfamily (Stewart 2007). Karyopherins direct their substrates over the NE via NPCs to ensure the maintenance of the differences in the molecular composition between the nucleus and the cytoplasm (Görlich and Kutay 1999).

Active transport is needed for molecules of < 40 kDa, which are either size-excluded at the NPC or their diffusion would take unreasonably long. These substrates are supplied with a NLS or a nuclear export signal (NES) (Stewart 2007, Strambio-De-Castillia *et al.* 2010). NLSs are short amino-acid sequences which interact with a specific or several karyopherins (Lusk *et al.* 2007). A cytoplasmic cargo with a classical NLS is recognized by an adaptor molecule importin α and transported to the nucleus together with importin β comprising a NPC binding domain (Lange *et al.* 2007, Lott & Cingolani 2010). Alternatively, a cargo with a non-classical or arginine-rich NLS can be transported to the NPC directly by importin β without interaction with importin α (Truant and Cullen 1999, Palmeri and Malim 1999, Cingolani *et al.* 2002, Singhal *et al.* 2006, Lusk *et al.* 2007). At the NPC, Nup 153 has a central role in interaction between the NPC and classical NLS-cargo transport complexes (Shah *et al.* 1998). Nup153, anchored on the nucleoplasmic basket, has a long mobile FG domain able to bind importin β with NLS cargo and contribute to its nuclear import (Fahrenkrog et al 2002, Cardarelli *et al.* 2012).

The directionality of the transport is determined by small GTPase (hydrolase enzyme of guanosine triphosphate) Ran gradient maintained by two guanine nucleotide exchange factors (GEF). These include the GTPase activating protein for Ran (Ran-GAP), which hydrolyzes GTP to GDP in the cytoplasm, and Ran-GEF in the nucleus which functions in reverse (Izaurralde *et al.* 1997, Moore 1998, Görlich and Kutay 1999). Consequently, Ran is mainly bound to GDP in the cytoplasm, whereas in the nucleus Ran is in its GTP-bound form. Ran is able to bind importins only in its GTP-bound state.

For incoming cargo, nuclear interaction with Ran-GTP triggers dissociation of the import complex and cargo release (Richards *et al.* 1997, Stewart 2007). After cargo release, importin β with RanGTP is recycled back to the cytoplasm, whereas importin α is exported via another β-karyopherin CAS and RanGTP. In the cytoplasm, RanGAP (Ran GTPase activating protein) generates RanGDP, which dissociates from the importins ready to begin a new import cycle (Stewart *et al.* 2007).

Many viruses take advantage of the described nuclear import machinery to gain nuclear access and to avoid provoking antiviral response (Greber and Fornerod 2004, Fontoura *et al.* 2005). Transport between the cytoplasm and the nucleus orchestrate the temporal and spatial regulation of cellular functions (Okada and Sato 2015). Nucleo-cytoplasmic transport is also an important part of the apoptotic programme which can be triggered in response to pathogen-induced stress (Ferrando-May 2005, Ashida *et al.* 2011).

2.4 Virus-nucleus interactions

Viruses are obligate intracellular parasites incapable of independent replication and the production of new progeny. In an arms race with cellular defences viruses have evolved sophisticated strategies to utilize the structural and functional organization of their hosts. Especially for viruses that replicate in the nucleus, interactions with nuclear components and the exploitation of nuclear functions are prerequisites for a successful infection. Extensive studies in recent years have expanded our knowledge of the mechanisms of virus-nucleus interactions and also have provided the molecular basis for virotherapy.

With the exception of pox- and vaccinia viruses, all DNA viruses replicate in the nucleus. These viruses include parvoviruses like canine parvovirus (CPV), orthohepadnaviruses like hepatitis B virus (HBV), herpesviruses like herpes simplex virus 1 (HSV1), baculoviruses, adenoviruses, papillomaviruses and polyomaviruses like simian virus 40 (SV40) (Schmid *et al.* 2014, Fay and Panté 2015). As an exception, a few RNA viruses such as retroviruses including HIV, orthomyxoviruses including influenza viruses, and bornaviruses, import their genome into the nucleus after reverse transcription and the formation of a pre-integration complex in the cytoplasm (Whelan 2013). All these viruses exploit the DNA reproduction machinery and other nuclear functions during genome replication, mRNA processing including capping, particle assembly and maturation. From another perspective, a viral infection can be used as a physiological model for studying nuclear function and architecture under cell stress.

2.4.1 Virus interactions with the NE, nuclear lamina and NPCs

Nuclear viruses interact with intranuclear components throughout an infection. During their life cycle, these viruses require function of molecular transport system, cellular transcription factors, subnuclear bodies, modification of chromatin architecture and gene expression, or the nucleoskeleton. Moreover, nuclear membranes can be exploited during import, maturation and nuclear egress. Consequently, infections affect the physical and mechanical properties of the nucleus by altering its architecture and functional organization.

Interactions between nuclear viruses and the NE are required for nuclear access in an early infection (Table 1). For this process, the preservation of the integrity of the NE is important for certain viruses, but interestingly, many viruses induce the disruption of the NE, lamina and/or NPCs (Smith and Helenius 2004, Kobiler *et al.* 2012, Fay and Panté 2015). Emerging mechanisms for the nuclear import of viral genomes are varied, but commonly restricted at the NPC by the size of the virus. Size-exclusion at the NE can be avoided by accomplishing nuclear entry as a nucleoprotein particle during mitosis and/or NE disintegration, as is the case for polyomaviruses like simian virus 40 (SV40), papillomaviruses like human papillomavirus (HPV) and most retroviruses, such as murine leukemia virus (MLV) (Aydin *et al.* 2014, Hamid *et al.* 2016). For SV40, also NPC mediated import of uncoated genome has been suggested (Fay and Panté 2015). In the same virus family, lentivirus simian immunodeficiency virus (SIV) undergoes a more massive disassembly in the cytoplasm followed by nucleoparticle docking at the NPCs and entering the nucleus (Hamid *et al.* 2016). Another lentivirus HIV first dock the NPCs followed by reverse transcription and formation of the pre-integration complex (Arhel *et al.* 2007). In contrast, herpesviruses and adenoviruses dock to the NPC as large, intact capsids triggering the nuclear import of their genome. However, there is a marked difference in the import mechanisms of these viruses. The HSV-1 genome is ejected from the NPC-bound capsid, whereas adenoviruses disassemble at the NPC as a result of interactions with Nups and microtubule motors and the disruption of the NPC (Strunze *et al.* 2011, Fay and Panté 2015). Intriguingly, viruses that are small enough to fit into the NPC core, such as HBV, enter the NPCs as intact particles (Fay and Panté 2015). Parvoviruses also dock to the NPCs, after which their capsid enters the nucleoplasm. To date, two different nuclear import mechanisms have been suggested. These include capsid translocation through the NPCs or entry during the transient disruption of the NE and the nuclear lamina (Vihinen-Ranta *et al.* 2000, Porwal at al. 2013, Kelich *et al.* 2015). Several viruses have been shown to induce the disintegration of the nuclear lamina when tethering to the nucleus (Fay and Panté 2015). However, the specific benefits of such strategy have remained unclear in the sense of the cellular antiviral response and signaling.

TABLE 1 Summary of the nuclear entry strategies of nuclear replicating viruses discussed in this thesis. Hepatitis B virus (HBV), herpes simplex virus 1 (HSV1), *Autographa californica* nucleopolyhedrovirus (AcMNPV), human immunodeficiency virus (HIV), simian immunodeficiency virus (SIV), murine leukemiavirus (MLV), minute virus of mice (MVM), rat parvovirus (H1), adeno-associated virus 2 (AAV2), canine parvovirus (CPV), simian virus 40 (SV40), human papillomavirus (HPV).

Nonenveloped			
Family	Virus	Strategy	Reference
Adenoviruses	Adenovirus	Docking, capsid disassembly and genome delivery at NPC	Hindley *et al.* 2007; Strunze *et al.* 2011
Parvoviruses	MVM, H1, AAV2, CPV	NPC docking, NE disruption and nuclear capsid delivery, or capsid delivery via NPC	Vihinen-Ranta *et al.* 2000; Porwal *et al.* 2013; Fay and Panté 2015; Kelich *et al.* 2015;
Polyomaviruses	SV40	Nucleoprotein particle delivery via NE disruption, or uncoated genome delivery via NPC	Fay and Panté 2015;
Papillomaviruses	HPV	NE breakdown during mitosis and nuclear delivery of partially disassembled capsid	Aydin *et al.* 2014
Enveloped			
Family	Virus	Strategy	Reference
Hepadnaviruses	HBV	Capsid delivery via NPC and nuclear disassembly	Fay and Panté 2015
Herpesviruses	HSV1	NPC docking & genome release	Cohen *et al.* 2011; Strunze *et al.* 2011
Baculoviruses	AcMNPV	Capsid delivery via NPC and nuclear disassembly	Fay and Panté 2015, Cohen *et al.* 2011
Retroviruses	HIV	NPC docking & genome release as a preintegration complex	Hamid *et al.* 2016; Arhel *et al.* 2007
	SIV	Massive disassembly in cytoplasm, nucleoparticle docking and nuclear delivery at NPC	Hamid *et al.* 2016
	MLV	Nucleoparticle delivery via NE disruption during mitosis	Hamid *et al.* 2016
Orthomyxoviruses	Influenza A	Ribonucleoprotein particle delivery via NPC	Wu *et al.* 2007
Bornaviruses	Bornavirus	Ribonucleoprotein particle delivery via NPC	Whelan 2013

Nuclear translocation at the NE is often mediated by virus capsid interactions with nuclear import receptors (importins and transportins) that recognize specific nuclear localization signals (NLSs) in the structure or the core proteins of the virus (Whittaker *et al.* 2000, Cohen *et al.* 2011). Interactions with importins are known to mediate the nuclear delivery of at least HSV-1, HBV, and AAV2 capsids, whereas the actions of transportin and importin-7/ importin β seem to be important for adenoviral DNA (Ojala *et al.* 2000, Rabe *et al.* 2003, Sonntag *et al.* 2006, Hindley *et al.* 2007, Nicholson and Samulski 2014, Fay and Panté 2015). Additionally, potential karyopherin tethering NLSs have been recognized in the capsid proteins of parvoviruses including CPV, minute virus of mice (MVM) and porcine parvovirus (PPV) (Vihinen-Ranta *et al.* 1998, Lombardo *et al.* 2002, Vihinen-Ranta *et al.* 2002, Boisvert *et al.* 2014). The N-terminal unique region of the CPV capsid protein VP1 contains a sequence comprising four basic amino acids (MAPPAKRARRGLV) that fulfils the minimal sequence requirement for the classical NLS (K-K/R-x-K/R) meaning that it should bind to importin β via importin α (Vihinen-Ranta *et al.* 1998, Vihinen-Ranta *et al.* 2002, Lange *et al.* 2007).

Interactions between viruses and NPCs during an infection are thought to attenuate the cellular antiviral response by the partial disruption of the NPCs. This induces the inhibition of the nucleo-cytoplasmic transport of molecules as is seen in an Epstein-Barr virus (EBV, a gammaherpesvirus) infection (Chang *et al.* 2015). Markedly, this phenomena seems not to be restricted to nuclear viruses, but is also detected in infections with other viruses, such as picornaviruses, which do not require nuclear access (Gustin and Sarnow 2002). Similarly, the inhibition of transport through the NPC can result in the repression of host gene expression by limiting mRNA trafficking as has been detected in infections by influenza virus, HSV-1, and even vesicular stomatitis virus of the rhabdovirus family, which does not replicate in the nucleus (Fortes *et al.* 1994, Hardy and Sandri-Goldin 1994, Her *et al.* 1997, Fontoura *et al.* 2005, Kuss *et al.* 2013). The degeneration of NPCs and the accumulation of Nups in the nucleus have been shown to promote viral replication in the nucleus (influenza A, HIV). Moreover, the disruption of NPCs commonly leads to an increase in the permeability of the NE promoting the nucleocytoplasmic shuttling of viral proteins (Leach *et al.* 2007, Le Sage and Mouland 2013, Chang *et al.* 2015).

Viruses can usurp or disrupt nuclear functions at the NE also in a late infection. During nuclear egress, the exploitation of the nuclear transport machinery, such as NPCs, and the function of exportins, such as chromosome region maintenance 1 (CRM1) protein, are emphasized in parvoviral, influenza A and HIV infections (Elton *et al.* 2001, Engelsma *et al.* 2008, Nagai-Fugataki *et al.* 2011). Furthermore, certain herpesviruses induce the redistribution of other NE-associated proteins, such as SUNs and emerin, affecting the rigidity and flexibility of the NE (Leach *et al.* 2007, Morris *et al.* 2007,). Possibly related to this, herpesviruses can exit the nucleus without the disintegration of nuclear membranes, while degrading the nuclear lamins (Lee *et al.* 2008, Johnson and Baines 2011). In a majority of infections, however, viruses disintegrate or

relocalize the lamins and the actins of the nucleoskeleton to promote their nuclear egress and transmission (Lee *et al.* 2008, Cibulka *et al.* 2012).

Although not extensively studied, viral reorganization or disintegration of the nuclear lamina might affect the distribution of NPCs as detected in HSV infection and even with reoviruses not replicating in the nucleus (Hoyt *et al.* 2004, Wild *et al.* 2008). For nuclear viruses, reorganization of NPCs, the nuclear lamina and LINC-complexes are seemingly required to overcome physical limitations preventing nuclear escape. These changes are also involved in regulating the expression of the host's genes and the cellular life cycle of the virus. Nuclear changes could also indicate apoptotic and mechanical stress, such as response to the expansion of the volume of the nucleus, structural modification of the cyto- and nucleoskeleton, altered genetic landscape, or innate immune response to viral infections (Wild *et al.* 2008, Ihalainen *et al.* 2009, Schoggins *et al.* 2011). In conclusion, interactions with the NE and associated components can be considered as a universal strategy for viral invasion and pathogenesis.

2.4.2 Virus interactions with chromatin

For viruses that replicate in the nucleus, the dynamic complexity of the nuclear chromatin architecture presents a challenge for gene expression and genome replication. Viruses need to overcome the spatial limitations set by the three-dimensional organization of chromatin and, furthermore, to hijack the chromatin-associated molecular machinery that is required for DNA synthesis, transcription and splicing (Fortes *et al.* 1994, Lieberman 2006, Everett 2013, Orzalli and Knipe 2014, Barichievy *et al.* 2015). This should be accomplished without provoking DNA damage recognition and/or gene silencing via chromatinization. Yet, viruses need to have regulatory control over the expression of the host's genes. Therefore, viruses need to adopt a genome structure that resembles that of the host and interact with chromatin – to become a "viral epigenome". During the last few decades, studies on the role of chromatin in regulating viral infections have expanded our knowledge of chromatin modifications induced by viruses, and the related interplay between viral proteins and the host chromatin.

From the host´s perspective, newly introduced DNA in the nucleus, such as viral genomes, is considered non-self or foreign presumably due to specific DNA sensing mechanisms (Goubau *et al.* 2010, Diner *et al.* 2015, Jungsan *et al.* 2015, Knipe 2015). Although the concept of nuclear DNA sensing is still widely enigmatic, the function of these sensory mechanisms seems to promote the assembly of histones on the naked DNA leading to transcriptional repression (Diner et al 2015). Recently, it was shown that one of the nuclear DNA sensory elements, human interferon-inducible protein IFI16 can mediate histone loading and the association of heterochromatin markers with the genomic DNA of HSV-1 (Orzalli *et al.* 2013, Johnson *et al.* 2014). Similarly, IFI16 loading promotes recognition of foreign DNA in cells (Sohn *et al.* 2015). In addition, tethering and integration of the viral genome with the host chromatin is characteristic of

persisting viruses such as herpesviruses, retroviruses and AAV2 (Linden *et al.* 1996, Aydin and Schelhaas 2016).

Chromatinization is known to occur in herpesvirus, polyomavirus and adenovirus infections where virus-encoded proteins promote transcriptional activation of chromatinized viral genomes during lytic infection (Nevels at al. 2004, Giberson et al 2012, Fang *et al.* 2015, Knipe 2015). Growing evidence suggests that these histone-associated viral genomes are epigenetically regulated and that viral proteins are required to enhance the acetylation of viral histones and the transcriptional activation of viral promoters (Ohshima *et al.* 2001, Huang *et al.* 2006, Ioudinkova *et al.* 2006, Hancock *et al.* 2010, Komatsu *et al.* 2011). Therefore, viruses exploit chromatinization to acquire effective activation of their genes. Viruses also tend to resist cellular chromatinization of their genomes and the mechanisms by which the host attempts to silence viral genomes become subverted. In latent HSV-1 infection a cellular repressor complex comprised of histone deacetylase, RE-1 silencing transcription factor (REST), REST corepressor 1 and lysine-specific demethylase is known to be suppressed by the virus (Du *et al.* 2010). Cellular chromatin regulation and remodeling are important in virus latency. For example, during the latent HSV infection latency-associated transcript (LAT) gene remains active, while the lytic genes are maintained in a transcriptionally-repressed state and packed into a nucleosomal structure like the host chromatin subjected to regulation by histone modification (Bloom *et al.* 2010, Watson *et al.* 2013).

Alteration of histone modification status is suggested to control the switch between virus latency and reactivation (Gu and Zheng 2016). Dependoparvovirus AAV has a bipartite life cycle including a productive phase in which the replication is dependent on coinfection with a helper virus such as adenovirus, and a latency where the viral genome integrates to the host genome in the absence of a helper virus (Stutika *et al.* 2016). These two modes have been shown to be regulated at the transcriptional level by the parvoviral nonstructural Rep proteins such as a 18-kDa Rep/VP of AAV2 analogous to NS2 of MVM (Stutika *et al.* 2016). Parvovirus B19 has been suggested to maintain a latent infection by transcriptionally regulating the STAT/PIAS pathway by the viral NS1 protein (Duechting *et al.* 2008). However, the role of histone modifications in the parvoviral transcriptional regulation and/or latency has remained unclear. Until date, latent infection has not been reported to CPV.

Viral transcription, replication, genome stabilization, capsid assembly and maturation all involve complex changes in chromatin organization. For instance, viruses that replicate in the nucleus are known to hijack chromatin remodeling complexes. On the minor conformational scale, nuclear viruses interact with chromatin associated proteins such as transcription factors required for the structural alteration of chromatin during the initiation of replication (Felton-Edkins *et al.* 2006, Ihalainen *et al.* 2012, Dembowski and DeLuca 2015). The most drastic forms of spatial reorganization include the marginalization of the host chromatin to the periphery of the nucleus and the enlargement of the interchromosomal space in order to correlate with the

enlargement of viral replication compartments. This has been shown to occur in parvovirus, baculovirus and herpesvirus infections (Monier at al. 2000, Nagamine *et al.* 2008, Ihalainen *et al.* 2009, Bosse *et al.* 2015). In a HSV-1 infection the nuclear marginalization of chromatin has been shown to be dependent on nuclear lamin A/C, but in general the mechanisms for chromatin remodeling remain unknown for most viruses (Silva *et al.* 2008). Alterations in chromatin architecture might be also beneficial for the nuclear egress of capsids as has been suggested for HSV (Simpson-Holley *et al.* 2004).

Viral interactions with chromatin alter the expression of host genes and the progress of the cell cycle (Gosh and Harter 2003, Chaurushiya and Weitzman 2009). Integration of HBV, EBV and SV40 is known to be associated with human cancers (Li *et al.* 2005). Furthermore, the epigenetic regulation of the host chromatin by viral proteins and the subversion of chromatin-associated histone modifying enzymes occurs in many virus infections, including even DNA viruses that do not require nuclear access for replication (Lilley *et al.* 2009, Herbein and Wendling 2010, Guise *et al.* 2013, Simões *et al.* 2015). The virus-induced spatial and structural reorganization of chromatin is evidently reflected in the nuclear architecture, since the distribution of nuclear lamins and NPCs and the attachment of chromatin to the NE are interdependent. However, the relationships are complex and thus have remained poorly characterized.

3 AIMS OF THE STUDY

Parvoviruses affect the architecture and functional organization of the nucleus during several phases of the infection. In this thesis, the interactions between CPV and nuclear components, as well as infection-induced effects on nuclear organization were characterized. The specific objectives of this thesis were:

I To characterize the interactions and dynamics of the nuclear import of viral capsids

II To analyze the chromatinization and histone acetylation of the viral genome

III To elucidate the effects of an infection on the structural organization of the nucleus

4 SUMMARY OF THE MATERIALS AND METHODS

This chapter summarizes the materials and methods used in the studies. A detailed description of the materials and methods can be found in the original publications indicated by their Roman numerals.

4.1 Viruses (I-III)

CPV type 2 and Alexa 594 conjugated CPV capsids were generous gifts from Colin Parrish (Cornell University, Ithaca, NY). CPV-2 was derived from an infectious plasmid clone p265 by the transfection of Norden laboratory feline kidney (NLFK) cells as described earlier (Parrish 1991, Parker *et al.* 2001). The viruses we grown, isolated and concentrated as described in Suikkanen et al., 2002. For infections, cells were inoculated with CPV (1–2) and incubated at 37°C in a humidified incubator (5 % CO_2) for the duration of the infection time. For synchronized infections, the cells were incubated on ice for 15 min prior to the addition of the virus. The cells were then inoculated on ice to allow the virus to adsorb for 30 min and washed once with PBS. Finally, 37°C medium was added and the cells were returned to a 37°C incubator. HBV capsids applied at an equivalent MOI of 5-7 pfu viruses per cell were a gift from Michael Kann (University of Bordeaux, Bordeaux, France).

4.2 Cellular markers, reagents and inhibitors (I-III)

Stable cell lines expressing fluorescent cellular markers (Table 2) were established by transfections with the Trans-IT 2020 reagent (Mirus Bio LLC, Madison, WI, USA). For immunofluorescence microscopy (I-III), the cells were fixed at set time intervals p.i. with PFA at RT. After fixation, the cells were permeabilized with Triton-X in PBS-BSA and washed with PBS-BSA. After

immunolabeling (Table 5) the cells were embedded in ProLong® antifade reagent with DAPI (Thermo Fisher Scientific) according to standard protocols.

TABLE 2 Fluorescent fusion constructs and reagents used in the publications.

Construct/Reagent	Source	Context (usage)	Publication
H3-EGFP	Clontech, USA	Microscopy: co-localization and correlation	II
Lamin C-EGFP	Juliet Ellis UK	Microscopy: Live cell imaging, image FCS analyses	I
Importin β-GFP	Enrico Gratton, USA	Microscopy: Live cell imaging, image FCS analyses	I
155 kDa TRITC-dextran	Thermo Fisher Scientific, USA	Cell manipulation: microinjection	I
Anacardic acid	Sigma-Aldrich, USA	Microscopy: NS1 and H3K27 localization Cell manipulation: enzymatic inhibition of HATs	II
DAPI	Thermo Fisher Scientific, USA	Microscopy	I, II, III

TABLE 3 Hypotonic gentle cell lysis buffer (I, III)

Concentration	Ingredient
10 mM	Tris-HCl pH 7.5
10 mM	NaCl
2 mM	EDTA
0.1%	Triton-X100
1 mM	PMSF
2 µg/ml	Aprotinin
2 µg/ml	Leupeptin
0.1 units/µl	RNasin

TABLE 4 Antibodies used in the publications.

Antibody (type)	Antigen	Source	Publication
A3B10 (Mab)	Intact CPV Capsid	Gift from Parrish CR, USA	II, III
VP2 (Ab)	CPV Capsid protein	Gift from Parrish CR, USA	II, III
NS1 (Mab)	NS1 protein	Gift from Astell C, Canada	II, III
PCNA (Ab)	PCNA protein	Abcam, UK	III
Mab414	FG-repeated Nups	Abcam, UK	I, II
Nup 153 (Mab)	Nup 153 and Nup 62 proteins	Abcam, UK	III
Importin β (Mab)	Importin β protein	Abcam, UK	I
Lamin B1 (Ab)	Lamin B1 protein	Abcam, UK	III
Lamin A/C (Mab)	Lamin A/C proteins	Abcam, UK	III
H3 (Ab)	Histone H3	Abcam, UK	II
H3K27ac (Ab)	Acetylation of histone H3 lysine 27	Abcam, UK	II
H3K9me3 (Ab)	Trimethylation of histone H3 lysine 9	Abcam, UK	II
Goat anti-mouse and anti-rabbit Alexa-488/555/633 conjugated IgG	Mouse or rabbit IgG	Thermo Fisher Scientific, USA	I, II, III
Goat anti-mouse and anti-rabbit horseradish peroxidase conjugated IgG	Mouse or rabbit IgG	Bio-Rad Laboratories, UK	I, III

4.3 Microinjection (I)

For co-microinjection studies (I) NLFK cells were grown to subconfluency (80 %) on glass cover slips. The injections were performed into the cytoplasm of living cells. The cells were co-internalized with HBV capsids or an importin β antibody and FITC-Dextran (Thermo Fisher Scientific) (Table 2, Table 4).

4.4 Confocal Microscopy Studies (I-III)

4.4.1 Fixed Cells (I-III)

Olympus FV1000 microscope (Olympus, Tokyo, Japan) was used with the appropriate excitation and emission settings for each dye (405-nm diode laser, 488/514-nm argon lasers and 633-nm Helium-Neon lasers). Pixel resolution of a 63x1.25 NA Plan-Neofluar oil immersion objective was adjusted according to Nyquist sampling to 50-69 nm/pixel (512x512 pixels/image). Z stacks were collected with a spacing of 150 nm. Image processing and analyses were performed in ImageJ (Abramoff *et al.* 2004) and Adobe Photoshop (C2) (Table 4, Table 5).

4.4.2 Live Cells (I)

Olympus FV1000 microscope at Laboratory for Fluorescence Dynamics (University of California, Irvine, CA, USA) was used with a 60x1.2NA water immersion objective with the appropriate excitation and emission settings for each dye to perform the two color fluorescence line scans over NLFK cells. The sample stage was heated to 37 °C prior the experiments. A pixel time of 2 us/pixel for 30 000 lines was used to obtain the fluorescence carpets for lamin C-EGFP (Table 1) and CPV-A594. Image frames were collected with different scan settings for the characterization of the dynamics (2μs/pixel and above).

4.4.3 Image FCS Analyses (I)

The image fluorescence correlation spectroscopy (FCS) analyses were carried out in the SimFCS program (Laboratory of Fluorescence Dynamics) and Matlab (The Mathworks Inc., 2010) (Table 1, Table 4). FCS-derived number and brightness analysis (N&B) was used to analyze intracellular dynamics of viral capsids (Digman *et al.* 2008). By using different time-averaging of the line scans, the transit events where divided in fast (transit ≤1.60 ms) and slow (transit ›160 ms). Autocorrelation function (ACF) was used to correlate the fluorescence intensity of a particle over time in space to see transition time of capsids. Pair

correlation function (PCF) was used to analyze the diffusion trajectories of capsids and importin β along the scanned line (Digman and Gratton 2009). Correlation was measured by the temporal cross correlation of the two objects at a given distance using image PCF detecting positive correlation from a pixel 300nm away (~size of 1 PSF) from any angle around. The intensity corresponded to a correlation integral of G(r, r+4).

4.5 SDS-PAGE, immunoblotting and chemiluminescence detection (I, III)

Immunoprecipitations (I) and the structural integrity of lamins and Nups (III) were analysed by SDS-PAGE, western blot and chemiluminescence detection according to the manufacturer´s instructions (SuperSignal West Pico Chemiluminescence Substrate, Pierce) (Table 4). Cells were collected by scraping and centrifugation. To produce a whole cell lysate, cells were lysed with a gentle hypotonic cell lysis buffer (Table 3, Table 5).

TABLE 5 Experimental procedures used in the publications.

Experimental procedure	Instrument or Program	Publication
Confocal imaging	Olympus FV1000	I, II, III
FCS[a] on confocal microscopy images	Olympus FV1000, SIM-FCS Matlab	I
Microinjection	Eppendorf Transjector 5246 & Micromanipulator 5171	I
Capillary pulling	Sutter instruments P97	I
AFM[b]	Veeco Multimode SPM, Nanoscope V SPM controller OTR4 AFM tips, Olympus	I
In situ PLA[c]	Duolink®	I, III
Transfection	-	I, II, III
Western blotting	-	III
Cell lysis	-	I, III
ChIP-seq[d]	Illumina Hiseq 2000	II
qPCR[e]	-	II

[a] Fluorescence correlation spectroscopy
[b] Atomic force microscopy
[c] Proximity ligation assay
[d] Chromatin immunoprecipitation combined with high-throughput sequencing
[e] Polymerase chain reaction

4.6 ChIP-seq and qPCR (II)

For ChIP-seq analyses, cells were fixed with PFA. Nuclei were isolated, lysed, and sonicated with a Covaris S220 ultrasonicator. The resulting nuclear extract was incubated overnight at 4 °C using Dynal Protein G beads pre-incubated with 5µg of H3K27ac (ab4729) or H3 (ab1791) Abs. The beads were washed. Bound complexes were eluted, and cross-links were reversed by heating at 65 °C. Precipitated and input DNA were purified with RNAse A, proteinase K, and a phenol-chloroform extraction. The precipitated DNA was analyzed by quantitative polymerase chain reaction (qPCR) using specific primers for the gp1, gp2 and gp5 regions of the CPV genome. Libraries were constructed from precipitated and input DNA with the NEBnext® Ultra™ DNA-library preparation kit from Illumina. DNA in the range of 150–350 bp was gel-purified after PCR amplification. The library was quantified using an Agilent bioanalyzer and subjected to 50 bp single-end read sequencing with an Illumina Hiseq 2000 at EMBL Genecore, Heidelberg. Quality metrics were obtained with FastQC. Adapter sequences were removed with cutadapt and the reads were aligned with Bowtie2 against cat (ICGSC Felis_catus 6.2) and CPV (NCBI Reference Sequence NC_001539.1) reference genomes. Sequencing reads were normalized to reads per genomic content (RPGC). Files were converted into BAM format with SAMtools, and visualized with deepTools.

4.7 Statistical analyses

For all experiments, three independent biological samples with equal sample sizes were analyzed. Amount of cells (n) used in the analyses ranged from 20-110. Statistical analysis was performed using Student's *t*-test (two-tailed, unequal variance). Results were considered statistically significant at $P<0.05$.

TABLE 6 Data analysis and processing used in the publications.

Data Analysis and Processing	Used Software	Publication
Colocalization and correlation	Image J (JACoP plugin) and Excel	II
Distance analysis	Image J (Euclidian distance transform (3D) plugin; in-house Java code)	II
Quantitative PLA analysis	Image J	II, III
Deconvolution	SVI Huygens Essential	I, II, III
Fluorescence intensity measurements	Image J (Measure plugin)	III
General Image Processing	Image J and Photoshop CS2	I, II, III
Correlation analyses	SimFCS; Matlab	I
Number and Brightness analysis	SimFCS	I
DNA-library preparation	NEBnext® Ultra™, Illumina	II
DNA-library quantification	Agilent bioanalyzer	II
Sequencing	Illumina Hiseq 2000, EMBL Genecore, Heidelberg	II
Quality metrics	FastQC	II
Sequence analysis	Bowtie2	II
File conversion	SAMtools	II
Data visualization	deepTools	II

5 RESULTS AND DISCUSSION

5.1 Nuclear import of CPV is mediated by importin β and nuclear pore complexes (I)

The role of active nuclear import receptors (importins) and NPCs in a CPV infection were studied using scanning fluorescence correlation spectroscopy analyses of confocal microscopy images, an *in situ* proximity ligation analysis (PLA), atomic force microscopy, co-microinjection and immunolabeling.

5.1.1 Cytoplasmic trafficking of CPV capsids is an active process mediated by importin beta leading to capsid disassembly in the nucleus

To analyse the translocation of the CPV capsids in the cytoplasm towards the NE, we used live cell imaging with fluorescence correlation spectroscopy analyses of confocal microscopy images, *in situ* PLA and co-microinjection of anti-importin β Ab combined with confocal microscopy.

We first observed the dynamics of virus-containing vesicles, and analyzed their temporal approach towards the NE in NLFK cells stably expressing lamin C-EGFP inoculated with a fluorescent virus (CPV-A594). At ~1h p.i. majority of the fluorescent capsids had accumulated in perinuclear vesicles, presumably endosomes in the proximity of the nucleus within an area of 0.7-4 μm away from the nuclear lamina. Later by ~2 h p.i. the virus-containing endosomes had enriched in the immediate vicinity of the nuclear rim. Movement of the capsid-containing vesicles towards the nuclear rim was accompanied by a loss of the CPV-A594 signal likely due to the release of endosomal viruses into the cytoplasm. These findings demonstrated a time-dependent accumulation of viral capsids near the NE. The perinuclear location of virus-containing endosomes is consistent with earlier studies showing that the maturation process of endosomes includes interactions with the perinuclear ER. When endosomes mature, they need to interact with the ER to modify endosomal signaling receptors and to control the association of endosomes with

microtubule motors, such as dynein, for delivery to perinuclear areas (Grove and Marsh 2011, Huotari and Helenius 2011, Raiborg *et al.* 2015). In agreement, our results showed the slow stepwise cytoplasmic transport of CPV-containing endosomal vesicles. The mode of transport is well in line with earlier studies on the endosomal trafficking of AAV2 (Seisenberger *et al.* 2001). In these studies, cytoplasmic translocation was shown to include phases of free and anomalous diffusion. Our results suggested that the endosomal release of viral capsids occurred in close vicinity of the NE. While the characteristics of these endosomes remains to be elucidated, the detected nuclear approach of CPV in endosomal vesicles is in line with earlier studies, where the entry and release of CPV into the cytoplasm were shown to occur from the low pH endosomes residing in the perinuclear periphery (Suikkanen *et al.* 2002, Grove and Marsh 2011). The acidic lysosomal environment triggers the activation of the viral PLA_2, which is located in the VP1 N-terminus required for release into the cytoplasm (Suikkanen *et al.* 2002). Endocytotic vesicles are mainly transported along microtubules, where the transport is driven by molecular motors such as dynein (Caviston *et al.* 2006). An increase in diameter is known to alter the motion of endosomal vesicles. As an example, the movement of lysosomes is greatly affected by size and includes combined modes of diffusion and active transport (Alberts *et al.* 2002, Luzio *et al.* 2007, Bálint *et al.* 2013). When the size of lysosomes increases such as in response to the presence of virus capsids, their diffusive motion decreases (Bandyopadhyay *et al.* 2014). This could explain why the movement of viruses in endosomes was found to be slow in our studies. The presence of cytoplasmic fast moving particles in close proximity to the nucleus is consistent with earlier studies showing that capsids are transported on microtubules in a dynein-dependent manner (Suikkanen *et al.* 2002).

To examine the cytoplasmic trafficking and the nuclear transport of A594-labelled viral capsids, we characterized their distribution and movement both in the cytoplasm and in the nucleoplasm. For this, confocal line scan acquisitions were performed across the NE of lamin C-EGFP expressing cells infected for 40-110 min to acquire the intensity and location of the nuclear lamina and capsids along the scanned line. The intensity trajectory analysis demonstrated accumulation of viral capsids close to the nuclear rim. Fluorescence fluctuations from the viral capsids around the nuclear lamina were characterized by ACF correlating the fluorescence intensity of a particle over time in space to see the transition time of the viral particle. These analyses confirmed the presence of dynamic virus capsids at the NE. PCF was used to record the movement of the single capsids into the nucleus. The PCF analysis demonstrated positive signals showing the transit trajectories across the lamin C verifying the nuclear entry of capsids. We also performed FCS derived computational Number and Brightness (N&B) analysis to specify the dynamics of the viral capsids from the time averaging of the line scans. The detected transit events where divided in fast (transit ≤160 ms) and slow (transit >160 ms) particle motion. The analysis showed that the slow particles arrived first in proximity to the nuclear lamina and then lost their brightness at 0.94 ± 0.25 µm away from the lamina likely demonstrating the location of endosomal escape of

the viral capsids. At 0.94 µm distance only the fast particles (transit ≤160ms) were detected to approach the nuclear lamina suggesting for a rapid transition of cytoplasmic capsids toward the nucleus. Fast particles were detected in the cytoplasm and in the nucleus with an equal brightness suggesting that no major conformational changes of capsids took place during the nuclear entry. In line with the correlation analysis, low numbers of bright particles were detected inside the nucleus indicating infrequent presence of nucleoplasmic particles and especially potential single particles suggesting that the nuclear import of capsids is a rare event. Moreover, the analysis showed translocation of the fast particles over the nuclear lamina accompanied with an increased presence of both slow and fast particles in the nucleus. This suggests that the nuclear transport of capsids was followed by restricted movement of intact capsids and fast movement of capsid remnants and/or detached fluorophores after disassembly in the nucleus.

Due to the averaging in the intensity carpets, the probability of capturing capsid movement is very small if the capsid moves very fast. However, the PCF fit finds the correlation of movement between pixels in the entire carpet making it more sensitive for detecting the movement of CPV. The PCF thus enabled a more sensitive method for the analysis of capsid transport through the cytoplasm which, until date, has been mainly studied by time-laps imaging and later by single-particle tracking. In line with our results, AAV2 particles have been found to translocate in a directed manner along microtubules towards the nucleus, which is suggestive of an active transport mode (Seisenberger *et al.* 2001, Xiao and Samulski 2012). In the cytoplasm the movement of larger molecules (>500 kDa) is restricted because of the interconnected web of the cytoskeleton, organelles and a high concentration of molecules (Luby-Phelps 2013, Goldstein and van de Meent 2015). Therefore, it can be concluded that the targeted movement of viruses in the cytoplasm cannot be a passive process.

To substantiate the importance of active nuclear transport for the nuclear entry of capsids and progress of infection, we blocked the importin β-mediated macromolecular transport with cytoplasmically microinjection of importin β monoclonal antibody (MAb). The infection progress was significantly inhibited or halted as assessed by quantifying the emergence of the viral replication compartments represented by VP1-3 proteins. These results suggested that the importin β -mediated nuclear transport pathway across the NPCs is essential for efficient progress of parvovirus infection. *In situ* PLA analysis indicated that in synchronized infection cytoplasmic capsids interacted with importin β at 1 h p.i., and that this interaction was increased in a time-dependent manner in early infection. The general pattern of the detected capsid-importin interactions in the cytoplasm possibly reflects the movement of the capsid on microtubules. As was shown previously, after endosomal escape into the cytoplasm, the CPV capsids utilize dynein-mediated transport along microtubules to move within the cytoplasm (Suikkanen *et al.* 2003). It has been documented that members of the importin β superfamily such as α/β could be microtubule associated transport motor adaptors, which direct cargo to the nucleus in a fast-track mode

(Harel and Forbes 2004). Since the NLS-containing VP1 N-terminus required for the recruitment of importins is exposed only after the capsid is released into the cytoplasm, the given time window reflects the timing of escape of the CPV capsid from the endosome (Vihinen-Ranta *et al.* 1998, Weichert *et al.* 1998, Vihinen-Ranta *et al.* 2002, Suikkanen *et al.* 2003). Notably, the results pointed to a somewhat earlier escape of the CPV capsid from the endosomes than was previously reported (~3-8 h p.i.) (Suikkanen *et al.* 2003), but they are in line with data obtained for other parvoviruses such as AAV2 (Seisenberger *et al.* 2001, Sonntag 2006, Xiao *et al.* 2012) and MVM (Zádori *et al.* 2001, Farr *et al.* 2005, Mani *et al.* 2006).

The dynamics of A594-labelled virus capsids and their interaction with importin β during nuclear transport was further analyzed at >50 min p.i. by time-laps imaging of infected cells stably expressing importin β-GFP labeling the nuclear rim, and correlation of the movement of importin β and capsids using PCF analysis. Movement of importin β was found in the cytoplasm, at the nuclear rim and in the nucleus beneath the nuclear rim. Movement of viral capsids occurred mainly in the cytoplasm and also at the nuclear rim and in the nucleoplasm. Importantly, this analysis revealed that the movement of a portion of the cytoplasmic particles correlated with that of importin β, and that the positive correlation of importin β and capsids extended over the NE showing the importin β-mediated capsid transport from the cytoplasm to the nucleoplasm. Our results showed that parvoviral capsids are selectively transported through NPCs by importin β -mediated process (Figure 3).

The nuclear transport machinery including importins, transportins and Nups is widely exploited by viruses (Cohen and Panté 2011). In a classical view, a NLS is required for importin mediated nuclear import of cargo (Adam and Geracet 1991, Görlich *et al.* 1995, Moroianu *et al.* 1995, Weiss *et al.* 1995). The N-terminal unique region of CPV capsid protein VP1 contains four basic amino acids (MAPPAKRARRGLV) fulfilling the minimal sequence requirement for the classical NLS (K-K/R-X-K/R) (Adam and Geracet 1991, Vihinen-Ranta *et al.* 1998, Lange *et al.* 2007). In cells, cargo with a classical NLS is recognized in the cytoplasm by the adaptor molecule importin α and translocated into the nucleus complexed with importin β comprising a NPC binding domain (Vihinen-Ranta *et al.* 2002, Lott *et al.* 2010). Besides the classical model for nuclear import, proteins are transported into the nucleus independently on importins via a direct interaction with the NPC proteins (Whitehurst *et al.* 2002, Tsuji *et al.* 2007, Xu *et al.* 2014). While the results substantiate the crucial role of importin β in the nuclear import of CPV capsids, they do not, however, exclude the possibility that importin α participates in the nuclear translocation of the capsid. Current models for the translocation of importin β through the NPC propose that the protein interacts with the FG repeat domains of specific Nups residing in the NPC. Importin β uses these interactions to translocate cargoes across the central channel (Cardarelli *et al.* 2012, Hülsmann *et al.* 2012, Ma *et al.* 2012). Taken together, our results suggest that an interaction with importin β is required prior to and during the nuclear import of CPV capsids at the initial

stage of an infection. These results also support the view of NPC mediated import of CPV (Figure 3).

To analyze the intranuclear dynamics of the viral capsids, we measured the diffusion coefficients of A594-labeled particles in the nucleoplasm by mathematical fitting of the nuclear ACF. The acquired intranuclear diffusion coefficients ranging from 0 to 70 $\mu m^2/s$ were plotted to 0-0.1 $\mu m^2/s$ (slow diffusion) and 0.1-100 $\mu m^2/s$ (faster diffusion), showing an average diffusion of 0.004 $\mu m^2/s$ for slow and 15 $\mu m^2/s$ for the fast particles. This was in line with our N&B analysis showing the presence of both slow and fast moving objects in the nucleus after the nuclear transport of capsids. In support of this, earlier studies with AAV2 reported intranuclear diffusion values of capsids ranging from 0.4 to 1.3 μm2/s (slow) corresponding velocities from 0.25 to 0.9 μm/s (Seisenberger *et al.* 2001). These previous studies were done by real-time imaging of single fluorescently labeled virus capsids, where particle disassembly cannot be addressed. In our study the ACF method includes analysis of all movement of labeled particles allowing detection of smaller particle species such as capsid remnants after disassembly. Previously, FCS analysis have showed diffusion coefficient of 17 $\mu m^2/s$ in buffer for virus like particles (Ihalainen *et al.* 2009). In the nucleus, however, the dense meshwork of chromatin would likely restrict diffusion of capsids. Our finding of relatively immobile nuclear capsids is in line with earlier results showing the presence of very-slow-diffusing intact parvoviral capsids in the nucleus (Ihalainen *et al.* 2009). The detected faster nuclear diffusion rates are in line with earlier observations where diffusion coefficient of 4.3 $\mu m^2/s$ was shown for the nuclear VP2 proteins (VP2-GFP) (Ihalainen *et al.* 2009). This verified that nuclear import of capsid is followed by their disassembly and nuclear emergence of viral capsid proteins. Altogether, these results suggested that both of slow intact capsids and fast disassembled capsid remnants were present in the nucleoplasm. Our findings revealed that the nuclear entry of parvoviral capsids is a dynamic process involving fast and slow movement of the capsids movements in the cytoplasm and also in the nucleus. The nuclear presence of the fast particles strongly suggests that nuclear entry of capsids is followed by their disassembly in the nucleoplasm.

5.1.2 Nuclear import of CPV occurs via nuclear pore complexes

Our results, which point to active importin β mediated capsid translocation across the NE in a CPV infection, led us to follow the nuclear import of CPV capsids more closely. Therefore, we investigated the interactions between capsids and NPCs at high resolution and near physiological conditions on the NE of *Xenopus laevis* oocytes by AFM. To introduce viral capsids to the NE, capsids were microinjected into the cytosol of oocytes. Isolated NEs were analyzed 1 h post microinjection.

We found that the viral capsids were localized on top of the NPCs, but not between them. The capsids were also seen to emerge from the nucleoplasmic side of the NPC in the accommodating nuclear basket showing the stepwise translocation of CPV across the NPC. The presence of viral capsids in the nuclear and cytoplasmic sides of the NPC was confirmed by capsid height-measurements. Moreover, an AFM cantilever deflection measurement indicated that the mechanical properties of capsids on the nucleoplasmic side of the NPC and on the hard surface were relatively similar. In agreement with this and our earlier observations (Suikkanen *et al.* 2003b), the AFM analysis of capsids in the nucleo- and cytoplasmic sides of the NPC confirmed that the capsids were intact after their nuclear translocation. In addition, blockage of NPCs in an early-infection with HBV capsids resulted in the complete inhibition of the infection. The size of a molecule is an important parameter that directly limits or at least determines the mode of transport through the NPCs. Intriguingly, at <30 nm in diameter the parvovirus capsid is small enough to theoretically fit through the central channel of the NPC, which has been reported to accommodate complexes of up to 39 nm in diameter (Panté and Kann 2002). Our AFM studies revealed the presence of CPV capsids on the top of the NPCs, and for the first time, the emergence of CPV capsids at the nucleoplasmic side of the complexes. This is in contradiction with the view that parvoviruses are imported into the nucleus with an NPC-independent mechanism (Hansen *et al.* 2001). The binding of the parvoviral capsid to, but not its entry into, the NPCs has been shown to be required for nuclear entry (Porwal *et al.* 2013). Our results support NPC binding, but also suggest that nuclear import can occur via the NPCs (Figure 3). In support of this, evidence for the NPC-mediated intranuclear localization of the recombinant capsids of another parvovirus, AAV2, was presented recently (Kelich *et al.* 2015). It might well be that capsid binding and/or entry into the nucleoplasm are required to trigger changes in the NE and in the underlining lamina. In our studies, the structural integrity of the lamina was not addressed.

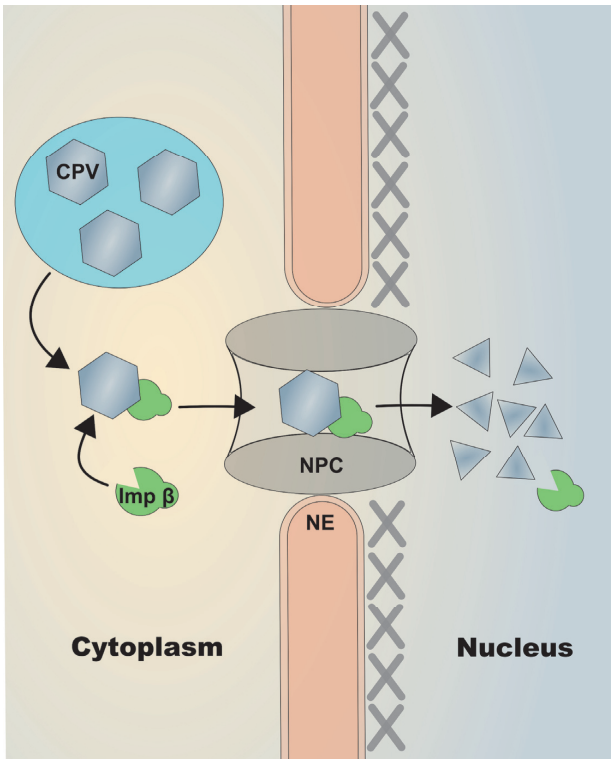

FIGURE 3 Schematic presentation of CPV nuclear import. Upon release from the endosomal vesicles near the NE, CPV capsids are actively transported via importin β followed by concomitant nuclear entry via NPCs. However, the possible involvement of importin α in this process remains to be addressed.

5.2 Chromatinization and epigenetic modifications are critical for the regulation of a CPV infection (II)

When introduced into cell nuclei, viral DNA is exposed to cellular responses against foreign DNA, including chromatinization and epigenetic silencing. In our study, we asked how the incoming parvoviruses can resists this cellular epigenetic down-regulation of their genes. To this end, confocal imaging techniques and *in situ* PLA complemented with chromatin immunoprecipitation coupled with high-throughput sequencing (ChIP-seq) were conducted in NLFK cells to study intracellular chromatinization, histone modification and their effects on the CPV genome and the progression of an infection. Transcriptionally active chromatin was detected with a specific marker, H3K27ac, while H3K9me, a marker for constitutive heterochromatin, was used to identify transcriptionally repressed chromatin.

Colocalization and Pearson´s correlation coefficient (PCC) analyses indicated that histone H3 and especially H3K27ac were enriched in APAR

bodies represented by the viral DNA-binding NS1 protein from 16 to 24 h p.i. These findings suggested that histones were associated with the viral genome in the APAR area bearing epigenetic modifications characteristic of active gene expression. To address this, the nuclear interaction between H3K27ac and NS1 was studied further by *in situ* PLA. This analysis demonstrated a time-dependent increase in the interaction or close proximity of H3K27ac with NS1 in the APAR bodies at >8 h p.i. followed by extensive interactions at 24 h p.i. This is consistent with our results obtained from immunofluorescence and PCC analyses of histones showing increased colocalization and correlation of H3K27ac and NS1 during the late-stages of infection, and suggests for presence of modified histones on the viral genome. However, these microscopy studies would have benefited from a marker or a fluorescent probe for parvoviral genome and use of such marker would be recommended in future studies. Post-translational modifications of core histone tails such as increased acetylation of histone H3 lysine 9 and lysine 14 and loss of H3 lysine 9 and H3 lysine 27 methylation (HSV-1 lytic cycle) and deposition of histones along the viral genome are known to play important roles in the regulation of herpes and adenoviral gene expression (Kent *et al.* 2004, Coleman *et al.* 2008, Kalamvoki and Roizman 2010, Komatsu and Nagata 2012). Consistently, evidence for the chromatinization of adeno-associated viruses, used as gene therapy vectors, and MVM genomes has been reported earlier (Ben-Asher *et al.* 1982, Marcus-Sekura and Carter 1983, Penaud-Budloo *et al.* 2008, Upadhyay *et al.* 2013).

5.2.1 Viral promoters become associated with acetylated histones

In autonomous parvoviruses, NS1 not only controls viral activities, but also regulates the expression host genes through histone acetylation by the recruitment of cellular proteins with a HAT-activity (Ohshima *et al.* 2001, Iseki *et al.* 2005). Interestingly, our PLA studies indicated that CPV NS1 was located in close proximity to H3K27ac in the enlarged APAR bodies. The close presence of H3K27ac with NS1 might be due to the accumulation of NS1 on the viral genome because of its involvement in transcription and replication (Cotmore *et al.* 2007, Niskanen *et al.* 2010, Niskanen *et al.* 2013). While the specific role of NS1 in viral histone modifications was not determined in our study, the results were in line with our colocalization and correlation analysis and demonstrated that an interaction or close proximity of H3K27ac with the viral NS1 increased temporally.

Earlier studies have indicated that CPV NS1 has two distinct binding sites in the viral genome (Ihalainen *et al.* 2007, Niskanen *et al.* 2010, Niskanen *et al.* 2013). It is thus tempting to speculate that NS1 is involved in the acetylation of histones at the viral P4 and P38 promoters by recruiting host proteins with an acetyl transferase activity. However, the involvement of NS1 in the regulation of histone acetylation on parvoviral promoters had not been reported earlier. In our study, ChIP-seq experiments showed that the CPV genome was chromatinized within the host nucleus and associated with H3K27ac-enriched nucleosomes. The H3K27ac was mainly enriched in the transcription start sites

of P4 promoter-driven transcriptional unit for NS1 and NS2 and P38-driven transcriptional unit for VP1 and VP, but was absent towards the right-hand (5´) end of the genome. The association of H3K27ac with the viral genome was confirmed with a targeted ChIP-qPCR analysis. Moreover, from the ChIP-qPCR of H3, we found that the viral genome was thoroughly chromatinized with uniformly distributed H3.

Our results verified the assumption that the parvoviral genome is chromatinized in the host nucleus during the late stages of an infection. Importantly, acetylated histones were observed to be enriched in viral promoter areas presumably to allow for the transcriptional activation of the viral genes.

5.2.2 Acetylation of viral histones is required for the progress of the infection

To study the importance of histone acetylation on the CPV genome, we determined the effect of the HAT inhibitor anacardic acid on viral protein synthesis during the early stages of an infection in NLFK cells. This approach showed that a treatment with the HAT inhibitor at -0.5 to 1 h p.i. resulted in a decrease in the percentage of cells with a nuclear NS1 (~5 %) and VPs (~2 %) compared to non-treated infected cells (~68 % and ~50.3 %, respectively). The early inhibition of histone acetylation significantly inhibited the infection. In addition, the HAT inhibitor was able to inhibit the progress of the infection and the nuclear translocation of proteins up to 3 h p.i.

The possibility that histone acetylation was not the only factor affecting viral protein production cannot be ruled out in this experiment. Because the acetylation status of chromatin is governed by HAT inhibitors, it might be that the genetic regulation of the cell cycle is affected upon treatment with anacardic acid. In our study, the concentration of anacardic acid was chosen according to the literature. It has been shown earlier that anacardic acid might induce cell cycle arrest into G1/S (Xiu *et al.* 2014). According to the literature, however, there is no consensus over how anacardic acid affects cell proliferation and cell cycle, whether the effects are related to a specific cell type, and whether it induces apoptosis (Tan *et al.* 2012, Xiu *et al.* 2014, Harsha Raj *et al.* 2016). However, in our study, cell viability was not affected as detected by DAPI, propidium iodide and annexin V stainings.

To characterize the role of anacardic-acid induced HAT inhibition on a late infection, we categorized the cells into four different types based on the intracellular localization of viral capsids. These categories included capsids localized to cytoplasmic endocytic vesicles (1), capsids localized to discrete foci scattered throughout the nucleus (2), capsids in enlarged APAR bodies enriched with NS1 (3), and capsids in both APAR bodies and the cytoplasm (4). The percentages of cells in these aforementioned categories were determined after a 6 h exposure to anacardic acid at 24 h p.i. As a result, the inhibition of histone acetylation correlated with the inhibition of the progress of a late-infection.

Parvoviral gene expression, the nuclear translocation of viral proteins, capsid assembly, genome replication and capsid maturation are known to be strictly dependent on the cell cycle (from G0/G1 through S into G2 phase) (Gil-

Ranedo *et al.* 2015). It has been shown that an arrest in the cell cycle in the G1 or early S phase interferes with the assembly of the viral capsid and retains parvoviral capsid proteins in the cytoplasm. Concomitantly, infection induced stress to cellular DNA synthesis uncouples the cell cycle-based controls of the replication of the parvoviral genome from the assembly of capsids. Newly synthesized viral proteins have been shown to immediately assemble into capsids upon nuclear import (Gil-Ranedo *et al.* 2015). In our study, cells were treated with anacardic acid at 6 h p.i. when the production of viral proteins had already begun (Ihalainen *et al.* 2012). Here, only the effect of the drug on the intracellular distribution of intact capsids was analyzed. Notably, the treatment at 6 h p.i. did not prevent the assembly of viral capsids or egress, but inhibited the progress of the infection suggesting that anacardic acid did not interfere with the cell cycle dependent regulation of the infection when added at a late stage. In conclusion, our study supported the importance of histone acetylation for the progress of a parvoviral infection by showing that the inhibition of histone acetylation was accompanied by an extensive repression of the infection.

Finally, we studied whether the timing of the viral histone acetylation was critical for the progress of a late infection. A treatment with the anacardic acid at 16 h p.i. resulted in the exclusion of H3K27ac from the NS1-positive APAR bodies, indicating that the viral genomes produced after the drug treatment at 16 h p.i. were not acetylated. However, the colocalization of H3K27ac with NS1 after exposure to the inhibitor at 20 h p.i. suggested that the modification of histones on the majority of the newly synthesized viral DNA continues until 16-20 h p.i. It can be speculated that the acetylation of viral histones correlates with the presence of suitable replication intermediates of the viral genome. Earlier studies have shown that the formation of templates for parvoviral gene transcription and intermediates for genome replication are temporally phased in an infection (Clemens and Pintel 1988, Schoborg and Pintel 1991, Tullis *et al.* 1994, Lieberman 2006). In line with these findings, our results suggest that parvoviral gene expression is regulated via histone acetylation in a temporal manner. These studies argue that the histone acetylation of viral genomes in an early infection plays an essential role in the production of viral proteins. Moreover, the acetylation of histones on newly synthesized viral genomes during the active phase of virus replication is necessary for accomplishing an infection. To summarize, our findings demonstrate that viral histone acetylation is essential for both the early and late steps of the parvoviral life cycle.

5.3 CPV induces the remodelling of the nuclear architecture (III)

The effect of a CPV infection on the composition of the nuclear envelope during the late stages of an infection in NLFK cells was studied by analysing NPCs and nuclear A- and B-type lamins, and the distribution of chromatin and chromatin-associated histone proteins.

5.3.1 CPV infection leads to the redistribution of chromatin and histones

To study the distribution of histones H3, H3K27ac, H3K9me3 and APAR bodies represented by viral NS1, we used NLFK cells stably expressing H3-EGFP in immunolabeling, deconvolution, line profile and PCC analyses. These studies indicated that H3 was mainly located distinctly separate from NS1 until 12 h p.i., whereas an increase in correlation was observed at 16 and 24 h p.i. To assess how H3-associated active and repressive chromatins were distributed in infected cells, we used H3K27ac and H3K9me3, as specific chromatin markers for active and repressive chromatin, respectively. The CPV infection began with the emergence of NS1-containing intranuclear foci at 12 h p.i., while H3K27ac and H3K9me3 showed a more uniform nuclear distribution and only a weak correlation with NS1. However, at 24 h p.i. APAR bodies represented by NS1 filled the nucleus and H3K27ac were concentrated significantly in these areas. Similarly, an increase in correlation was detected from 16 h to 24 h p.i. instead of earlier time-points. Therefore, the colocalization of H3 and H3K27ac correlated time-dependently with the enlargement of APAR bodies. In comparison, no correlation between NS1 and H3K9me3 was observed in this study. These results indicated the time-dependent presence of actively transcribed chromatin in the APAR areas.

Additionally, we applied a quantitative 3D distribution analysis of H3K27ac and H3K9me3 as a function of distance from the nuclear rim to study intranuclear distribution of the modifications. The H3K27ac signal was found in the center of the nucleus in both infected (24 h p.i.) and noninfected cells. Intriquingly, in infected cells H3K9me3 was enriched at the nuclear periphery with a decreased intensity toward the center, while in noninfected cells, the H3K9me3 signal was distributed throughout the nucleus. Concomitantly, the infection induced the compaction of the DAPI-stained host chromatin and its dislocation into the nuclear periphery and around the nucleolus at 24 h p.i. Marginalization of cellular chromatin is a known phenomenon in infections of nuclear replicating viruses although the nature of the marginalized chromatin is less well known (Monier *et al.* 2000, Nagamine *et al.* 2008, Ihalainen *et al.* 2009, Bosse *et al.* 2015). Spatial organization of chromatin, the intranuclear distribution of euchromatin and facultative and constitutive heterochromatin, fluctuates during the cell cycle and occupy specific locations in the nucleus. These locations have also been shown to be consistent between cells of the same cell type (O´Keefe *et al.* 1992, Dekker 2014). In the early S-phase replicative euchromatin is homogenously distributed throughout the nucleoplasm excluding the nucleoli, which is in line with our results in mock-infected control cells, and in infected cells as parvoviruses have been shown to induce S-phase arrest. Later in S-phase replication of the euchromatin decreases while the peripheral heterochromatin becomes more actively replicated concomitantly with increased presence of late-replicating chromatin around the nucleoli (O´Keefe *et al.* 1992, Guetg and Santoro 2012). However, the transcriptionally

inactive nature of nucleolus-associated heterochromatin is relatively unknown (van Koningsbruggen *et al.* 2010, Németh and Längst 2011).

H3K9me3 is a marker for transcriptionally repressed heterochromatin. Particularly, it is found in the constitutive, pericentric heterochromatin, which has been hypothesized to act as a silencing compartment. Moreover, the distance to the nuclear periphery has been shown to positively correlate with gene silencing (Takizawa *et al.* 2008, Szczerbal *et al.* 2009). The tethering of chromatin to the nuclear lamina at the nuclear periphery has also been shown to induce transcriptional repression (Finlan *et al.* 2008, Reddy *et al.* 2008). It might be that infection induced repression of the cellular gene expression results in increased presence of transcriptionally inactive heterochromatin in the perinuclear area and around the nucleoli (Kalverda *et al.* 2008, Pombo and Dillon 2015). Repression of cellular genes might be a beneficial strategy for the virus to regulate host transcription as it is the case with bovine papillomavirus (You *et al.* 2004). These changes could be also related to infection induced cellular defense or apoptotic changes. CPV is known to induce condensation and fragmentation of DNA, and accumulation of high levels of histone H2A.X phosphorylation coinciding with severe DNA damage and apoptosis in late infection leading to cellular lysis (Nykky *et al.* 2010). It is tempting to speculate that CPV influences the transcriptional status and architecture of the host chromatin from the loosely packed, transcriptionally active euchromatin towards a more inactive, condensed heterochromatin. However, these interactions remain to be determined by future studies.

5.3.2 CPV infection induces the reorganization of nuclear pore complexes and nuclear lamins

The effect of CPV infection on the organization of NPCs and nuclear lamins was studied using immunofluorescence labelling, deconvolution and Western blotting in NLFK cells at 24 h p.i. We examined the spatial distributions of NPCs at the apical and basal sides of nuclei in infected and mock-infected S- or G1/G2-phase cells. PCNA was used as a marker for cell cycle phases and the presence of parvoviral replication bodies.

In non-infected cells, NPCs stained by anti-Nup 153 were unevenly distributed. In these cells, the number of NPCs at the apical side was ~31% higher than that at the basal side. Concomitantly, the overall NPC densities on both the apical and basal sides were significantly reduced in the infection. The most prominent reduction was seen at the basal side of the nuclei of infected-cells, where the NPC density was ~25 % lower than in the mock-infected G-phase (G1/G2) cells and ~30 % lower than in the S-phase cells. Moreover, a western blot analysis indicated that the infection preserved the abundance and integrity but induced other structural modification of Nup 153.

In previous studies, the distribution of NPCs on the basal side of the nucleus has been considered to describe the overall nuclear density of NPCs. Nowadays, nuclei are known to be polarized compartments, where structures and functions are unevenly organized between the apical and basal surfaces

(Kim and Wirtz 2015). Despite this, the distribution of NPCs between the apical and basal sides of the nucleus has not been comparatively determined. Our results showed that an infection was accompanied by a profound modification of the NPC network. Earlier studies have shown that a cell cycle dependent increase in the amount of NPCs and the nuclear volume occur simultaneously, but are regulated by distinct mechanisms (Dultz and Ellenberg 2010, Maeshima *et al.* 2010). The frequency of NPC biogenesis fluctuates during the cell cycle, being at its highest in the S and G2 phases (Maul *et al.* 1972, Winey *et al.* 1997, Maeshima *et al.* 2006, Antonin *et al.* 2008, Maeshima *et al.* 2010). A CPV infection is accompanied by a cell cycle arrest in the S phase (Nykky *et al.* 2010). Notably, in contrast with the high density of NPCs seen in S-phase cells, we observed a significant decrease in their density in infected cells.

In relation to this, no major differences in the abundance or integrity of Nup 153 were detected in biochemical assays. Therefore, the change in the organization of NPCs was not due to virus induced degradation. Yet, the increased molecular weight of Nup 153 might reflect a posttranslational modification of Nup 153, such as an increase in phosphorylation. In many virus infections, Nup 153 undergoes structural modifications to support viral replication and spread. As an example, viruses use the phosphorylation of Nups to alter the nucleocytoplasmic transport of the host (Porter and Palmenberg 2009). Furthermore, the phosphorylation of Nups can occur in response to DNA damage, commonly detected in parvovirus infections (Cotmore and Tattersall 2013, Luo and Qiu 2013), and can indicate an infection-induced functional change of Nup 153 (Güttinger *et al.* 2009, Wan *et al.* 2013). Our analyses do not exclude the possibility that Nup 153 becomes detached from the NPCs during an infection. However, the unchanged amount of homogenously distributed Nup 153 in the cytoplasm argues against it. Taken together, these results demonstrate that a CPV infection is accompanied by the accumulation of NPCs at the apical side of the nucleus along with a decrease in the overall density of the complexes and structural modification of Nup153.

Concomitantly, the infection induced changes to the nuclear lamina. In the mock-infected cells, an analysis of the intensity ratio between the apical and basal surfaces revealed that the intensities of lamins A/C and B1 were always higher at the apical side than at the basal side. At the apical side, the intensity of lamin A/C was significantly higher than that of lamin B1. In virus-infected cells, similarly to NPCs, lamin B1 was enriched in clusters along the apical side of the NE with a slightly increased intensity, whereas the intensity of lamin A/C remained similar to that of the mock-infected cells. Interestingly, a western blot analysis showed that both lamins remained intact and their expression levels remained unaltered during the infection. To study if these changes were related to the nuclear egress of the progeny viruses across the NE, we analyzed the local distributions of lamin B1, Nup153, and newly formed CPV capsids during a late infection by immunolabeling, deconvolution and intensity measurements. An analysis of confocal yz-cross sections showed that an infection was accompanied by an increase in the apical positioning of the

NPCs. In addition, the apical side of the nucleus contained lamin B1-rich areas, while the overall intensity of lamin A/C was reduced. B-type lamins are known to concentrate in NPC-rich regions, whereas A-type lamins are found in pore-free islands (Maeshima *et al.* 2006, Maeshima *et al.* 2010). Accordingly, changes in the distribution of NPCs are known to correlate with nuclear lamina reorganization during the cell cycle (Fisherova and Goldberg 2010, Maeshima *et al.* 2010). It can be speculated that the detected changes in NPC and lamin B1 distribution are related to the infection driven proceeding of the cell cycle into late S/G2-phase preventing mitotic entry (Adeyemi and Pintel 2014, Gil-Ranedo *et al.* 2015). Approaching the mitosis might induce compositional changes of the NE, however, the relation of the cell cycle and the reorganization of NPCs and lamins in parvovirus infection remain to be investigated in future studies. Concomitant with the apical enrichment of NPCs and lamin B1, intact intranuclear capsids concentrated beneath the apical NPCs prior to their nuclear egress.

Our results are in agreement with earlier data showing that parvoviral nuclear egress does not induce the degradation of lamins (Nüesch *et al.* 2005). The results suggested that the structural integrity of the lamina was retained in a late CPV infection, but its composition or the accessibility of lamin epitopes might have been affected. Recently, it was shown that access to lamin A/C epitopes is regulated by cytoskeletal tension (Ihalainen *et al.* 2015). Mechanical forces related to the previously reported increase in nuclear volume and changes in cellular metabolism might influence the nuclear architecture and the conformation of lamins (Nüesch *et al.* 2005, Ihalainen *et al.* 2009). Instead of inducing degradation, a parvovirus infection might influence the organizational and/or functional status of nuclear lamins. It might be that the infection induces altered post-translational modification of the lamina. For example, phosphorylation of lamins is known to affect their structural properties and signaling functions (Torvaldson *et al.* 2015). On the another hand, knowing that lamins and NPCs mediate forces between the cytoplasm and the nucleoplasm, it might be that the reorganization of lamins occurs as a response to the altered mechanical requirements of the nucleus due to pathogenic stress induced by the virus (Guo and Zhen 2015). The cell stress might result from infection induced cytopathic effects and apoptotic signaling. For CPV and other parvoviruses such as B19, H1 and aleutian mink disease virus mechanisms of cell death and cell cycle arrest are known to promote the viral lifecycle (Chen and Qiu 2010). In CPV infection, apoptosis has been shown to be caspase-dependent (Nykky *et al.* 2010). Therefore, CPV induced activation of caspases 9, 8, and 3/7, whose function is related to functional and structural changes of the NE such as degradation of nuclear lamins and NPCs, might be connected to the reorganization of the NE detected in our study (Ferrando-May *et al.* 2001, Chen and Qiu 2010, Nykky *et al.* 2010, Shalini *et al.* 2015). Changes in nuclear lamina might also be related to the increased volume of the nucleus in CPV infection (Ihalainen *et al.* 2009). Enlargement of the nucleus might require changes of the cytoskeleton. Change in the cytoskeletal tension is known to alter the differential basal-to-apical accessibility of lamin A/C epitopes in the nuclear

lamina, which might partly explain our results (Ihalainen *et al.* 2015). However, additional experimentation would be required to address this question.

6 CONCLUSIONS

The main conclusions of this thesis are:

1. After endosomal escape, the translocation of CPV into the nucleus is actively mediated by the nuclear transport receptor importin β. CPV particles translocate to the NPCs and into the nucleus across the intact nuclear lamina. The nuclear entry of viruses triggers an overall instability in the nuclear lamina.

2. In the chromatinized CPV genome, the two viral promoter areas are rich in histone H3 bearing a post-translational modification, acetylation of lysine 27 (K27ac), which is characteristic of transcriptionally active chromatin. The inhibition of HAT activity efficiently interferes with the expression of viral proteins and the progress of the infection. Acetylation of viral histones and its temporal control are essential for viral gene expression and the completion of the viral life cycle.

3. A CPV infection is followed by the reorganization of the nuclear architecture. The nuclear pore complexes and lamin B1 accumulate, while the level of lamin A/C decreases on the apical side of the nucleus. These changes are accompanied by the apical localization of newly formed CPV capsids in close proximity to the NPCs. This suggests that a late parvoviral infection induces the reorganization of nuclear pore complexes and the lamina to enhance the nuclear egress of capsids. A CPV infection results in the redistribution of the host chromatin and its marginalization to the periphery of the nucleus in association with the H3K9me, an epigenetic marker for transcriptionally repressed chromatin.

Parvoviruses are dependent on nuclear functions throughout their infectious cycle. However, the host cell´s structure, transport pathways and defense mechanisms pose a challenge for the progression of the viral life cycle. Although much is known about the cytoplasmic entry and nuclear replication

and gene expression of parvoviruses, little is known about the dynamics of nuclear entry, chromatinization of the viral genome, and virus-induced changes in the structure of the NE. This thesis shed light on these events. Moreover, while the roles of the NE in protecting the nuclear genome and mediating nucleo-cytoplasmic transport are well known, its dynamic behavior in response to parvoviral infections is less well understood. Also this aspect was elucidated in this thesis.

This thesis shows that parvoviruses hijack the nuclear transport machinery enabling the translocation of their capsids into the nucleus. The nuclear import of parvoviruses is an active process mediated by the nuclear transport machinery. The results reveal the dynamics of the transportation of parvovirus capsids into the nucleoplasm.

Our studies describe the critical role of epigenetic modifications in the regulation of a parvovirus infection. Intranuclear chromatinization and histone acetylation are exploited in the activation of parvoviral gene expression and to ensure progress of the infection. We demonstrated, for the first time, that a successful parvovirus infection is characterized by the deposition of nucleosomes with active histone acetylation on the viral promoter areas.

Finally, we showed that the late stages of a parvovirus infection are accompanied by the reorganization of the NE, including NPCs and the nuclear lamina. These changes might be required to facilitate the infection, and/or be direct consequences of disrupting nuclear metabolism and the regulation of host gene expression. Our results extend our previous knowledge of profound virus-induced changes in nuclear organization.

For cell cycle dependent autonomous parvoviruses, the regulatory control over the NE and nuclear organization can be beneficial because the NE actively controls genomic activity and directly modifies the genetic landscape. In addition, regulatory control over the organization of NPCs can be beneficial for the virus, since a gating function in nucleocytoplasmic transport empowers the viral control of signaling pathways, cell cycle progression, and antiviral mechanisms.

As an outcome, new insights into the molecular interactions of the nuclear import parvoviruses, to the epigenetic regulation of parvoviral gene expression and to the impact of an infection on nuclear organization are provided - all of these aspects are important for understanding the mechanisms of the virus-nucleus interactions required for developing oncolytic virotherapies and parvovirus-based gene therapies (*Marchini et al.* 2015).

Acknowledgements

This study was performed in the University of Jyväskylä, at the Department of Biological and Environmental Science, Division of Molecular Biology.

I want to express my deepest gratitude to my supervisor Docent Maija Vihinen-Ranta for her infinite support and endless encouragement. I also want to thank her for giving me the scientific freedom to investigate, learn and to perform research. She always enabled me to attend meetings and courses where I could grow as a person and to develop into an independent scientist.

I am grateful for my second supervisor Professor Michael Kann for enthusiastic discussions and advice. He taught me to think outside the box and to adopt new ideas, to be open for all possibilities and to enjoy science in all its freedom. I want to thank my follow-up committee, Doctor Kari Airenne and Professor Markku Kulomaa for excellent support and discussions in the National Doctoral Programme for Informative and Structural Biology (ISB). Additionally, I want to thank Mark Johnsson and Fredrik Karlsson, the heart and soul of ISB, for all courses and events, discussions and thoughts. I also want to thank all fellow scientists in ISB for unforgettable moments.

Since my master´s studies I have had the privilege to follow the example of two excellent researchers, Doctor Einari Niskanen and Doctor Teemu Ihalainen. Without you, your advice and discussions, I wouldn´t be the researcher I am today. I am very grateful for your kindest help and endless source of real interest and love for science.

I want to acknowledge my co-authors of the original publications: Kari, Pekka, Lassi, Mikko, Olli, Vesa, Jenu, Ian, Carmine, Doctor Keijo Viiri, Doctor Michelle Digman, Professor Jussi Timonen, Professor Enrico Gratton and Professor Victor Shahin. I express my gratitude to the official reviewers of my thesis, Doctor Johanna Laakkonen and Professor Veijo Hukkanen. Your comments were highly appreciated and they improved the quality of my thesis. I want to thank Professor Klaus Hedman for suggestions and checking the language of all of the original articles. I thank Helen Cooper for excellent language check of this thesis.

I have had the chance to supervise talented master´s students. Thanks to Anniina, Kateryna, Anna, Visa and Jori for the great moments and discussions in the corridors. Similarly, I am grateful to all of my colleagues in the JYU Nanoscience center, especially Eleonora Nykänen, and in the Laboratory for Fluorescence Dynamics for cheering me up and all the smiles and help. Many thanks to all great laboratory technicians for your kindest assistance in the research projects. Allu, Ine, Alli, Laura and Milka: I can´t thank you enough.

I also thank my parents, my sisters Hanna and Anniina, their husbands, and my sister-in-law Maija and her family for your support and faith. Thank you for believing in me. I also want to thank my dearest friends, especially Kaisa, for being there for me.

Finally, I express my deepest gratitude to my husband Jussi and my precious kids Helmi and Reino. Your eternal love and support were lifesavers and mean the world to me. This thesis is dedicated to you.

YHTEENVETO (RÉSUMÈ IN FINNISH)

Parvoviruksen ja tuman väliset vuorovaikutukset

Lähes kaikki DNA-virukset tarvitsevat isäntäsolun tumassa sijaitsevia tekijöitä perimänsä monistamiseen ja uusien virussukupolvien tuottamiseen. Näihin viruksiin lukeutuvat myös parvovirukset, jotka ovat pieniä, yksijuosteista DNA:a sisältäviä, vaipattomia viruksia. Tässä väitöskirjassa tutkittiin parvovirusten ja isäntäsolun tuman välisiä vuorovaikutuksia sekä infektiomekanismeja. Lääketieteen näkökulmasta parvovirukset ovat lupaavia työvälineitä virusvälitteisessä geeniterapiassa. Geeniterapian tarkoituksena on parantaa sairauksia korvaamalla solujen puuttuvia tai virheellisiä geenejä ja niiden tuotteita. Tästä syystä johtuen, parvovirusten ja tuman välisten vuorovaikutusten tuntemus on ensiarvoisen tärkeää.

Tässä väitöskirjassa malliviruksena käytettiin *Parvovirinae*-heimoon kuuluvaa koiran parvovirusta, joka on koirien merkittävimpiä taudinaiheuttajia. Se aiheuttaa veristä ripulia, sydänlihastulehdusta, kuumetta sekä ruokahaluttomuutta johtaen hoitamattomana kuolemaan. Ympäri maailmaa koiranpennut rokotetaan tätä virusta vastaan, sillä tällä hetkellä ei ole olemassa tehokasta hoitomuotoa sen aiheuttamiin oireisiin. Jotta uusia hoitomuotoja voitaisiin kehittää, parvovirusten infektiomekanismien ja solusisäisten vaikutusten tutkiminen on tarpeen.

Väitöskirja koostuu kolmesta osatyöstä, joissa selvitettiin viruksen tumakuljetuksen dynamiikkaa, tumassa tapahtuvaa virusperimän aktivoitumista sekä infektiosta aiheutuvia muutoksia tumakalvossa. Ensimmäisessä osatyössä parvoviruksen näytettiin ensimmäistä kertaa kulkeutuvan tumaan aktiivisesti tumakuljetusreseptori importiini β:n välittämää reittiä. Tumakuljetusta edelsi virusten kulkeutuminen endosomaalisissa kalvorakkuloissa lähelle tumaa, niiden vapautuminen solulimaan ja kulkeutuminen kohti tumakalvoa. Tätä tietoa voidaan hyödyntää kehitettäessä hoitomuotoja parvoviruksia vastaan ja ennen kaikkea tehostettaessa parvovirusvälitteisten geeniterapiavektoreiden kohdentamista solun sisällä.

Väitöskirjan toisessa osatyössä tutkittiin koiran parvoviruksen perimän kromatinisaatiota ja sen sisältämien geenien ilmentämisen aktivoitumista. Tutkimuksessa osoitettiin, että tumassa parvoviruksen perimä kromatinisoitiin liittäen siihen H3 histoneita. Geenien aktiivisuudesta kertovan, epigeneettisesti muokatun H3K27ac muodon osoitettiin rikastuvan erityisesti perimän promoottorialueille. Lisäksi huomattiin, että histoneiden asetylaatiota välittävien entsyymien kohdennettu estäminen hidasti viruksen proteiinien ilmentämistä ja infektion etenemistä. Tämän tutkimuksen tuloksia voidaan pitää ensimmäisenä suorana osoituksena parvoviruksen geenien epigeneettisen säätelyn merkittävyydestä viruksen geenien ilmentämiselle ja infektion etenemiselle. Nämä tulokset selittävät osaltaan sekä parvovirusinfektion pysyvyyttä kudoksissa, että parvoviruksiin kuuluvan AAV geeniterapiavektorin geenien ilmentämisen pitkää kestoa. Täten tästä

tutkimuksesta saatua tietoa voidaan hyödyntää sekä infektion hoidon, että geeniterapiavektoreiden kehittämisessä.

Viimeisessä osatyössä selvitettiin parvovirusinfektiosta aiheutuvia muutoksia tumakalvon (tumahuokosten ja tumalaminan) rakenteelliselle järjestäytyneisyydelle. Viruksen havaittiin lisäävän tumahuokosten epäsymmetristä jakautumista tuman yläpinnalle ja aiheuttavan myös rakenteellisia muutoksia Nup 153 proteiiniin tumahuokosessa. Tuman yläpinnalla korostuivat pääasiallisesti lamiini B1:sta muodostuvat alueet, kun taas lamiini A/C:n kirkkaus väheni tumassa kauttaaltaan. Tumahuokosten ja lamiini B1:a sisältävien alueiden jakauman osoitettiin olevan yhtenevät. Lisäksi uusien virusten huomattiin hakeutuvan näiden alueiden läheisyyteen tuman yläpinnalle odottamaan tumasta poistumista. Tässä tutkimuksessa parvovirusinfektion osoitettiin aiheuttavan tuman rakenteiden merkittävää uudelleenjärjestäytymistä. Tulokset lisäävät tietämystä parvovirusten infektiomekanismeista ja tuman käyttäytymisestä stressitilanteessa.

Väitöskirjan tulokset osoittavat, että vuorovaikutukset isännän tumakuljetus- ja kromatinisaatiokoneiston kanssa ovat elintärkeitä viruksen lisääntymiselle. Lisäksi osatöissä tutkittujen tuman rakenteiden ja niiden muutosten tiedetään osallistuvan tuman ja soluliman väliseen signaalin välitykseen sekä kromatiinin järjestäytyneisyyteen. Täten parvoviruksen aiheuttamien tuman rakennemuutosten voidaan myös ajatella liittyvän isäntäsolun infektion seurauksena muuttuneeseen geneettiseen säätelyyn ja toimintaan.

REFERENCES

Abràmoff M.D., Magalhães P.J. & Ram S.J. 2004. Image processing with ImageJ. *Biophotonics Int* 11 (7): 36 – 42.

Adam S. A. 2001. The nuclear pore complex. *Genome Biol* 2 (9), reviews0007.1–reviews0007.6.

Adam S.A. & Geracet L. Cytosolic proteins that specifically bind nuclear location signals are receptors for nuclear import. *Cell* 66: 837–847.

Adeyemi R. O. & Pintel D. J. 2014. Parvovirus-induced depletion of cyclin B1 prevents mitotic entry of infected cells. *PLoS Pathog* 10(1), e1003891.

Agbandje M. & Chapman M.S. 2006. Correlating structure with function in the viral capsid. Teoksessa: Kerr J., Cotmore S.F., Bloom M.E., Linden R.M. & Parrish C.R. (toim.), *Parvoviruses*, s. 125–139.

Akhtar A. & Gasser S.M. 2007. The nuclear envelope and transcriptional control. *Nat Rev Genet* 8: 507–517.

Alberts B., Johnson A., Lewis J., Raff M., Roberts K. & Walter P. 2002. Molecular biology of the cell. 4th edition. New York, Garland Science.

Alexander J. M. & Lomvardas S. 2014. Nuclear Architecture as an Epigenetic Regulator of Neural Development and Function. *Neuroscience* 264: 39–50.

Allison A.B., Kohler D.J., Ortega A., Hoover E.A., Grove D.M., Holmes E.C. & Parrish C.R. 2014. Host-Specific Parvovirus Evolution in Nature Is Recapitulated by *In Vitro* Adaptation to Different Carnivore Species. *PLoS Pathog* 10: e1004475.

Antonin W., Ellenberg J. & Dultz E. 2008. Nuclear pore complex assembly through the cell cycle: Regulation and membrane organization. *FEBS Lett* 582: 2004–2016.

Arhel N.J., Souquere-Besse S., Munier S., Souque P., Guadagnini S., Rutherford S., Prévost M., Allen T.D. & Charneau P. 2007. HIV-1 DNA Flap formation promotes uncoating of the pre-integration complex at the nuclear pore. *EMBO J* 26: 3025–3037.

Ashida H., Mimuro H., Ogawa M., Kobayashi T., Sanada T., Kim M. & Sasakawa C. 2011. Cell death and infection: A double-edged sword for host and pathogen survival. *J Cell Biol* 195: 931–942.

Aydin I. & Schelhaas M. 2016. Viral genome tethering to host cell chromatin: cause and consequences. *Traffic* 17(4): 327–340.

Aydin I., Weber S., Snijder B., Samperio Ventayol P., Kühbacher A., Becker M., Day P. M., Schiller J. T., Kann M., Pelkmans L., Helenius A. & Schelhaas M. 2014. Large scale RNAi reveals the requirement of nuclear envelope breakdown for nuclear import of human papillomaviruses. *PLoS Pathog* 10 (5), e1004162.

Bálint Š., Verdeny Vilanova I., Sandoval Álvarez Á. & Lakadamyali M. 2013. Correlative live-cell and superresolution microscopy reveals cargo transport dynamics at microtubule intersections. *Proc Natl Acad Sci USA* 110: 3375–3380.

Ball L. 2007. Viral replication strategies. In: Knipe D.M. & Howley P.M. (eds.), *Fields Virology*, 5th edition, Lippincott Williams & Wilkins, PA, USA, s. 119–139.

Bandyopadhyay D., Cyphersmith A., Zapata J.A., Kim Y.J. & Payne C.K. 2014. Lysosome Transport as a Function of Lysosome Diameter. *PLoS ONE* 9: e86847.

Barichievy S., Naidoo J. & Mhlanga M. 2015. Non-coding RNAs and HIV: viral manipulation of host dark matter to shape the cellular environment. *Front Gen* 6(108).

Bashir T., Hörlein R., Rommelaere J. & Willwand K. 2000. Cyclin A activates the DNA polymerase delta-dependent elongation machinery in vitro: A parvovirus DNA replication model. *Proc Natl Acad Sci USA* 97: 5522–5527.

Ben-Asher E., Bratosin S. & Aloni Y. 1982. Intracellular DNA of the parvovirus minute virus of mice is organized in a minichromosome structure. *J Virol* 41: 1044–1054.

Bernad R., van der Velde H., Fornerod M. & Pickersgill H. 2004. Nup358/RanBP2 Attaches to the Nuclear Pore Complex via Association with Nup88 and Nup214/CAN and Plays a Supporting Role in CRM1-Mediated Nuclear Protein Export. *Mol Cell Biol* 24: 2373–2384.

Biamonti G. & Vourc´h C. 2010. Nuclear Stress Bodies. Cold Spring Harb Perspect Biol 2 (6), a000695.

Bianchi A. & Lanzuolo C. 2015. Into the chromatin world: Role of nuclear architecture in epigenome regulation. *AIMS Biophys* 2 (4): 585–612.

Bloom D. C., Giordani N. V. & Kwiatkowski D. L. 2010. Epigenetic regulation of latent HSV-1 gene expression. *Biochim Biophys Acta* 1799 (3-4): 246–256.

Boisvert M., Bouchard-Levesque V., Fernandes S. & Tijssen P. 2014. Classic nuclear localization signals and a novel nuclear localization motif are required for nuclear transport of porcine parvovirus capsid proteins. *J Virol* 88.

Bosse J.B., Hogue I.B., Feric M., Thiberge S.Y., Sodeik B., Brangwynne C.P. & Enquist L.W. 2015. Remodeling nuclear architecture allows efficient transport of herpesvirus capsids by diffusion. *Proc Natl Acad Sci USA* 112: E5725–E5733.

Bouwman B. A. M. & de Laat W. 2015. Getting the genome in shape: the formation of loops, domains and compartments. *Genome Biol* 16 (1): 1–9.

Breuer M. & Ohkura H. 2015. A negative loop within the nuclear pore complex controls global chromatin organization. *Genes & Development* 29: 1789–1794.

Briggs J. A. G., Wilk T., Welker R., Kräusslich H. & Fuller S. D. 2003. Structural organization of authentic, mature HIV-1 virions and cores. *EMBO J* 22 (7): 1707–1715.

Brohawn S.G., Partridge J.R., Whittle J.R.R. & Schwartz T.U. 2009. The Nuclear Pore Complex has entered the Atomic Age. *Structure* 17(9):1156–68 .

Burke B. & Stewart C.L. 2013. The nuclear lamins: flexibility in function. *Nat Rev Mol Cell Biol* 14: 13–24.

Bär S., Daeffler L., Rommelaere J. & Nüesch J.P.F. 2008. Vesicular Egress of Non-Enveloped Lytic Parvoviruses Depends on Gelsolin Functioning. *PLoS Pathog* 4: e1000126.

Cain N.E. & Starr D.A. 2015. SUN proteins and nuclear envelope spacing. *Nucleus* 6(1): 2–7.

Cain N.E., Tapley E.C., McDonald K.L., Cain B.M. & Starr D.A. 2014. The SUN protein UNC-84 is required only in force-bearing cells to maintain nuclear envelope architecture. *J Cell Biol* 206: 163–172.

Capelson M., Liang Y., Schulte R., Mair W., Wagner U. & Hetzer M.W. 2010. Chromatin-bound nuclear pore components regulate gene expression in higher eukaryotes. *Cell* 140(3):372–83.

Cardarelli F., Lanzano L. & Gratton E. 2012. Capturing directed molecular motion in the nuclear pore complex of live cells. *Proc Natl Acad Sci USA* 109: 9863–9868.

Carmo-Fonseca M., Berciano M. T. & Lafarga M. 2010. Orphan nuclear bodies. Cold Spring Harb Perspect Biol 2 (9), a000703.

Casey A.K., Chen S., Novick P., Ferro-Novick S. & Wente S.R. 2015. Nuclear pore complex integrity requires Lnp1, a regulator of cortical endoplasmic reticulum. *Mol Biol Cell* 26: 2833–2844.

Caviston J.P. & Holzbaur E.L.F. 2006. Microtubule motors at the intersection of trafficking and transport. *Trends Cell Biol* 16: 530–537.

Chang C., Lee C., Su M., Tsai C. & Chen M. 2015. BGLF4 Kinase Modulates the Structure and Transport Preference of the Nuclear Pore Complex To Facilitate Nuclear Import of Epstein-Barr Virus Lytic Proteins. *J Virol* 89: 1703–1718.

Chang W., Worman H.J. & Gundersen G.G. 2015a. Accessorizing and anchoring the LINC complex for multifunctionality. *J Cell Biol* 208: 11–22.

Chang W., Antoku S., Ã–stlund C., Worman H.J. & Gundersen G.G. 2015b. Linker of nucleoskeleton and cytoskeleton (LINC) complex-mediated actin-dependent nuclear positioning orients centrosomes in migrating myoblasts. *Nucleus* 6: 77–88.

Chapman M.S. & Agbandje-McKenna M. 2006. Atomic structure of viral particles. In: Kerr J., Cotmore S.F., Bloom M.E., Linden M.R. & Parrish C.R. (eds.), *Parvoviruses*, s. 107–123.

Chaurushiya M.S. & Weitzman M.D. 2009. Viral manipulation of DNA repair and cell cycle checkpoints. *DNA repair* 8: 1166–1176.

Chen A. Y. & Qiu J. 2010. Parvovirus infection-induced cell death and cell cycle arrest. *Future Virol* 5 (6): 731–743.

Christensen J., Cotmore S.F. & Tattersall P. 1997. A novel cellular site-specific DNA-binding protein cooperates with the viral NS1 polypeptide to initiate parvovirus DNA replication. *J Virol* 71: 1405–1416.

Christensen J., Cotmore S.F. & Tattersall P. 1995. Minute virus of mice transcriptional activator protein NS1 binds directly to the transactivation region of the viral P38 promoter in a strictly ATP-dependent manner. *J Virol* 69: 5422–5430.

Christensen J. & Tattersall P. 2002. Parvovirus initiator protein NS1 and RPA coordinate replication fork progression in a reconstituted DNA replication system. *J Virol* 76: 6518–6531.

Ciabrelli F. & Cavalli G. 2015. Chromatin-driven behavior of topologically associating domains. *J Mol Biol* 427 (3): 608–625.

Cibulka J., Fraiberk M. & Forstova J. 2012. Nuclear actin and lamins in viral infections. *Viruses* 4: 325–347.

Cingolani G., Bednenko J., Gillespie M.T. & Gerace L. 2002. Molecularb for the recognition of a nonclassical nuclear localization signal by importin β. *Mol Cell* 10: 1345–1353.

Clemens K.E. & Pintel D.J. 1988. The two transcription units of the autonomous parvovirus minute virus of mice are transcribed in a temporal order. *J Virol* 62: 1448–1451.

Cohen S., Etingov I. & Panté N. 2012. Effect of viral infection on the nuclear envelope and nuclear pore complex. *Int Rev Cell Mol Biol* 299: 117–159.

Cohen S., Au S. & Panté N. 2011. How viruses access the nucleus. *Biochim Biophys Acta* 1813: 1634–1645.

Cohen S., Marr A.K., Garcin P. & Panté N. 2011. Nuclear envelope disruption involving host caspases plays a role in the parvovirus replication cycle. *J Virol* 85: 4863–4874.

Coleman H. M., Connor V., Cheng Z. S. C., Grey F., Preston C. M. & Efstathiou S. 2008. Histone modifications associated with herpes simplex virus type 1 genomes during quiescence and following ICP0-mediated de-repression. *J Gen Virol* 89: 68–77.

Collepardo-Guevara R., Portella G., Vendruscolo M., Frenkel D., Schlick T. & Orozco M. 2015. Chromatin Unfolding by Epigenetic Modifications Explained by Dramatic Impairment of Internucleosome Interactions: A Multiscale Computational Study. *J Am Chem Soc* 137: 10205–10215.

Cotmore S.F. & Tattersall P. 2006. A rolling-hairpin strategy: basic mechanisms of DNA replication in the parvoviruses. In: Kerr J.R., Cotmore S.F., Bloom M.E., Linden R.M. & Parrish C.R. (eds.), *Parvoviruses*, s. 171–188.

Cotmore S.F. & Tattersall P. 1989. A genome-linked copy of the NS-1 polypeptide is located on the outside of infectious parvovirus particles. *J Virol* 63: 3902–3911.

Cotmore S.F., Agbandje-McKenna M., Chiorini J.A., Mukha D.V., Pintel D.J. & Qiu J. 2014. The family Parvoviridae. *Arch Virol* 159(5): 1239–47.

Cotmore S.F. & Tattersall P. 2013. Parvovirus Diversity and DNA Damage Responses. *Cold Spring Harbor Perspect Biol* 5(2). pii: a012989.

Cotmore S.F. & Tattersall P. 1998. High-mobility group 1/2 proteins are essential for initiating rolling-circle-type DNA replication at a parvovirus hairpin origin. *J Virol* 72: 8477–8484.

Cotmore S.F., Gottlieb R.L. & Tattersall P. 2007. Replication initiator protein NS1 of the parvovirus minute virus of mice binds to modular divergent sites distributed throughout duplex viral DNA. *J Virol* 81: 13015–13027.

Cotmore S.F., Christensen J. & Tattersall P. 2000. Two widely spaced initiator binding sites create an HMG1–dependent parvovirus rolling–hairpin replication origin. *J Virol* 74: 1332–1341.

Cotmore S.F., D'abramo Jr. A.M., Carbonell L.F., Bratton J. & Tattersall P. 1997. The NS2 polypeptide of parvovirus MVM is required for capsid assembly in murine cells. *Virology* 231: 267–280.

Crisp M., Liu Q., Roux K., Rattner J.B., Shanahan C., Burke B., Stahl P.D. & Hodzic D. 2006. Coupling of the nucleus and cytoplasm: role of the LINC complex. *J Cell Biol* 172: 41–53.

Daigle N., Beaudouin J., Hartnell L., Imreh G., Hallberg E., Lippincott-Schwartz J. & Ellenberg J. 2001. Nuclear pore complexes form immobile networks and have a very low turnover in live mammalian cells. *J Cell Biol* 154: 71–84.

D'Angelo M.A., Anderson D.J., Richard E. & Hetzer M.W. 2006. Nuclear pores form de novo from both sides of the nuclear envelope. *Science* 312: 440–443.

D'Angelo M., Gomez-Cavazos J., Mei A., Lackner D. & Hetzer M. 2012. A change in nuclear pore complex composition regulates cell differentiation. *Dev Cell* 22: 446–458.

Dawson T.R., Lazarus M.D., Hetzer M.W. & Wente S.R. 2009. ER membrane-bending proteins are necessary for de novo nuclear pore formation. *J Cell Biol* 184: 659–675.

Decaro N. & Buonavoglia C. 2012. Canine parvovirus - A review of epidemiological and diagnostic aspects, with emphasis on type 2c. *Vet Microbiol* 155 (1): 1–12.

Dechat T., Adam S.A., Taimen P., Shimi T. & Goldman R.D. 2010. Nuclear Lamins. *Cold Spring Harb Perspect Biol* 2(11): a000547.

Dekker, J. 2014. Two ways to fold the genome during the cell cycle: insights obtained with chromosome conformation capture. *Epigenet Chromatin* 7:25.

Dembowski J.A. & DeLuca N.A. 2015. Selective Recruitment of Nuclear Factors to Productively Replicating Herpes Simplex Virus Genomes. *PLoS Pathog* 11: e1004939.

Duechting A., Tschöpe C., Kaiser H., Lamkemeyer T., Tanaka N., Aberle S., Lang F., Torresi J., Kandolf R. & Bock C. 2008. Human parvovirus B19 NS1 protein modulates inflammatory signaling by activation of STAT3/PIAS3 in human endothelial cells. *J Virol* 82 (16): 7942–7952.

Digman M.A., Dalal R., Horwitz A.F., Gratton E. 2008. Mapping the number of molecules and brightness in the laser scanning microscope. *Biophys J* 94: 2320–2332.

Digman M.A., Gratton E. 2009. Imaging barriers to diffusion by pair correlation functions. *Biophys J* 97: 665–673.

Diner B.A., Lum K.K. & Cristea I.M. 2015. The Emerging Role of Nuclear Viral DNA Sensors. *J Biol Chem* 290: 26412–26421.

Dittmer T.A. & Misteli T. 2011. The lamin protein family. *Genome Biol* 12: 222–222.

Du T., Zhou G., Khan S., Gu H. & Roizman B. 2010. Disruption of HDAC/CoREST/REST repressor by dnREST reduces genome silencing and increases virulence of herpes simplex virus. *Proc Natl Acad Sci* 107 (36):15904–15909.

Dultz E. & Ellenberg J. 2010. Live imaging of single nuclear pores reveals unique assembly kinetics and mechanism in interphase. *J Cell Biol* 191: 15–22.

Dundr M. & Misteli T. 2010. Biogenesis of nuclear bodies. *Cold Spring Harb Perspect Biol* 2(12): a000711.

Eichwald V., Daeffler L., Klein M., Rommelaere J. & Salomé N. 2002. The NS2 proteins of parvovirus minute virus of mice are required for efficient nuclear egress of progeny virions in mouse cells. *J Virol* 76: 10307–10319.

Elton D., Simpson-Holley M., Archer K., Medcalf L., Hallam R., McCauley J. & Digard P. 2001. Interaction of the influenza virus nucleoprotein with the cellular CRM1-mediated nuclear export pathway. *J Virol* 75: 408–419.

Engelsma D., Valle N., Fish A., Salomé N., Almendral J.M. & Fornerod M. 2008. A supraphysiological nuclear export signal is required for parvovirus nuclear export. *Mol Biol Cell* 19: 2544–2552.

Everett R.D. 2013. The spatial organization of DNA virus genomes in the nucleus. *PLoS Pathog* 9: e1003386.

Fahrenkrog B., Köser J. & Aebi U. 2004. The nuclear pore complex: a jack of all trades? *Trends Biochem Sci* 29: 175–182.

Fang C.Y., Shen C.H., Wang M., Chen P.L., Chan M.W., Hsu P.H. & Chang D. 2015. Global profiling of histone modifications in the polyomavirus BK virion minichromosome. *Virology* 483: 1–12.

Farr G.A., Zhang L.G. & Tattersall P. 2005. Parvoviral virions deploy a capsid-tethered lipolytic enzyme to breach the endosomal membrane during cell entry. *PNAS* 102(47):17148–17153.

Fay N. & Panté N. 2015. Nuclear entry of DNA viruses. *Front Microbiol* 6(467): 1–16.

Felton-Edkins Z.A., Kondrashov A., Karali D., Fairley J.A., Dawson C.W., Arrand J.R., Young L.S. & White R.J. 2006. Epstein-barr virus induces cellular transcription factors to allow active expression of EBER genes by RNA polymerase III. *J Biol Chem* 281: 33871–33880.

Ferrando-May E. 2005. Nucleocytoplasmic transport in apoptosis. *Cell Death Differ* 12: 1263–1276.

Ferrando-May E., Cordes V., Biller–Ckovric I., Mirkovic J., Görlich D. & Nicotera P. 2001. Caspases mediate nucleoporin cleavage, but not early redistribution of nuclear transport factors and modulation of nuclear permeability in apoptosis. *Cell Death Differ* 8(5): 495–505.

Fichtman B., Ramos C., Rasala B., Harel A. & Forbes D.J. 2010. Inner/outer nuclear membrane fusion in nuclear pore assembly: biochemical demonstration and molecular analysis. *Mol Biol Cell* 21: 4197–4211.

Finlan L.E., Sproul D., Thomson I., Boyle S., Kerr E., Perry P., Ylstra B., Chubb J.R. & Bickmore W.A. 2008. Recruitment to the nuclear periphery can alter expression of genes in human cells. *PLoS Genet* 4: e1000039.

Fiserova J. & Goldberg M. 2010. Relationships at the nuclear envelope: lamins and nuclear pore complexes in animals and plants. *Biochem Soc Trans* 38 (3): 829–831.

Flatt J.W. & Greber U.F. 2015. Misdelivery at the nuclear pore complex - stopping a virus dead in its tracks. *Cells* 4: 277–296.

Fortes P., Beloso A. & Ortín J. 1994. Influenza virus NS1 protein inhibits pre-mRNA splicing and blocks mRNA nucleocytoplasmic transport. *EMBO J* 13: 704–712.

Fried H. & Kutay U. 2003. Nucleocytoplasmic transport: taking an inventory. *Cell Mol Life Sci* 60: 1659–1688.

Fu S., Imai K. & Horton P. 2011. Prediction of leucine-rich nuclear export signal containing proteins with NESsential. *Nucleic Acids Res* 39: e111–e111.

Ghosh M.K. & Harter M.L. 2003. A Viral Mechanism for remodeling chromatin structure in G0 cells. *Mol Cell* 12: 255–260.

Giberson A.N., Davidson A.R. & Parks R.J. 2011. Chromatin structure of adenovirus DNA throughout infection. *Nucleic Acids Res* 40: 2369–2376.

Gil–Ranedo J., Hernando E., Riolobos L., Domínguez C., Kann M. & Almendral J.M. 2015. The mammalian cell cycle regulates parvovirus nuclear capsid assembly. *PLoS Pathog* 11: e1004920.

Goldman R. D., Gruenbaum Y., Moir R. D., Shumaker D. K. & Spann T. P. 2002. Nuclear lamins: building blocks of nuclear architecture. *Genes Dev* 16 (5): 533–547.

Goldstein R.E. & van de Meent. 2015. A physical perspective on cytoplasmic streaming. *Interface Focus* 5: 20150030.

Gomez-Cavazos J.S. & Hetzer M.W. 2015. The nucleoporin gp210/Nup210 controls muscle differentiation by regulating nuclear envelope/ER homeostasis. *J Cell Biol*208: 671–681.

Goryaynov A. & Yang W. 2014. Role of molecular charge in nucleocytoplasmic transport. *PLoS ONE* 9: e88792.

Goubau D., Rehwinkel J. & Reis e.S. 2010. PYHIN proteins: center stage in DNA sensing. *Nat Immunol* 11: 984–986.

Grewal S.I.S. & Jia S. 2007. Heterochromatin revisited. *Nat Rev Genet* 8: 35–46.

Grossman E., Medalia O. & Zwerger M. 2012. Functional architecture of the nuclear pore complex. *Annu Rev Biophys* 41: 557–584.

Grove J. & Marsh M. 2011. The cell biology of receptor–mediated virus entry. *J Cell Biol*195: 1071–1082.

Greber U.F. & Fornerod M. 2004. Nuclear Import in Viral Infections. In: Marsh M. (ed.), *Membrane Trafficking in Viral Replication*, Springer Berlin Heidelberg, Berlin, Heidelberg, s. 109–138.

Gruenbaum Y. & Medalia O. 2015. Lamins: the structure and protein complexes. *Curr Opin Cell Biol* 32: 7–12.

Gruenbaum Y., Margalit A., Goldman R.D., Shumaker D.K. & Wilson K.L. 2005. The nuclear lamina comes of age. *Nat Rev Mol Cell Biol* 6: 21–31.

Gu H. & Zheng Y. 2016. Role of ND10 nuclear bodies in the chromatin repression of HSV–1. *Virol J* 13(1): 1–8.

Guelen L., Pagie L., Brasset E., Meuleman W., Faza M. B., Talhout W., Eussen B. H., de Klein A., Wessels L., de Laat W. & van Steensel B. 2008. Domain organization of human chromosomes revealed by mapping of nuclear lamina interactions. *Nature* 453(7197): 948–951.

Guetg C. & Santoro R. 2012. Formation of nuclear heterochromatin: The nucleolar point of view. *Epigenetics* 7 (8): 811–814.

Guise A.J., Budayeva H.G., Diner B.A. & Cristea I.M. 2013. Histone deacetylases in herpesvirus replication and virus–stimulated host defense. *Viruses* 5: 1607–1632.

Guo Y. & Zheng Y. 2015. Lamins position the nuclear pores and centrosomes by modulating dynein. *Mol Biol Cell* 26: 3379–3389.

Guo Y., Kim Y., Shimi T., Goldman R.D. & Zheng Y. 2014. Concentration-dependent lamin assembly and its roles in the localization of other nuclear proteins. *Mol Biol Cell* 25: 1287–1297.

Gustin K.E. & Sarnow P. 2002. Inhibition of nuclear import and alteration of nuclear pore complex composition by rhinovirus. *J Virol* 76: 8787–8796.

Güttinger S., Laurell E. & Kutay U. 2009. Orchestrating nuclear envelope disassembly and reassembly during mitosis. *Nat Rev Mol Cell Biol* 10: 178–191.

Görlich D. & Kutay U. 1999. Transport between the cell nucleus and the cytoplasm. *Annu Rev Cell Dev Biol* 15: 607–60.

Görlich D., Kostka S., Kraft R., Dingwall C., Laskey R.A., Hartmann E. & Prehn S. 1995. Two different subunits of importin cooperate to recognize nuclear localization signals and bind them to the nuclear envelope. *Current Biology* 5: 383–392.

Hamid F.B., Kim J. & Shin C. 2016. Cellular and viral determinants of retroviral nuclear entry. *Can J Microbiol* 62: 1–15.

Hancock M.H., Cliffe A.R., Knipe D.M. & Smiley J.R. 2010. Herpes simplex virus VP16, but not ICP0, is required to reduce histone occupancy and enhance histone acetylation on viral genomes in U2OS osteosarcoma cells. *J Virol* 84: 1366–1375.

Hancock R. 2004. Internal organisation of the nucleus: assembly of compartments by macromolecular crowding and the nuclear matrix model. *Biol Cell* 96: 595–601.

Hansen J., Qing K. & Srivastava A. 2001. Infection of Purified Nuclei by Adeno-associated Virus 2. *Mol Ther* 4: 289–296.

Hanson N.D. & Rhode S.L. 1991. Parvovirus NS1 stimulates P4 expression by interaction with the terminal repeats and through DNA amplification. *J Virol* 65: 4325–4333.

Harsha Raj M., Yashaswini B., Rössler J. & Salimath B. P. 2016. Combinatorial treatment with anacardic acid followed by TRAIL augments induction of apoptosis in TRAIL resistant cancer cells by the regulation of p53, MAPK and NFκβ pathways. *Apoptosis* 21(5):578–593.

Harel A. & Forbes D.J. 2004. Importin beta: conducting a much larger cellular symphony. *Mol Cell* 16: 319–330.

Hawryluk–Gara L., Shibuya E.K. & Wozniak R.W. 2005. Vertebrate Nup53 interacts with the nuclear lamina and is required for the assembly of a Nup93–containing complex. *Mol Biol Cell* 16: 2382–2394.

Her L., Lund E. & Dahlberg J.E. 1997. Inhibition of ran guanosine triphosphatase–dependent nuclear transport by the matrix protein of vesicular stomatitis virus. *Science* 276: 1845–1848.

Herbein G. & Wendling D. 2010. Histone deacetylases in viral infections. *Clin Epigenetics* 1: 13–24.

Hetzer M.W. 2010. The Nuclear Envelope. *Cold Spring Harbor Perspect Biol* 2: a000539.

Hetzer M.W., Walther T.C. & Mattaj I.W. 2005. Pushing the envelope: structure, function, and dynamics of the nuclear periphery. *Annu Rev Cell Dev Biol* 21: 347–380.

Hindley C.E., Lawrence F.J. & Matthews D.A. 2007. A Role for transportin in the nuclear import of adenovirus core proteins and DNA. *Traffic* 8: 1313–1322.

Ho C.Y. & Lammerding J. 2012. Lamins at a glance. *J Cell Sci* 125: 2087–2093.

Holoch D. & Moazed D. 2015. RNA-mediated epigenetic regulation of gene expression. *Nat Rev Genet* 16 (2): 71–84.

Hoyt C.C., Bouchard R.J. & Tyler K.L. 2004. Novel nuclear herniations induced by nuclear localization of a viral protein. *J Virol* 78: 6360–6369.

Huang J., Kent J.R., Placek B., Whelan K.A., Hollow C.M., Zeng P., Fraser N.W. & Berger S.L. 2006. Trimethylation of histone H3 lysine 4 by Set1 in the lytic infection of human herpes simplex virus 1. *J Virol* 80: 5740–5746.

Huotari J. & Helenius A. 2011. Endosome maturation. *EMBO J* 30: 3481–3500.

Hutchison C.J. 2002. Lamins: building blocks or regulators of gene expression? *Nat Rev Mol Cell Biol* 3: 848–858.

Hutten S. & Kehlenbach R.H. 2007. CRM1-mediated nuclear export: to the pore and beyond. *Trends Cell Biol* 17: 193–201.

Hülsmann B., Labokha A. & Görlich D. 2012. The permeability of reconstituted nuclear pores provides direct evidence for the selective phase model. *Cell* 150: 738–751.

Ihalainen T.O., Aires L., Herzog F.A., Schwartlander R., Moeller J. & Vogel V. 2015. Differential basal-to-apical accessibility of lamin A/C epitopes in the nuclear lamina regulated by changes in cytoskeletal tension. *Nat Mater* 14: 1252–1261.

Ihalainen T.O., Niskanen E.A., Jylhävä J., Paloheimo O., Dross N., Smolander H., Langowski J., Timonen J. & Vihinen-Ranta M. 2009. Parvovirus induced alterations in nuclear architecture and dynamics. *PLoS ONE* 4: e5948.

Ihalainen T.O., Niskanen E.A., Jylhävä J., Turpeinen T., Rinne J., Timonen J. & Vihinen–Ranta M. 2007. Dynamics and interactions of parvoviral NS1 protein in the nucleus. *Cell Microbiol* 9: 1946–1959.

Ihalainen T.O., Willman S.F., Niskanen E.A., Paloheimo O., Smolander H., Laurila J.P., Kaikkonen M.U. & Vihinen-Ranta M. 2012. Distribution and dynamics of transcription–associated proteins during parvovirus infection. *J Virol* 86: 13779–13784.

Ioudinkova E., Arcangeletti M.C., Rynditch A., De Conto F., Motta F., Covan S., Pinardi F., Razin S.V. & Chezzi C. 2006. Control of human cytomegalovirus gene expression by differential histone modifications during lytic and latent infection of a monocytic cell line. *Gene* 384: 120–128.

Iseki H., Shimizukawa R., Sugiyama F., Kunita S., Iwama A., Onodera M., Nakauchi H. & Yagami K. 2005. Parvovirus nonstructural proteins induce an epigenetic modification through histone acetylation in host genes and revert tumor malignancy to benignancy. *J Virol* 79: 8886–8893.

Izaurralde E., Kutay U., von Kobbe C., Mattaj I.W. & Görlich D. 1997. The asymmetric distribution of the constituents of the Ran system is essential for transport into and out of the nucleus. *EMBO J* 16: 6535–6547.

Jang S.H., Byun J.K., Jeon W., Choi S.Y., Park J., Lee B.H., Yang J.E., Park J.B., O'Grady S.M., Kim D., Ryu P.D., Joo S. & Lee S.Y. 2015. Nuclear localization and functional characteristics of voltage-gated potassium channel Kv1.3. *J Biol Chem* 290: 12547–12557.

Ji J.Y., Lee R.T., Vergnes L., Fong L.G., Stewart C.L., Reue K., Young S.G., Zhang Q., Shanahan C.M. & Lammerding J. 2007. Cell nuclei spin in the absence of lamin B1. *J Biol Chem* 282: 20015–20026.

Johnson D.C. & Baines J.D. 2011. Herpesviruses remodel host membranes for virus egress. *Nat Rev Micro* 9: 382–394.

Johnson K.E., Bottero V., Flaherty S., Dutta S., Singh V.V. & Chandran B. 2014. IFI16 restricts HSV-1 replication by accumulating on the HSV-1 genome, repressing HSV-1 gene expression, and directly or indirectly modulating histone modifications. *PLoS Pathogens* 10: e1004503.

Kabachinski G. & Schwartz T. U. 2015. The nuclear pore complex - structure and function at a glance. *J Cell Sci* 128 (3): 423–429.

Kalamvoki M. & Roizman B. 2010. Circadian CLOCK histone acetyl transferase localizes at ND10 nuclear bodies and enables herpes simplex virus gene expression. *Proc Natl Acad Sci* 107: 17721–17726.

Kalverda B., Röling M.D. & Fornerod M. 2008. Chromatin organization in relation to the nuclear periphery. *FEBS Lett* 582: 2017–2022.

Kelich J.M., Ma J., Dong B., Wang Q., Chin M., Magura C.M., Xiao W. & Yang W. 2015. Super-resolution imaging of nuclear import of adeno-associated virus in live cells. *Mol Ther Methods Clin Dev* 2: 15047.

Kent J. R., Zeng P., Atanasiu D., Gardner J., Fraser N. W. & Berger S. L. 2004. During lytic infection herpes simplex virus type 1 is associated with histones bearing modifications that correlate with active transcription. *J Virol* 78 (18): 10178–10186.

Kim D. & Wirtz D. 2015. Cytoskeletal tension induces the polarized architecture of the nucleus. *Biomaterials* 48: 161–172.

Knipe D.M. 2015. Nuclear sensing of viral DNA, epigenetic regulation of herpes simplex virus infection, and innate immunity. *Virology* 479–480: 153–159.

Kobiler O., Drayman N., Butin–Israeli V. & Oppenheim A. 2012. Virus strategies for passing the nuclear envelope barrier. *Nucleus* 3: 526–539.

Komatsu T. & Nagata K. 2012. Replication-Uncoupled Histone Deposition during Adenovirus DNA Replication. *J Virol* 86: 6701–6711.

Komatsu T., Haruki H. & Nagata K. 2011. Cellular and viral chromatin proteins are positive factors in the regulation of adenovirus gene expression. *Nucleic Acids Res* 39: 889–901.

Korfali N., Wilkie G.S., Swanson S.K., Srsen V., de l.H., Batrakou D.G., Malik P., Zuleger N., Kerr A.R.W., Florens L. & Schirmer E.C. 2012. The nuclear envelope proteome differs notably between tissues. *Nucleus* 3: 552–564.

Köster S., Weitz D.A., Goldman R.D., Aebi U. & Herrmann H. 2015. Intermediate filament mechanics in vitro and in the cell: from coiled coils to filaments, fibers and networks. *Curr Opin Cell Biol* 32: 82–91.

Kouzarides T. 2007. Chromatin modifications and their function. *Cell* 128: 693–705, doi:10.1016/j.cell.2007.02.005.

Kuss S.K., Mata M.A., Zhang L. & Fontoura B.M.A. 2013. Nuclear imprisonment: viral strategies to arrest host mRNA nuclear export. *Viruses* 5: 1824–1849.

Kuznetsov Y. G., Victoria J. G., Robinson W. E. & McPherson A. 2003. Atomic force microscopy investigation of human immunodeficiency virus (HIV) and HIV–infected lymphocytes. *J Virol* 77(22): 11896–11909.

Lallemand-Breitenbach V. & de Thé H. 2010. PML Nuclear Bodies. *Cold Spring Harb Perspect Biol* 2(5): a000661.

Lammerding J., Schulze P.C., Takahashi T., Kozlov S., Sullivan T., Kamm R.D., Stewart C.L. & Lee R.T. 2004. Lamin A/C deficiency causes defective nuclear mechanics and mechanotransduction. *J Clin Invest* 113: 370–378.

Lange A., Mills R.E., Lange C.J., Stewart M., Devine S.E. & Corbett A.H. 2007. Classical nuclear localization signals: definition, function, and interaction with importin alpha. *J Biol Chem* 282: 5101–5105.

Le Sage V. & Mouland A.J. 2013. Viral subversion of the nuclear pore complex. *Viruses* 5: 2019–2042.

Leach N., Bjerke S.L., Christensen D.K., Bouchard J.M., Mou F., Park R., Baines J., Haraguchi T. & Roller R.J. 2007. Emerin is hyperphosphorylated and redistributed in herpes simplex virus type 1-infected cells in a manner dependent on both UL34 and US3. *J Virol* 81: 10792–10803.

Lee C., Huang Y., Lin S., Chang Y., Chang Y., Takada K. & Chen M. 2008. Epstein-barr virus BGLF4 kinase induces disassembly of the nuclear lamina to facilitate virion production. *J Virol* 82: 11913–11926.

Lee J.S.H., Hale C.M., Panorchan P., Khatau S.B., George J.P., Tseng Y., Stewart C.L., Hodzic D. & Wirtz D. 2007. Nuclear lamin A/C deficiency induces defects in cell mechanics, polarization, and migration. *Biophys J* 93: 2542–2552.

Lee J. T. 2012. Epigenetic regulation by long noncoding RNAs. *Science* 338(6113): 1435–1439.

Li H.P., LEU Y.W. & Chang Y.S. 2005. Epigenetic changes in virus–associated human cancers. *Cell Res* 15: 262–271.

Li J., Bonifati S., Hristov G., Marttila T., Valmary–Degano S., Stanzel S., Schnölzer M., Mougin C., Aprahamian M., Grekova S. P., Raykov Z., Rommelaere J. & Marchini A. 2013. Synergistic combination of valproic acid and oncolytic parvovirus H–1 PV as a potential therapy against cervical and pancreatic carcinomas. *EMBO Mol Med* 5 (10): 1537–1555.

Liang Y. & Hetzer M.W. 2011. Functional interactions between nucleoporins and chromatin. *Curr Opin Cell Biol* 23: 65–70.

Lieberman P.M. 2006. Chromatin regulation of virus infection. *Trends Microbiol* 14: 132–140.

Linden R.M., Ward P., Giraud C., Winocour E. & Berns K.I. 1996. Site-specific integration by adeno-associated virus. *Proc Natl Acad Sci USA* 93: 11288–11294.

Lombardo E., Ramirez J.C., Agbandje–McKenna M. & Almendral J.M. 2000. A beta–stranded motif drives capsid protein oligomers of the parvovirus minute virus of mice into the nucleus for viral assembly. *J Virol* 74(8):3804–14.

Lombardo E., Ramírez J.,C., Garcia J. & Almendral J.M. 2002. Complementary roles of multiple nuclear targeting signals in the capsid proteins of the parvovirus minute virus of mice during assembly and onset of infection. *J Virol* 76: 7049–7059.

Lord C.L., Timney B.L., Rout M.P. & Wente S.R. 2015. Altering nuclear pore complex function impacts longevity and mitochondrial function in S. cerevisiae. *J Cell Biol* 208: 729–744.

Lorson, C., Pearson, J., Burger, L. & Pintel, D. J. 1998. An SP1–binding site and TATA element are sufficient to support full transactivation by proximally bound NS1 protein of minute virus of mice. *Virology* 240(2): 326–337.

Lorson C., Burger L.R., Mouw M. & Pintel D.J. 1996. Efficient transactivation of the minute virus of mice P38 promoter requires upstream binding of NS1. *J Virol* 70: 834–842.

Lott K. & Cingolani G. 2010. The importin β binding domain as a master regulator of nucleocytoplasmic transport. *Biochim Biophys Acta* 1813: 1578–1592.

Luby–Phelps K. 2013. The physical chemistry of cytoplasm and its influence on cell function: an update. *Mol Biol Cell* 24: 2593–2596.

Lund E. & Collas P. 2013. Nuclear lamins: making contact with promoters. *Nucleus* 4: 424–430.

Luo Y. & Qiu J. 2013. Parvovirus infection-induced DNA damage response. *Future virology* 8: 245–257.

Lusk C.P., Blobel G. & King M.C. 2007. Highway to the inner nuclear membrane: rules for the road. *Nat Rev Mol Cell Biol* 8: 414–420.

Luzio J.P., Pryor P.R. & Bright N.A. 2007. Lysosomes: fusion and function. *Nat Rev Mol Cell Biol* 8: 622–632.

Ma J., Goryaynov A., Sarma A. & Yang W. 2012. Self-regulated viscous channel in the nuclear pore complex. *Proc Natl Acad Sci USA* 109: 7326–7331.

Maeshima K., Yahata K., Sasaki Y., Nakatomi R., Tachibana T., Hashikawa T., Imamoto F. & Imamoto N. 2006. Cell-cycle-dependent dynamics of nuclear pores: pore-free islands and lamins. *J Cell Sci* 119: 4442–4451.

Maeshima K., Iino H., Hihara S., Funakoshi T., Watanabe A., Nishimura M., Nakatomi R., Yahata K., Imamoto F., Hashikawa T., Yokota H. & Imamoto N. 2010. Nuclear pore formation but not nuclear growth is governed by cyclin-dependent kinases (Cdks) during interphase. *Nat Struct Mol Biol* 17: 1065–1071.

Mani B., Baltzer C., Valle N., Almendral J.M., Kempf C. & Ros C. 2006. Low pH-dependent endosomal processing of the incoming parvovirus minute virus of mice virion leads to externalization of the VP1 N–terminal sequence (N-VP1), N-VP2 cleavage, and uncoating of the full-length genome. *J Virol* 80 (2): 1015–24.

Marchini A., Bonifati S., Scott E.M., Angelova A.L. & Rommelaere J. 2015. Oncolytic parvoviruses: from basic virology to clinical applications. *Virol J* 12: 6.

Marcus–Sekura C. & Carter B.J. 1983. Chromatin-like structure of adeno–associated virus DNA in infected cells. *J Virol* 48: 79–87.

Mariño–Ramíerz L., Kann M.G., Shoemaker B.A. & Landsman D. 2005. Histone structure and nucleosome stability. *Expert Rev Proteomics* 2: 719–729.

Maroto B., Valle N., Saffrich R. & Almendral J.M. 2004. Nuclear export of the nonenveloped parvovirus virion is directed by an unordered protein signal exposed on the capsid surface. *J Virol* 78(19): 10685–10694.

Matzke A.J.M., Weiger T.M. & Matzke M. 2010. Ion channels at the nucleus: electrophysiology meets the genome. *Mol Plant* 3: 642–652.

Maul G.G., Maul H.M., Scogna J.E., Lieberman M.W., Stein G.S., Hsu B.Y. & Borun T.W. 1972. Time sequence of nuclear pore formation in phytohemagglutinin-stimulated lymphocytes and in HeLa cells during the cell cycle. *J Cell Biol* 55: 433–447.

Meng F., Na I., Kurgan L. & Uversky V. N. 2015. Compartmentalization and functionality of nuclear disorder: intrinsic disorder and protein-protein interactions in intra–nuclear compartments. *Int J Mol Sci* 17(1): pii E24.

Mohr D., Frey S., Fisher T., Güttler T. & Görlich D. 2009. Characterisation of the passive permeability barrier of nuclear pore complexes. *The EMBO J* 28: 2541–2553.

Monier K., Armas J.C.G., Etteldorf S., Ghazal P. & Sullivan K.F. 2000. Annexation of the interchromosomal space during viral infection. *Nat Cell Biol* 2: 661–665.

Moore M.S. 1998. Ran and nuclear transport. *J Biol Chem* 273: 22857–22860.

Morita E., Nakashima A., Asao H., Sato H. & Sugamura K. 2003. Human parvovirus B19 nonstructural protein (NS1) induces cell cycle arrest at G(1) phase. *J Virol* 77: 2915–2921.

Morris J.B., Hofemeister H. & O'Hare P. 2007. Herpes simplex virus infection induces phosphorylation and delocalization of emerin, a key inner nuclear membrane protein. *J Virol* 81: 4429–4437.

Naeger L.K., Cater J. & Pintel D.J. 1990. The small nonstructural protein (NS2) of the parvovirus minute virus of mice is required for efficient DNA replication and infectious virus production in a cell-type-specific manner. *J Virol* 64: 6166–6175.

Nagai–Fukataki M., Ohashi T., Hashimoto I., Kimura T., Hakata Y. & Shida H. 2011. Nuclear and cytoplasmic effects of human CRM1 on HIV-1 production in rat cells. *Genes Cells* 16: 203–216.

Nagamine T., Kawasaki Y., Abe A. & Matsumoto S. 2008. Nuclear marginalization of host cell chromatin associated with expansion of two discrete virus-induced subnuclear compartments during baculovirus infection. *J Virol* 82: 6409–6418.

Nelson C.D.S., Palermo L.S., Hafenstein S.L. & Parrish C.R. 2007. Different mechanisms of antibody-mediated neutralization of parvoviruses revealed using the Fab fragments of monoclonal antibodies. *Virology* 361: 283–293.

Németh A. & Längst G. 2011. Genome organization in and around the nucleolus. *Trends Genet* 27 (4): 149–156.

Nandi S. & Kumar M. 2010. Canine parvovirus: current perspective. *Indian J Virol* 21: 31–44.

Nevels M., Paulus C. & Shenk T. 2004. Human cytomegalovirus immediate-early 1 protein facilitates viral replication by antagonizing histone deacetylation. *Proc Natl Acad Sci U S A* 101: 17234–17239.

Nicolson S.C. & Samulski R.J. 2014. Recombinant adeno-associated virus utilizes host cell nuclear import machinery to enter the nucleus. *J Virol* 88: 4132–4144.

Niskanen E.A., Kalliolinna O., Ihalainen T.O., Häkkinen M. & Vihinen-Ranta M. 2013. Mutations in DNA binding and transactivation domains affect the dynamics of parvovirus NS1 protein. *J Virol* 87: 11762–11774.

Niskanen E.A., Ihalainen T.O., Kalliolinna O., Häkkinen M.M. & Vihinen-Ranta M. 2010. Effect of ATP binding and hydrolysis on dynamics of canine parvovirus NS1. *J Virol* 84: 5391–5403.

Nizami Z., Deryusheva S. & Gall J.G. 2010. The cajal body and histone locus body. *Cold Spring Harb Perspect Biol* 2(7): a000653.

Nüesch J.P. & Rommelaere J. 2006. NS1 interaction with CKII alpha: novel protein complex mediating parvovirus-induced cytotoxicity. *J Virol* 80: 4729–4739.

Nüesch J.P.F., Lachmann S. & Rommelaere J. 2005. Selective alterations of the host cell architecture upon infection with parvovirus minute virus of mice. *Virology* 331: 159–174.

Nüesch J.P.F., Cotmore S.F. & Tattersall P. 1995. Sequence motifs in the replicator protein of parvovirus MVM essential for nicking and covalent attachment to the viral origin: identification of the linking tyrosine. *Virology* 209: 122–135.

Nykky J., Tuusa J.E., Kirjavainen S., Vuento M. & Gilbert L. 2010. Mechanisms of cell death in canine parvovirus-infected cells provide intuitive insights to developing nanotools for medicine. *Int J Nanomedicine* 5: 417–428.

Nykky J., Vuento M. & Gilbert L. 2014. Role of mitochondria in parvovirus pathology. *PLoS One* 9(1): e86124.

O´Keefe R.T., Henderson S. & Spector D.L. 1992. Dynamic organization of DNA replication in mammalian cell nuclei: spatially and temporally defined replication of chromosome-specific alpha-satellite DNA sequences. *J Cell Biol* 116(5): 1095–1110.

Ohshima T., Yoshida E., Nakajima T., Yagami K. & Fukamizu A. 2001. Effects of interaction between parvovirus minute virus of mice NS1 and coactivator CBP on NS1- and p53-transactivation. *J Mol Med* 7: 49–103.

Ojala P.M., Sodeik B., Ebersold M.W., Kutay U. & Helenius A. 2000. Herpes simplex virus type 1 entry into host cells: reconstitution of capsid binding and uncoating at the nuclear pore complex in vitro. *Mol Cell Biol* 20(13): 4922–4931.

Okada N. & Sato M. 2015. Spatiotemporal regulation of nuclear transport machinery and microtubule organization. *Cells* 4: 406–426.

Organtini L.J., Allison A.B., Lukk T., Parrish C.R. & Hafenstein S. 2015. Global displacement of canine parvovirus by a host–adapted variant: structural comparison between pandemic viruses with distinct host ranges. *J Virol* 89(3):1909–1912.

Orzalli M.H. & Knipe D.M. 2014. Cellular sensing of viral DNA and viral evasion mechanisms. *Annu Rev Microbiol* 68: 477–492.

Orzalli M.H., Conwell S.E., Berrios C., DeCaprio J.A. & Knipe D.M. 2013. Nuclear interferon-inducible protein 16 promotes silencing of herpesviral and transfected DNA. *Proc Natl Acad Sci USA* 110: E4492–E4501.

Osmanagic-Myers S., Dechat T. & Foisner R. 2015. Lamins at the crossroads of mechanosignaling. *Genes Dev* 29: 225–237.

Palmeri D. & Malim M.H. 1999. Importin beta can mediate the nuclear import of an arginine-rich nuclear localization signal in the absence of importin alpha. *Mol Cell Biol* 19: 1218–1225.

Panté N. & Kann M. 2002. Nuclear pore complex is able to transport macromolecules with diameters of ~39 nm. *Mol Biol Cell* 13: 425–434.

Parker J.S.L., Murphy W.J., Wang D., O'Brien S.,J. & Parrish C.R. 2001. Canine and feline parvoviruses can use human or feline transferrin receptors to bind, enter, and infect cells. *J Virol* 75: 3896–3902.

Parrish C.R. 1991. Mapping specific functions in the capsid structure of canine parvovirus and feline panleukopenia virus using infectious plasmid clones. *Virology* 183: 195–205.

Parrish C.R. & Kawaoka Y. 2005. The origins of new pandemic viruses: the acquisition of new host ranges by canine parvovirus and influenza A viruses. *Annu Rev Microbiol* 59: 553–586.

Parrish C., O'Connell P., Evermann J. & Carmichael L. 1985. Natural variation of canine parvovirus. *Science* 230: 1046–1048.

Pederson T. 2011. The Nucleolus. *Cold Spring Harb Perspect Biol* 3(3): pii: a000638.

Penaud–Budloo M., Le Guiner C., Nowrouzi A., Toromanoff A., Chérel Y., Chenuaud P., Schmidt M., von Kalle C., Rolling F., Moullier P. & Snyder

R.O. 2008. Adeno-associated virus vector genomes persist as episomal chromatin in primate muscle. *J Virol* 82: 7875–7885.

Pombo A. & Dillon N. 2015. Three-dimensional genome architecture: players and mechanisms. *Nat Rev Mol Cell Biol* 16: 245–257.

Porwal M., Cohen S., Snoussi K., Popa–Wagner R., Anderson F., Dugot–Senant N., Wodrich H., Dinsart C., Kleinschmidt J., Panté N. & Kann M. 2013. Parvoviruses Cause Nuclear Envelope Breakdown by Activating Key Enzymes of Mitosis. *PLoS Pathog* 9: e1003671.

Rabe B., Vlachou A., Panté N., Helenius A. & Kann M. 2003. Nuclear import of hepatitis B virus capsids and release of the viral genome. *Proc Natl Acad Sci USA* 100: 9849–9854.

Raiborg C., Wenzel E.M., Pedersen N.M., Olsvik H., Schink K.O., Schultz S.W., Vietri M., Nisi V., Bucci C., Brech A., Johansen T. & Stenmark H. 2015. Repeated ER-endosome contacts promote endosome translocation and neurite outgrowth. *Nature* 520: 234–238.

Rajgor D. & Shanahan C.M. 2013. Nesprins: from the nuclear envelope and beyond. *Expert Reviews in Molecular Medicine* 15: e5.

Reddy K.L., Zullo J.M., Bertolino E. & Singh H. 2008. Transcriptional repression mediated by repositioning of genes to the nuclear lamina. *Nature* 452: 243–247.

Reed A.P., Jones E.V. & Miller T.J. 1988. Nucleotide sequence and genome organization of canine parvovirus. *J Virol* 62: 266–276.

Richards S.A., Carey K.L. & Macara I.G. 1997. Requirement of guanosine triphosphate-bound Ran for signal-mediated nuclear protein export. *Science* 276: 1842–1844.

Richter K., Nessling M. & Lichter P. 2007. Experimental evidence for the influence of molecular crowding on nuclear architecture. *J Cell Sci* 120: 1673–1680.

Riolobos L., Reguera J., Mateu M. G. & Almendral J. M. 2006. Nuclear transport of trimeric assembly intermediates exerts a morphogenetic control on the icosahedral parvovirus capsid. *J Mol Biol* 357 (3): 1026–1038.

Roux K.J., Kim D.I., Raida M. & Burke B. 2012. A promiscuous biotin ligase fusion protein identifies proximal and interacting proteins in mammalian cells. *J Cell Biol* 196: 801–810.

Saksouk N., Simboeck E. & Déjardin J. 2015. Constitutive heterochromatin formation and transcription in mammals. *Epigenetics Chromatin* 8: 3.

Sánchez–Martínez C., Grueso E., Carroll M., Rommelaere J. & Almendral J.M. 2012. Essential role of the unordered VP2 n-terminal domain of the parvovirus MVM capsid in nuclear assembly and endosomal enlargement of the virion fivefold channel for cell entry. *Virology* 432(1):45–56.

Schirmer E.C. & Gerace L. The nuclear membrane proteome: extending the envelope. *Trends Biochem Sci* 30: 551–558.

Schmid M., Arib G., Laemmli C., Nishikawa J., Durussel T. & Laemmli U.K. 2006. Nup–PI: The nucleopore-promoter interaction of genes in yeast. *Mol Cell* 21: 379–391.

Schmid M., Speiseder T., Dobner T. & Gonzalez R.A. 2014. DNA virus replication compartments. *J Virol* 88: 1404–1420.

Schoborg R.V. & Pintel D.J. 1991. Accumulation of MVM gene products is differentially regulated by transcription initiation, RNA processing and protein stability. *Virology* 181: 22–34.

Schoggins J.W., Wilson S.J., Panis M., Murphy M.Y., Jones C.T., Bieniasz P. & Rice C.M. 2011. A diverse array of gene products are effectors of the type I interferon antiviral response. *Nature* 472: 481–485.

Schreiber K. & Kennedy B. 2013. When lamins go bad: nuclear structure and disease. Cell 152 (6): 1365–1375.

Shalini S., Dorstyn L., Dawar S. & Kumar S. 2015. Old, new and emerging functions of caspases. *Cell Death Differ* 22 (4): 526–539.

Shumaker D.K., Solimando L., Sengupta K., Shimi T., Adam S.A., Grunwald A., Strelkov S.V., Aebi U., Cardoso M.C. & Goldman R.D. 2008. The highly conserved nuclear lamin Ig–fold binds to PCNA: its role in DNA replication. *J Cell Biol* 181: 269–280.

Silva L., Cliffe A., Chang L. & Knipe D.M. 2008. Role for A-type lamins in herpesviral DNA targeting and heterochromatin modulation. *PLoS Pathog* 4: e1000071.

Simões M., Rino J., Pinheiro I., Martins C. & Ferreira F. 2015. Alterations of nuclear architecture and epigenetic signatures during african swine fever virus infection. *Viruses* 7(9):4978–96.

Simon D.N. & Wilson K.L. 2011. The nucleoskeleton as a genome-associated dynamic 'network of networks'. *Nat Rev Mol Cell Biol* 12: 695–708.

Simpson-Holley M., Baines J., Roller R. & Knipe D.M. 2004. Herpes simplex virus 1 U(L)31 and U(L)34 gene products promote the late maturation of viral replication compartments to the nuclear periphery. *J Virol* 78: 5591–5600.

Singhal P.K., Kumar P.R., Rao M.R.K.S., Kyasani M. & Mahalingam S. 2006. Simian immunodeficiency virus Vpx is imported into the nucleus via importin alpha-dependent and -independent pathways. *J Virol* 80: 526–536.

Smith A.E. & Helenius A. 2004. How viruses enter animal cells. *Science* 304(5668): 237–242.

Sohn J., Morrone S., Wang T. & Hooy R. 2015. The cooperative assembly of IFI16 filaments on dsDNA provides insights into host defense strategy. *Biophys J* 108: 40a.

Somech R., Shaklai S., Geller O., Amariglio N., Simon A.J., Rechavi G. & Gal–Yam E. 2005. The nuclear-envelope protein and transcriptional repressor LAP2 beta interacts with HDAC3 at the nuclear periphery, and induces histone H4 deacetylation. *J Cell Sci* 118: 4017–4025.

Sonntag F., Bleker S., Leuchs B., Fisher R. & Kleinschmidt J. 2006. Adeno–associated virus type 2 capsids with externalized VP1/VP2 trafficking domains are generated prior to passage through the cytoplasm and are maintained until uncoating occurs in the nucleus. *J Virol* 80: 11040–11054.

Sood V. & Brickner J.H. 2014. Nuclear pore interactions with the genome. *Curr Opin Genet Dev* 25: 43–49.

Soutoglou E. & Misteli T. 2007. Mobility and immobility of chromatin in transcription and genome stability. *Curr Opin Genet Dev* 17: 435–442.

Spector D.L. & Lamond A.I. 2011. Nuclear Speckles. *Cold Spring Harbor Perspect Biol* 3(2): pii: a000646.

Splinter D., Tanenbaum M.E., Lindqvist A., Jaarsma D., Flotho A., Yu K.L., Grigoriev I., Engelsma D., Haasdijk E.D., Keijzer N., Demmers J., Fornerod M., Melchior F., Hoogenraad C.C., Medema R.H. & Akhmanova A. 2010. Bicaudal D2, dynein, and kinesin-1 associate with nuclear pore complexes and regulate centrosome and nuclear positioning during mitotic entry. *PLoS Biol* 8: e1000350.

Starr D.A. & Fisher J.A. 2005. KASH 'n Karry: The KASH domain family of cargo-specific cytoskeletal adaptor proteins. *Bioessays* 27: 1136–1146.

Stewart M. 2007. Molecular mechanism of the nuclear protein import cycle. *Nat Rev Mol Cell Biol* 8: 195–208.

Strambio–De–Castillia C., Niepel M. & Rout M.P. 2010. The nuclear pore complex: bridging nuclear transport and gene regulation. *Nat Rev Mol Cell Biol* 11: 490–501.

Strunze S., Engelke M., Wang I., Puntener D., Boucke K., Schleich S., Way M., Schoenenberger P., Burckhardt C. & Greber U. 2011. Kinesin-1-mediated capsid disassembly and disruption of the nuclear pore complex promote virus infection. *Cell Host & Microbe* 10: 210–223.

Stutika C., Gogol-Döring A., Botschen L., Mietzsch M., Weger S., Feldkamp M., Chen W. & Heilbronn R. 2016. A comprehensive RNA sequencing analysis of the adeno-associated virus (AAV) type 2 transcriptome reveals novel AAV transcripts, splice variants, and derived proteins. *J Virol* 90 (3): 1278–1289.

Suikkanen S., Antila M., Jaatinen A., Vihinen-Ranta M. & Vuento M. 2003a. Release of canine parvovirus from endocytic vesicles. *Virology* 316(2): 267–280.

Suikkanen S., Aaltonen T., Nevalainen M., Välilehto O., Lindholm L., Vuento M. & Vihinen-Ranta M. 2003b. Exploitation of microtubule cytoskeleton and dynein during parvoviral traffic toward the nucleus. *J Virol* 77: 10270–10279.

Suikkanen S., Sääjärvi K., Hirsimäki J., Välilehto O., Reunanen H., Vihinen-Ranta M. & Vuento M. 2002. Role of recycling endosomes and lysosomes in dynein–dependent entry of canine parvovirus. *J Virol* 76: 4401–4411.

Swami M. 2015. Technology: dropping in on single-cell epigenetic profiles. *Nat Rev Gen* 16 (12): 684–685.

Szczerbal I., Foster H.A. & Bridger J.M. 2009. The spatial repositioning of adipogenesis genes is correlated with their expression status in a porcine mesenchymal stem cell adipogenesis model system. *Chromosoma* 118: 647–663.

Takizawa T., Gudla P.R., Guo L., Lockett S. & Misteli T. 2008. Allele-specific nuclear positioning of the monoallelically expressed astrocyte marker GFAP. *Genes Dev* 22: 489–498.

Talamas J.A. & Capelson M. 2015. Nuclear envelope and genome interactions in cell fate. *Front Gen* 6: 95.

Tan J., Chen B., He L., Tang Y., Jiang Z., Yin G., Wang J. & Jiang X. 2012. Anacardic acid (6-pentadecylsalicylic acid) induces apoptosis of prostate cancer cells through inhibition of androgen receptor and activation of p53 signaling. *Chin J Cancer Res* 24: 275–283.

Tanay A. & Cavalli G. 2013. Chromosomal domains: epigenetic contexts and functional implications of genomic compartmentalization. *Curr Opin Genetics Dev* 23 (2): 197–203.

Tapley E.C. & Starr D.A. 2013. Connecting the nucleus to the cytoskeleton by SUN-KASH bridges across the nuclear envelope. *Curr Opin Cell Biol* 25: 57–62.

Torvaldson E., Kochin V. & Eriksson J. E. 2015. Phosphorylation of lamins determine their structural properties and signaling functions. *Nucleus* 6 (3): 166–171.

Truant R. & Cullen B.R. 1999. The arginine-rich domains present in human immunodeficiency virus type 1 Tat and Rev function as direct importin beta–dependent nuclear localization signals. *Mol Cell Biol* 19: 1210–1217.

Tsao J., Chapman M.S., Agbandje M., Keller W., Smith K. & Wu H. 1991. The three-dimensional structure of canine parvovirus and its functional implications. *Science* 251(5000): 1456–1464.

Tsuji T., Sheehy N., Gautier V.W., Hayakawa H., Sawa H. & Hall W.W. 2007. The nuclear import of the human T lymphotropic virus type I (HTLV-1) tax protein is carrier- and energy-independent. *J Biol Chem* 282(18): 13875–13883.

Tullis G., Schoborg R.V. & Pintel D.J. 1994. Characterization of the temporal accumulation of minute virus of mice replicative intermediates. *J Gen Virol* 75: 1633–1646.

Upadhyay M., Samal J., Kandpal M., Vasaikar S., Biswas B., Gomes J. & Vivekanandan P. 2013. CpG dinucleotide frequencies reveal the role of host methylation capabilities in parvovirus evolution. *J Virol* 87 (24): 13816–13824.

van Koningsbruggen, S., Gierliṅski M., Schofield P., Martin D., Barton G. J., Ariyurek Y., den Dunnen J.,T. & Lamond A. I. 2010. High-resolution whole-genome sequencing reveals that specific chromatin domains from most

human chromosomes associate with nucleoli. *Mol Biol Cell* 21 (21): 3735–3748.

Vázquez-Martínez R. & Malagón M.M. 2011. Rab proteins and the secretory pathway: the case of Rab18 in neuroendocrine cells. *Front Endocrin* 2: 1–9.

Verma A. D. & Parnaik V. K. 2015. Identification of tissue-specific regulatory region in the zebrafish lamin A promoter. *Gene* 567(1): 73–80.

Vihinen-Ranta M., Wang D., Weichert W.S. & Parrish C.R. 2002. The VP1 N-terminal sequence of canine parvovirus affects nuclear transport of capsids and efficient cell infection. *J Virol* 76: 1884–1891.

Vihinen-Ranta M., Kalela A., Mäkinen P., Kakkola L., Marjomäki V. & Vuento M. 1998. Intracellular route of canine parvovirus entry. *J Virol* 72: 802–806.

Vihinen-Ranta M., Yuan W. & Parrish C.R. 2000. Cytoplasmic trafficking of the canine parvovirus capsid and its role in infection and nuclear transport. *J Virol* 74: 4853–4859.

Vihinen-Ranta M., Kakkola L., Kalela A., Vilja P. & Vuento M. 1997. Characterization of a nuclear localization signal of caninep capsid proteins. *Eur J Biochem* 250: 389–394.

Wagner N. & Krohne G. 2007. LEM-domain proteins: new insights into lamin-interacting proteins. *Int Rev Cytol* 261: 1–46.

Walther T.C., Fornerod M., Pickersgill H., Goldberg M., Allen T.D. & Mattaj I.W. 2001. The nucleoporin Nup 153 is required for nuclear pore basket formation, nuclear pore complex anchoring and import of a subset of nuclear proteins. *EMBO J* 20: 5703–5714.

Wan G., Zhang X., Langley R.R., Liu Y., Hu X., Han C., Peng G., Ellis L.M., Jones S.N. & Lu X. 2013. DNA damage-induced nuclear export of precursor microRNAs is regulated by the ATM–AKT pathway. *Cell Rep* 3: 2100–2112.

Ward G.E. & Kirschner M.W. 2014. Identification of cell cycle-regulated phosphorylation sites on nuclear lamin C. *Cell* 61: 561–577.

Watson Z., Dhummakupt A., Messer H., Phelan D. & Bloom D. 2013. Role of polycomb proteins in regulating HSV-1 latency. *Viruses* 5 (7): 1740–1757.

Weichert W.S., Parker J.S., Wahid A.T., Chang S.F., Meier E. & Parrish C.R. 1998. Assaying for structural variation in the parvovirus capsid and its role in infection. *Virology* 250(1): 106–17.

Wente S.R. & Rout M.P. 2010. The nuclear pore complex and nuclear transport. *Cold Spring Harbor Perspect Biol* 2: a000562.

Whelan S.P. 2013. Viral replication strategies. In: Knipe D.M. & Howley P.M. (eds.), *Fields Virology*. 6th edition, Lippincott Williams & Wilkins, Philadelphia, s. 105–126.

Whittaker G.R., Kann M. & Helenius A. 2000. Viral entry into the nucleus. *Annu Rev Cell Dev Biol* 16: 627–651.

Wild P., Senn C., Manera C., Sutter E., Schraner E.M., Tobler K., Ackermann M., Ziegler U., Lucas M.S. & Kaech A. 2008. Exploring the nuclear envelope of herpes simplex virus 1-infected cells by high–resolution microscopy. *J Virol* 83: 408–419.

Wilk T., Gross I., Gowen B. E., Rutten T., de Haas F., Welker R., Kräusslich H., Boulanger P. & Fuller S. D. 2001. Organization of immature human immunodeficiency virus type 1. *J Virol* 75 (2): 759–771.

Wilson K.L. & Berk J.M. 2010. The nuclear envelope at a glance. *J Cell Sci* 123: 1973–1978.

Wilson K.L. & Foisner R. 2010. Lamin-binding proteins. *Cold Spring Harb Perspect Biol* 2: a000554.

Winey M., Yarar D., Giddings T.H. & Mastronarde D.N. 1997. Nuclear pore complex number and distribution throughout the saccharomyces cerevisiae cell cycle by three-dimensional reconstruction from electron micrographs of nuclear envelopes. *Mol Biol Cell* 8: 2119–2132.

Wolter S., Richards R. & Armentrout R.W. 1980. Cell cycle-dependent replication of the DNA of minute virus of mice, a parvovirus. *Biochim Biophys Acta* 607: 420–431.

Woodcock C.L. & Ghosh R.P. 2010. Chromatin higher-order structure and dynamics. *Cold Spring Harb Perspect Biol* 2: a000596.

Wozniak R. 2014. Sculpting the chromatin landscape: a role for nuclear pore complexes in gene silencing (238.2). *The FASEB J* 28.

Wu W. W. H., Sun Y. B. & Panté N. 2007. Nuclear import of influenza A viral ribonucleoprotein complexes is mediated by two nuclear localization sequences on viral nucleoprotein. *Virol J* 4: 49.

Xiao P. & Samulski R.J. 2012. Cytoplasmic trafficking, endosomal escape, and perinuclear accumulation of adeno-associated virus type 2 particles are facilitated by microtubule network. *J Virol* 86: 10462–10473.

Xie Q. & Chapman M.S. 1996. Canine parvovirus capsid structure, analyzed at 2.9 Å resolution. *J Mol Biol* 264: 497–520.

Xiu Y., Zhao Y., Gou W., Chen S., Takano Y. & Zheng H. 2014. Anacardic acid enhances the proliferation of human ovarian cancer cells. *PLoS ONE* 9: e99361.

Xu J., Guo H.C., Wei Y.Q., Dong H., Han S.C. & Ao D. 2014. Self–assembly of virus–like particles of canine parvovirus capsid protein expressed from Escherichia coli and application as virus-like particle vaccine. *Appl Microbiol Biot* 98(8): 3529–3538.

You J., Croyle J. L., Nishimura A., Ozato K. & Howley P. M. 2004. Interaction of the bovine papillomavirus E2 protein with Brd4 tethers the viral DNA to host mitotic chromosomes. *Cell* 117 (3): 349–360.

Zádori Z., Szelei J., Lacoste M., Li Y., Gariépy S., Raymond P., Allaire M., Nabi I. & Tijssen P. 2001. A viral phospholipase A_2 is required for parvovirus infectivity. *Dev Cell* 1: 291–302.

Zhang G., Estéve P., Chin H., Terragni J., Dai N., Corréa I.,R. & Pradhan S. 2015. Small RNA-mediated DNA (cytosine–5) methyltransferase 1 inhibition leads to aberrant DNA methylation. *Nucleic Acids Res* 43 (12): 6112–6124.

Zhu L. & Brangwynne C. P. 2015. Nuclear bodies: the emerging biophysics of nucleoplasmic phases. *Curr Opin Cell Biol* 34: 23–30.

ORIGINAL PAPERS

I

SINGLE–PARTICLE ANALYSIS UNVEILS DYNAMICS OF PARVOVIRUS CAPSID PASSAGE THROUGH NUCLEAR PORE COMPLEX

by

Elina Mäntylä, Jenu Chacko, Carmine Di Rienzo, Colin Parrish, Michael Kann, Victor Shahin, Michelle Digman, Enrico Gratton & Maija Vihinen-Ranta

Manuscript

II

PROMOTER TARGETED HISTONE ACETYLATION OF CHROMATINIZED PARVOVIRAL GENOME IS ESSENTIAL FOR INFECTION PROGRESS

by

Elina Mäntylä*, Kari Salokas*, Mikko Oittinen, Vesa Aho, Pekka Mäntysaari, Lassi Palmujoki, Olli Kalliolinna, Teemu O. Ihalainen, Einari A. Niskanen, Jussi Timonen, Keijo Viiri & Maija Vihinen-Ranta 2016
* Equal contribution

J Virol 90: 4059-4066

AMERICAN SOCIETY FOR MICROBIOLOGY | Journal of Virology

Promoter-Targeted Histone Acetylation of Chromatinized Parvoviral Genome Is Essential for the Progress of Infection

Elina Mäntylä,[a] Kari Salokas,[a] Mikko Oittinen,[b] Vesa Aho,[c] Pekka Mäntysaari,[a] Lassi Palmujoki,[a] Olli Kalliolinna,[a] Teemu O. Ihalainen,[d] Einari A. Niskanen,[e] Jussi Timonen,[c] Keijo Viiri,[b] Maija Vihinen-Ranta[a]

Department of Biological and Environmental Science and Nanoscience Center, University of Jyvaskyla, Jyvaskyla, Finland[a]; Tampere Center for Child Health Research, University of Tampere, Tampere, Finland[b]; Department of Physics and Nanoscience Center, University of Jyvaskyla, Jyvaskyla, Finland[c]; NeuroGroup, BioMediTech, University of Tampere, Tampere, Finland[d]; Institute of Biomedicine, University of Eastern Finland, Kuopio, Finland[e]

ABSTRACT

The association of host histones with parvoviral DNA is poorly understood. We analyzed the chromatinization and histone acetylation of canine parvovirus DNA during infection by confocal imaging and *in situ* proximity ligation assay combined with chromatin immunoprecipitation and high-throughput sequencing. We found that during late infection, parvovirus replication bodies were rich in histones bearing modifications characteristic of transcriptionally active chromatin, i.e., histone H3 lysine 27 acetylation (H3K27ac). H3K27ac, in particular, was located in close proximity to the viral DNA-binding protein NS1. Importantly, our results show for the first time that in the chromatinized parvoviral genome, the two viral promoters in particular were rich in H3K27ac. Histone acetyltransferase (HAT) inhibitors efficiently interfered with the expression of viral proteins and infection progress. Altogether, our data suggest that the acetylation of histones on parvoviral DNA is essential for viral gene expression and the completion of the viral life cycle.

IMPORTANCE

Viral DNA introduced into cell nuclei is exposed to cellular responses to foreign DNA, including chromatinization and epigenetic silencing, both of which determine the outcome of infection. How the incoming parvovirus resists cellular epigenetic downregulation of its genes is not understood. Here, the critical role of epigenetic modifications in the regulation of parvovirus infection was demonstrated. We showed for the first time that a successful parvovirus infection is characterized by the deposition of nucleosomes with active histone acetylation on the viral promoter areas. The results provide new insights into the regulation of parvoviral gene expression, which is an important aspect of the development of parvovirus-based virotherapy.

Nuclear chromatin is composed of DNA and histone proteins (1). The histone proteins assemble DNA into nucleosomes, the composition and spacing of which contribute to higher-order chromatin packing. The chromatin is organized into regions of less-condensed actively transcribed chromatin (euchromatin) and highly condensed transcriptionally repressed chromatin (heterochromatin). Epigenetic modifications of histone proteins have been shown to correlate with the spatial distribution of active and repressed chromatin (2, 3). The acetylation of lysine 9 or 27 of histone H3 (H3K9ac and H3K27ac, respectively) and trimethylation of lysine 4 (H3K4me3) correlate with transcriptional activity, while repressed chromatin is characterized by, e.g., trimethylation or dimethylation of the same H3 lysine residues (H3K9me3 and H3K27me3 as well as H3K9me2 and H3K27me2) (4–8).

Foreign DNA introduced into mammalian cells can be recognized as a threat by the host cell. The cellular responses to the foreign DNA, such as viral DNA, include the chromatinization of the entering DNA, leading to its transcriptional silencing (9–11). How viruses resist cellular chromatinization and silencing is known for only a few viruses (9, 12, 13). These include herpes simplex viruses (HSVs) (14–16), polyomaviruses (17, 18), adenoviruses (19), and cytomegaloviruses (20, 21), all of which encode proteins that promote transcriptionally activating histone modifications on chromatinized viral genomes during lytic infection.

In parvovirus infection, the nuclear entry of viral single-stranded DNA is followed by the formation of double-stranded replicative intermediates, the nuclear accumulation of viral proteins and DNA, and the formation of autonomous parvovirus-associated replication (APAR) bodies (22–25). Viral gene expression and DNA replication are dependent on the S phase of the cell cycle. In infected cells, the transcription of viral nonstructural protein 1 (NS1) at 4 h postinfection (p.i.) is followed by viral genome replication (26). Replication continues throughout the infection and leads to the production of viral capsids and their nuclear egress at 20 to 24 h p.i. The intranuclear chromatinization of the parvoviral genome, the modification of the assembled histones, and the effect of these events on viral gene expression are not well understood. To provide answers to these questions, we analyzed the infection of an autonomous protoparvovirus, canine

Received 17 December 2015 **Accepted** 31 January 2016

Accepted manuscript posted online 3 February 2016

Citation Mäntylä E, Salokas K, Oittinen M, Aho V, Mäntysaari P, Palmujoki L, Kalliolinna O, Ihalainen TO, Niskanen EA, Timonen J, Viiri K, Vihinen-Ranta M. 2016. Promoter-targeted histone acetylation of chromatinized parvoviral genome is essential for the progress of infection. J Virol 90:4059–4066. doi:10.1128/JVI.03160-15.

Editor: G. McFadden, University of Florida

Address correspondence to Keijo Viiri, keijo.viiri@uta.fi, or Maija Vihinen-Ranta, maija.vihinen-ranta@jyu.fi.

K.S. and M.O. contributed equally to this work.

parvovirus (CPV), by confocal imaging techniques and *in situ* proximity ligation assays (PLA) complemented with chromatin immunoprecipitation coupled with high-throughput sequencing (ChIP-seq). Our results demonstrated the enrichment of acetylated histones (H3K27ac) in close proximity to viral DNA-binding NS1 in APAR bodies and especially H3K27ac accumulated in the viral promoters. The inhibition of histone acetyltransferase (HAT) activity led to the interruption of the viral life cycle. These results reveal that histone acetylation on chromatinized parvoviral genomes is necessary for the expression of viral genes and successful progression of infection.

MATERIALS AND METHODS

Cells, viruses, and constructs. Norden Laboratories feline kidney (NLFK; Quality Control of Pfizer Animal Health, Lincoln, NE) cells were grown in Dulbecco's modified Eagle medium (DMEM) supplemented with 10% fetal bovine serum (Gibco, Paisley, United Kingdom) at 37°C in the presence of 5% CO_2. CPV-2d isolates originated from an infectious plasmid clone (a gift from C. R. Parrish, Cornell University, Ithaca, NY [27]). The viruses had been isolated as described by Suikkanen et al. (28). For infection, the cells were inoculated with CPV (multiplicity of infection [MOI] of 1 to 2) and kept at 37°C until fixation. In order to synchronize infections, the cells were incubated on ice at 4°C for 20 min prior to virus addition. The cells then were inoculated on ice to allow for virus adsorption to occur for 30 min. The cells next were rinsed at 4°C with phosphate-buffered saline (PBS) containing 0.3% bovine serum albumin (BSA) followed by the addition of 37°C medium. The plasmid encoding fluorescent H3-enhanced green fluorescent protein (EGFP) was a generous gift from J. Langowski (German Cancer Research Center, Heidelberg, Germany). An NLFK cell line stably expressing H3-EGFP was established by transfection (TransIT-LT1 reagent; Thermo Fisher Scientific Inc., Waltham, MA) with an expression vector at 24 h after seeding. After 2 days, the DMEM was replaced by DMEM containing 1 mg/ml Geneticin (Sigma-Aldrich, St. Louis, MO). The cells then were seeded at different intervals until stable expression was observed by microscopy.

Confocal microscopy. For immunolabeling, cells seeded on round coverslips were infected with CPV and fixed at 8, 10, 12, 16, and 24 h p.i. with 4% paraformaldehyde (PFA; 15 min at room temperature). Viral proteins were detected with an NS1-specific monoclonal antibody (MAb) (generous gift from Caroline Astell) (29), an intact capsid MAb, and a polyclonal capsid-protein VP2 antibody (Ab; generous gifts from Colin R. Parrish) (27), followed by goat anti-mouse or anti-rabbit Alexa-555- or Alexa-633-conjugated secondary Abs (Molecular Probes, Life technologies, Grand Island, NY). Modified histones were labeled with rabbit Abs against H3K9me3 and H3K27ac (Abcam, Cambridge, MA) followed by goat anti-rabbit Alexa 633-conjugated secondary Abs. For deacetylation and hyperacetylation studies, cells were either pretreated for 30 min prior to virus inoculation or treated at 0 to 6 h p.i. with 0.1 mM anacardic acid prepared in 100% dimethyl sulfoxide (DMSO) (Sigma-Aldrich, St. Louis, MO). Cell viability was assessed using propidium iodide (Sigma) and annexin V Alexa 647 (Molecular Probes) staining by following the manufacturer's instructions (data not shown). All cells were fixed at 24 h p.i. with 4% PFA and permeabilized with 0.1% Triton X-100 in PBS supplemented with 1% BSA and 0.01% sodium azide. Imaging was done with an Olympus FV-1000 confocal microscope with the UPLSAPO 60× oil-immersion objective (numeric aperture, 1.35). EGFP was excited with a 488-nm argon laser, and fluorescence was collected with a 515/30-nm band-pass filter. Alexa 555 and the proximity ligation assay (PLA) reagent with a fluorophore, 594 nm, were excited with a 543-nm He-Ne laser, and fluorescence was collected with a 570-nm to 620-nm band-pass filter and a 560IF band-pass filter, respectively. Alexa 633 was excited with a 633-nm He-Ne laser, and the fluorescence was collected with a 647-nm long-pass filter. Image size was between 512 by 512 and 1,600 by 1,600 pixels with a pixel resolution of 66 to 69 nm. Deconvolution was performed with Huygens Essential software (SVI, Netherlands). The point-spread function was averaged, the iterative deconvolution was performed with a signal-to-noise ratio of 5, and the quality threshold was 0.01. Image analysis was done with ImageJ (30).

Correlation analysis was done with ImageJ using the JACoP plugin (31). Distance analysis of the fixed-cell samples was done first by making a Euclidian distance map from an image of interest and then plotting the original image against the distance map. The data from every cell were combined and arranged to 0.1-μm-wide bins based on the distance of the voxels from the nuclear envelope. The average intensity then was plotted for each bin. Distance maps were done in ImageJ with the exact Euclidian distance transform (3D) plugin, and the data analysis was done with an in-house Java code. Student's *t* test (two-tailed, unequal variance) was used to evaluate statistical significance in the change of the recovery time point values.

Analysis of protein interactions. For *in situ* PLA (32), cells were grown on 8-well chamber slides (Nunc Lab-Tek II chamber slide system; Nalgene Nunc International, Penfield, NY) to 80 to 90% confluence and fixed with 4% PFA. PLA was done with a DuolinkII kit (Olink Bioscience, Uppsala, Sweden) and primary Abs against NS1 and H3K27ac. After labeling the cells with the primary Abs, the PLA probes (oligonucleotide-conjugated secondary anti-mouse and anti-rabbit IgGs diluted in 3% BSA in PBS) were incubated for 1 h at 37°C in a humidified chamber, followed by ligation and amplification according to the manufacturer's instructions. Samples were embedded in ProLong gold antifade mounting medium with 4′,6-diamidino-2-phenylindole (DAPI). The specificity of the assay was confirmed using positive, negative, and technical control readings. Positive and negative controls consisted of infected and noninfected cells, respectively, labeled with anti-VP2 and intact capsid-specific Abs or anti-NS1 and anti-H3K27ac Abs. For a technical control, noninfected cells were labeled only with PLA probes. Quantitative analysis was done with ImageJ by determining the arithmetic mean of the total number of signals per cell. The PLA signal was normalized as PLA = NA − NT, where NA is the total number of nuclear PLA dots in infected and noninfected cells labeled with H3K27ac Ab and NS1 MAb and NT is the average number of nuclear PLA dots in the technical control. Student's *t* test (two-tailed, unequal variance) was used to evaluate statistical significance.

ChIP-seq and qPCR. Cells were fixed with formaldehyde, and nuclei were isolated, lysed, and sonicated with a Covaris S220 ultrasonicator. The resulting nuclear extract was incubated overnight at 4°C with Dynal protein G beads preincubated with 5 μg of H3K27ac (ab4729) or H3 (ab1791) Abs. Beads were washed and bound complexes eluted, and cross-links were reversed by heating at 65°C. Immunoprecipitation (IP) and input DNA then were purified by a treatment with RNase A, proteinase K, and phenol-chloroform extraction. Before moving forward to ChIP-seq, precipitated DNA was analyzed by quantitative PCR (qPCR) using primers specific for gp1, gp2, and gp5 regions. Libraries were constructed from IP and input DNA by a NEBnext Ultra DNA library preparation kit for Illumina. DNA in the range of 150 to 350 bp was gel purified after PCR amplification. The library was quantified using an Agilent bioanalyzer and subjected to 50-bp single-end read sequencing with an Illumina HiSeq 2000 at EMBL Genecore, Heidelberg, Germany. Quality metrics for sequenced reads were gathered with FastQC (www.bioinformatics.babraham.ac.uk/projects/fastqc/). Adapter sequences were removed with cutadapt (33). Reads then were aligned with Bowtie2 (34) to cat (ICGSC Felis_catus 6.2) and CPV (NCBI reference sequence NC_001539.1) reference genomes. Sequencing reads of H3K27ac ChIP-seq from infected cells were normalized to CPV reads per genomic content (RPGC). File conversions to the BAM format were done with SAMtools (35), and visualizations were done with deepTools (36).

Accession number. The ChIP-seq data reported in this paper have been deposited in the NCBI Gene Expression Omnibus (GEO) database under accession number GSE77785.

RESULTS

Temporal changes in localization of modified histones in infection. To analyze the chromatinization of the CPV genome at various times postinfection (p.i.), we used H3-EGFP-expressing cells to identify the distribution of histone H3 and APAR bodies represented by NS1. The line profiles showed that at 12 h p.i. H3 was mostly located distinctly from NS1, whereas at 24 h p.i. increased colocalization of H3 with NS1 was observed (Fig. 1A and B). Similarly, Pearson correlation coefficient (PCC) analysis indicated the correlation of H3-EGFP with NS1 at 16 h p.i. (0.61 ± 0.29; $n = 22$; *P* value [Student's *t* test] at 16 and 24 h p.i. compared to results at 10 h p.i., <0.05) and 24 h p.i. (0.77 ± 0.21; $n = 26$; $P < 0.01$) but not at earlier times (Fig. 1G). To assess how H3-associated active and repressed chromatin is distributed in infected cells, we used H3K27ac and H3K9me3 as markers of active and repressed chromatin, respectively. Immunolabeling indicated that at 12 h p.i., distinct NS1 foci began to emerge, while H3K27ac and H3K9me3 showed a thorough nuclear distribution. The line profiles of H3K27ac and H3K9me3 with NS1 at 12 h p.i. indicated only a weak colocalization (Fig. 1C and E). However, at 24 h p.i. H3K27ac concentrated in the enlarging APAR bodies (Fig. 1D). Similarly, PCC of NS1 with H3K27ac was significantly higher at 16 h p.i. (0.83 ± 0.22; $n = 18$; $P < 0.01$) and at 24 h p.i. (0.87 ± 0.08; $n = 23$; $P < 0.01$) than at earlier times (Fig. 1G). No correlation of H3K9me3 with NS1 was observed by the line profile and PCC analyses (Fig. 1E to G). Colocalization of NS1 with H3 and H3K27ac correlated time dependently with the enlargement of APAR bodies. Quantitative 3D distribution analysis of H3K27ac and H3K9me3 as a function of distance from the nuclear rim indicated that the H3K27ac signal was located in the nuclear center in both infected (24 h p.i.) and noninfected cells ($n = 20$; 1,000 spots/cell counted) (Fig. 1H). In infected cells, the 0.7-μm-thick region at the nuclear periphery in particular was enriched in H3K9me3, and its intensity decreased toward the nuclear center. In noninfected cells, the H3K9me3 signal was distributed throughout the nucleus ($n = 20$; 1,000 spots/cell counted) (Fig. 1I).

In summary, these data showed that in the infected cells both H3K27ac and H3-EGFP were enriched in APAR bodies. At the same time, H3K9me3 was found to accumulate in the nuclear periphery, an area known to harbor the layer of marginalized cellular chromatin. This suggests that the histones associated with the viral genome in the APAR area bear modifications that are characteristic of active gene expression.

Time-dependent intranuclear interplay of H3K27ac and NS1. In order to address the nuclear interaction of H3K27ac with viral DNA-bound NS1, *in situ* PLA was performed. PLA is an immunodetection technique that generates a fluorescent signal only when two antigens of interest are within 40 nm of each other (32). To assess the nuclear interactions of H3K27ac and NS1, we analyzed infected cells by PLA at 8 to 24 h p.i. Noninfected control cells exhibited only a faint nuclear signal (PLA signal per cell, 1.1 ± 0.19; $n = 111$). At 8, 10, 12, and 16 h p.i., a time-dependent increase in the amount of punctate intranuclear PLA signals was detected (0.14 ± 0.16, $n = 105$; 0.81 ± 0.30, $n = 92$; 3.43 ± 0.91, $n = 110$; 19.46 ± 3.39, $n = 90$), with a maximal signal at 24 h p.i. (36.49 ± 3.97, $n = 99$) (Fig. 2A) in the nuclear interior with low levels of DAPI (Fig. 2B). The infection-induced compaction of the host chromatin and its dislocation into the nuclear periphery and around the nucleolus at 24 h p.i. were visualized with DAPI.

In summary, these results demonstrated a time-dependent increase in the interaction or close proximity of H3K27ac with NS1 after 10 h p.i., followed by extensive interaction at 24 h p.i. This finding is consistent with the results of immunofluorescence and PCC analyses of infected cells, which showed increased colocalization and correlation of H3K27ac and NS1 during late stages of infection.

CPV promoters are rich in acetylated histones. The prominent colocalization and interaction of NS1 with H3K27ac in the nucleus at 24 h p.i. prompted us to study whether the CPV genome *per se* is chromatinized with H3K27ac-enriched nucleosomes. To this end, ChIP-seq with H3K27ac Ab for the infected cells was performed. First, the success of ChIP was assessed with genome-wide occupancy of H3K27ac in infected cells showing a typical occupancy of this histone marker at ±2 kb around the transcription start sites (TSSs) of ~35% of the genes (data not shown). We found that 9.23% of the total reads (2.23×10^7 reads) were aligned with the viral genome in a unique manner (0.00% in noninfected cells) (37). The alignment of these reads with the genome, after normalization to reads per CPV genomic content, revealed that H3K27ac is mostly enriched in the TSSs of P4 promoter-driven transcriptional units for NS1 and NS2 (gp1 loci) and P38-driven transcriptional units for VP1 and VP2 (gp2 loci) (Fig. 3A) (38).

The viral genome was mostly devoid of this histone marker toward the right end (gp5 loci). The location of gp1 loci was very similar to that of the P4 promoter of the parvovirus minute virus of mice (MVM; nucleotides 1 to 260), and the location of gp2 was similar to that of the CPV P38 promoter (1355 to 2260) (39). The targeted ChIP-qPCR of H3 with gp1-, gp2-, and gp5-specific primers showed that the CPV genome is thoroughly chromatinized with uniformly distributed H3 (Fig. 3B and data not shown). Finally, targeted ChIP-qPCR analysis confirmed the occupancy of H3K27ac in the genome (Fig. 3C).

In conclusion, our data verified that the parvoviral genome is chromatinized with histones during late stages of infection. Importantly, acetylated histones were observed to be enriched in viral promoters to allow for the transcriptional activation of the viral NS and VP genes.

Viral histone acetylation is important for infection progress. In order to determine the importance of histone acetylation of parvoviral genomes during early stages of infection, the effect of the HAT inhibitor anacardic acid on viral protein synthesis was determined. Treatment with anacardic acid very early during infection (−0.5 to 1 h p.i.) resulted in a decrease in the percentage of cells with nuclear NS1 (~5%) and VP2 (~2%) at 24 h p.i. compared to the level for nontreated infected cells (68.0 and 50.3%, respectively; $n \geq 250$). This suggests that the early inhibition of histone acetylation induced an almost complete block of infection. While the early treatment exerted a maximal effect, anacardic acid was able to inhibit the infection progress when introduced later, up to 3 h postinfection (Fig. 4A). Here, we cannot rule out the possibility that histone acetylation was not the only factor affecting viral protein production. Cell cycle progression also could be involved. Of note, the treatment did not affect cell viability (data not shown). Our results suggest that histone acetylation is required during very early infection for the production of viral proteins necessary for the efficient progress of infection.

We next studied if the anacardic acid-induced inhibition of histone acetylation affected late infection. For this, we divided the

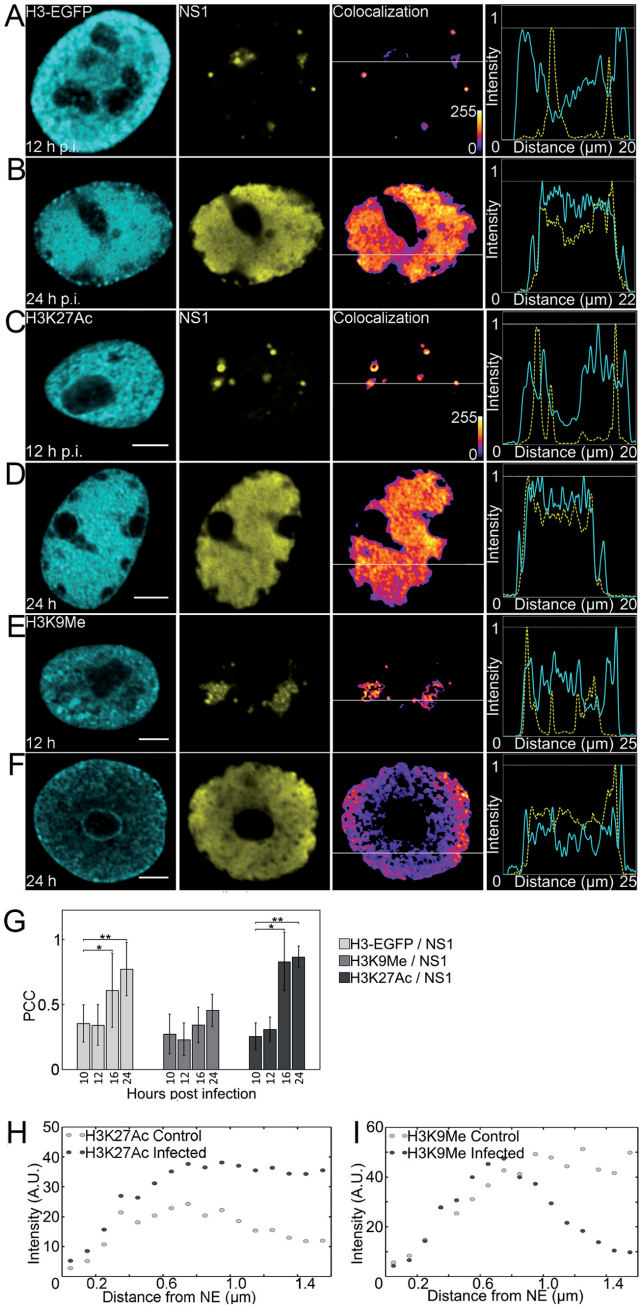
A
H3-EGFP
NS1
Colocalization
12 h p.i.
255
0
Intensity
1
0
Distance (μm) 20
B
24 h p.i.
Distance (μm) 22
C
H3K27Ac
12 h p.i.
Distance (μm) 20
D
24 h
Distance (μm) 20
E
H3K9Me
12 h
Distance (μm) 25
F
24 h
Distance (μm) 25
G
PCC
Hours post infection
H3-EGFP / NS1
H3K9Me / NS1
H3K27Ac / NS1
H
H3K27Ac Control
H3K27Ac Infected
Intensity (A.U.)
Distance from NE (μm)
I
H3K9Me Control
H3K9Me Infected
Intensity (A.U.)
Distance from NE (μm)

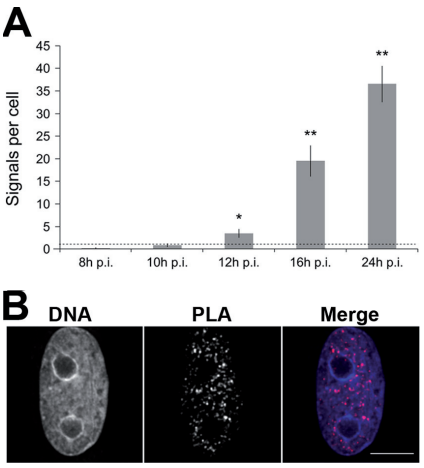

FIG 2 *In situ* PLA of H3K27ac interaction with NS1 in infected cells. (A) Number of PLA signals in infected cells at 8, 10, 12, 16, and 24 h p.i. The mean values of PLA signals ± standard errors from ~100 cells per time point are shown. The negative control, PLA signal in noninfected cells, is shown by a dashed line. Statistical significance of PLA signals per cell at 12, 16, and 24 h p.i. compared to that of the negative control is shown (*P* values [Student's *t* test]: *, $P < 0.05$; **, $P < 0.01$). (B) Distribution of PLA signals in DAPI-stained nuclei at 24 h p.i. Scale bar, 10 μm.

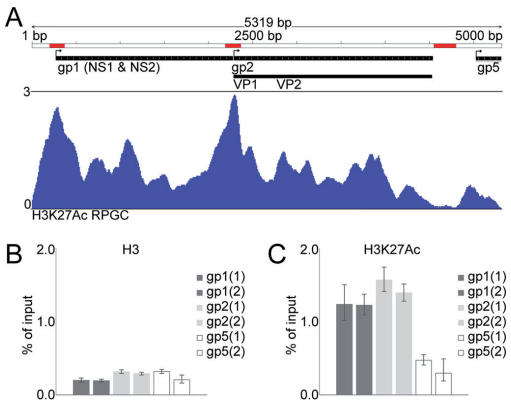

FIG 3 Enrichment of acetylated histones on gp1 and gp2 transcription start sites and effect on gene expression. (A) Histogram depicts occupancy of H3K27ac at CPV genome. Sequencing reads of H3K27ac ChIP-seq from infected cells at 24 h p.i. are normalized to RPGC. Bent arrows indicate TSSs of transcriptional units for NS1 and NS2 (gp1), VP1 and VP2 (gp2), and right-hand terminal gp5 loci, and red bars depict regions where qPCR primers anneal. ChIP-qPCRs for targeted measurements of H3 (B) and H3K27ac (C) levels at gp1 and gp2 TSSs and the VP2-gp5 interregion is shown as an enrichment of DNA relative to the level for input DNA. Two primer pairs for each of the three regions were used; columns represent the means ± SD from triplicate wells of two independent ChIP experiments.

infected cells in four categories based on intracellular localization of capsids at 24 h p.i. The categories were (i) capsids localized into cytoplasmic endocytic vesicles due to inhibition of infection or secondary infection (24), (ii) capsids localized in discrete foci scattered throughout the nucleus, (iii) capsids in enlarged APAR bodies enriched with NS1, and (iv) capsids in both APAR bodies and the cytoplasm (egress initiated) (Fig. 4B). The localization of capsids next was determined at 24 h p.i. in cells exposed to anacardic acid at 6 h p.i. Studies indicated that levels of category II, III, and IV cells were reduced in treated cells (4.9%, 12.5%, and 21.2%; $n \geq 250$) compared to the level of the nontreated infected control cells (7.9%, 26.8%, and 26.8%; $n \geq 250$). Moreover, an increase in category I cells was detected in treated cells (61.1%; $n \geq 250$) compared to the level in control cells (36.6%, 1.9%; $n \geq 250$) (Fig. 4B). These results demonstrated that efficient progress of infection correlates with histone acetylation in APAR areas at late stages of infection.

Finally, we studied whether the timing of viral histone acetylation was critical for the progress of late-stage infection. Here, the distribution of H3K27ac and NS1, positioned on the viral genome, was analyzed at 24 h p.i. in cells treated with anacardic acid. The inhibitor treatment at 16 h p.i. resulted in the exclusion of H3K27ac from the NS1-positive APAR bodies (Fig. 4C). This indicated that the viral genomes produced after drug treatment at 16 h p.i. were not acetylated. However, H3K27ac colocalized with NS1 after exposure to inhibitor at 20 h p.i. (Fig. 4C). These results suggested that histone acetylation on the majority of newly synthesized viral DNA occurs until 16 to 20 h p.i.

These inhibition studies provided evidence that the histone acetylation of intranuclear viral genomes early during infection plays an essential role in the production of viral proteins. Similarly, the acetylation of histones on newly synthesized viral genomes during active virus replication is necessary for the efficient accomplishment of infection. In summary, our findings demonstrate that viral histone acetylation is essential for both early and late steps in the parvoviral life cycle.

DISCUSSION

Although much is known about nuclear replication and gene expression of parvoviruses, little is known about the chromatinization of parvoviral genomes and histone modifications and the effect of these events on the progress of infection. For some DNA

FIG 1 Intranuclear distribution of H3-EGFP, modified histones, and viral NS1 protein. (A and B) Confocal microscopy images of cells stably expressing H3-EGFP (cyan) at 12 (A) and 24 (B) h p.i. labeled with NS1 (yellow) antibody. (C to F) Infected cells at 12 h p.i. and 24 h p.i. labeled with antibodies for H3K27ac (cyan) (C and D), H3K9me3 (cyan) (E and F), and NS1 (yellow). In order to clarify the changes in colocalization, pseudocolor images are shown with intensity increasing from blue to yellow. Fluorescence line profile analysis of the intensity of H3-EGFP/H3K27ac/H3K9me3 (cyan) and NS1 (yellow) in a single optical section through the center of the nucleus is shown beside each image. Analysis was performed with ImageJ and the Plot RGB Profile plugin. Scale bars, 5 μm. (G) Quantitative colocalization analysis of H3K27ac, H3K9me3, and H3-EGFP with NS1. The mean PCC values and standard deviations (SD) are shown. Statistical significance of colocalization at 16 and/or 24 h p.i. compared to that at 10 h p.i. is shown (*P* values [Student's *t* test]: *, $P < 0.05$; **, $P < 0.01$). (H and I) Plots of intensity of H3K27ac (H) and H3K9me3 (I) in infected cells at 24 h p.i. and in noninfected cells as a function of distance from the nuclear envelope (NE). A.U., arbitrary units.

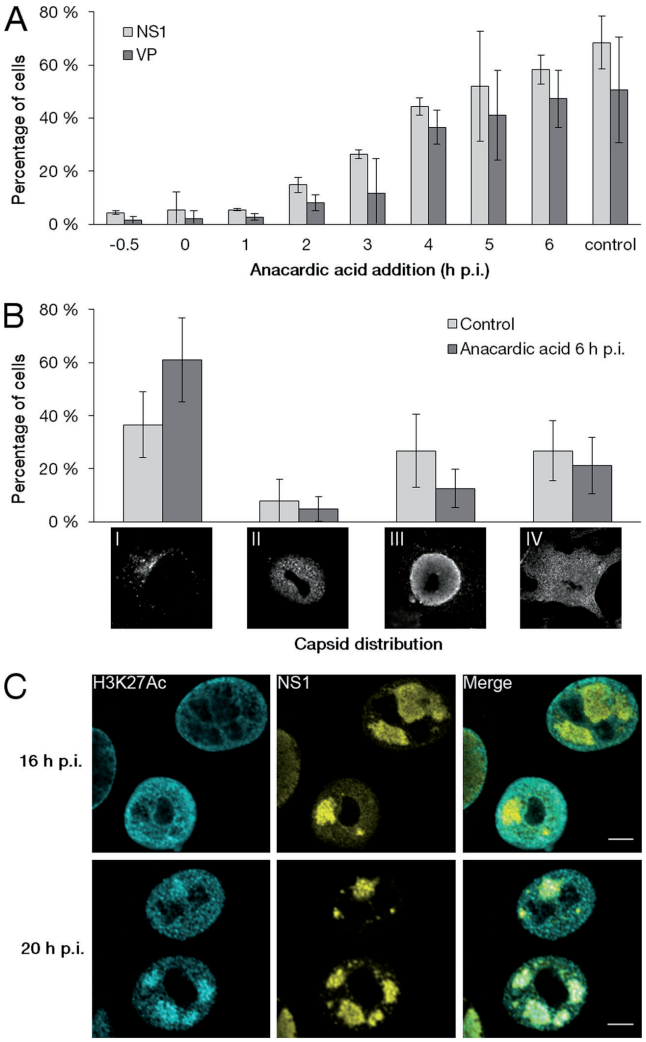

FIG 4 Importance of acetylation on progress of infection. (A) Percentage of cells showing viral NS1 and VP proteins in the nucleus in the cells exposed to the HAT inhibitor anacardic acid (0.1 mM). Cells were either pretreated for 30 min with the drugs prior to infection or treated at 0 to 6 h p.i., and the treatment continued until fixation at 24 h p.i. (B) Effect of anacardic acid treatment on localization of viral capsids. Images of cells representing four type categories based on the intracellular localization of capsids at 24 h p.i. and percentages of cells showing various types after treatment at 6 or 16 h p.i. The mean values ± SD are shown. (C) Distribution of H3K27ac compared to that of NS1 at 24 h p.i. in cells treated with anacardic acid at 16 or 20 h p.i. Scale bars, 10 μm.

viruses, such as herpesviruses and adenoviruses, epigenetic mechanisms, including histone modifications, play an important role in the regulation of viral gene expression. During herpesvirus lytic infection, the viral genomes are associated with histones immediately after injection into the nucleus, and viral proteins are required to enhance histone acetylation to allow for efficient viral gene expression (40–44). Moreover, studies of infection by an adenovirus have shown that viral proteins mediate the transcriptional activation of viral promoter regions (45–47). In this work, we first observed that the progress of CPV infection was accompanied by the enrichment of H3 histones in the enlarged APAR body area. This is consistent with earlier studies showing nuclear chromatinization of adeno-associated parvoviruses, used as gene therapy vectors, and MVM genomes (48–51). We next addressed

the existence of histone modifications in the parvoviral APAR bodies and revealed the accumulation of histones with modifications characteristic of transcriptionally active chromatin (H3K27ac). Moreover, our analysis demonstrated that H3K27ac was located in close proximity to the viral NS1 protein in the APAR bodies. This interaction likely is caused by the accumulation of NS1 on viral genomes because of its involvement in transcription and replication (52–54). NS1 of autonomous parvoviruses not only controls the viral activities but also regulates host gene expression through histone acetylation in cancer cells by recruiting innate proteins with HAT activity (55, 56). To date, evidence for the involvement of NS1 in the regulation of histone acetylation on parvoviral promoters has not been reported. Here, our PLA studies revealed that CPV NS1 was located in close proximity to H3K27ac in the enlarged APAR bodies. Our earlier studies indicated that CPV NS1 has two distinct binding sites in the viral genome (53, 54, 57). It is tempting to speculate that NS1 is involved in the histone acetylation of viral P4 and P38 promoters by recruiting host proteins with acetyltransferase activity. However, the specific role and interactions of NS1 in viral histone modifications remain to be determined. Our ChIP-seq analyses demonstrated for the first time that in the extensively chromatinized parvoviral genome, H3K27ac accumulated in viral P4 and P38 promoter areas. This suggests that parvoviral gene expression is regulated by histone acetylation in promoter areas. The importance of histone acetylation for the progress of infection was supported by our results showing that the inhibition of histone acetylation was accompanied by extensive repression of infection. Earlier studies showed that the formation of parvoviral gene transcription templates and intermediates for genome replication are temporally phased in infection (58–61). In line with this, our results suggest that parvoviruses regulate their gene expression via histone acetylation in a temporal fashion.

In summary, the CPV genome is chromatinized inside the nuclei of infected cells, and histone modifications associated with transcriptional activation are enriched in viral promoters. Our results highlight a critical role of epigenetic modification in the progression of the parvoviral life cycle.

ACKNOWLEDGMENTS

We are grateful to Klaus Hedman for comments on the manuscript. We thank The Sequencing Service GeneCore Sequencing Facility (EMBL, http://www.genecore.embl.de) for DNA sequencing.

FUNDING INFORMATION

Jane and Aatos Erkko Foundation provided funding to Jussi Timonen and Maija Vihinen-Ranta. Suomen Akatemia (Academy of Finland) provided funding to Einari A. Niskanen under grant number 135609. Suomen Akatemia (Academy of Finland) provided funding to Teemu O. Ihalainen under grant number 267471. Suomen Akatemia (Academy of Finland) provided funding to Maija Vihinen-Ranta under grant number 138388. Suomen Akatemia (Academy of Finland) provided funding to Keijo Viiri under grant number 265575. Päivikki ja Sakari Sohlbergin Säätiö (Päivikki and Sakari Sohlberg Foundation) provided funding to Keijo Viiri and Mikko Oittinen.

REFERENCES

1. **Luger K, Mäder AW, Richmond RK, Sargent DF, Richmond TJ.** 1997. Crystal structure of the nucleosome core particle at 2.8 A resolution. Nature **389:**251–260. http://dx.doi.org/10.1038/38444.
2. **Venkatesh S, Workman JL.** 2015. Histone exchange, chromatin structure and the regulation of transcription. Nat Rev Mol Cell Biol **16:**178–189. http://dx.doi.org/10.1038/nrm3941.
3. **Kornberg RD.** 1974. Chromatin structure: a repeating unit of histones and DNA. Science **184:**868–871. http://dx.doi.org/10.1126/science.184.4139.868.
4. **Ferrari KJ, Scelfo A, Jammula S, Cuomo A, Barozzi I, Stützer A, Fischle W, Bonaldi T, Pasini D.** 2014. Polycomb-dependent H3K27me1 and H3K27me2 regulate active transcription and enhancer fidelity. Mol Cell **53:**49–62. http://dx.doi.org/10.1016/j.molcel.2013.10.030.
5. **Smolle M, Workman JL.** 2013. Transcription-associated histone modifications and cryptic transcription. Biochim Biophys Acta **1829:**84–97. http://dx.doi.org/10.1016/j.bbagrm.2012.08.008.
6. **Bannister AJ, Kouzarides T.** 2011. Regulation of chromatin by histone modifications. Cell Res **21:**381–395. http://dx.doi.org/10.1038/cr.2011.22.
7. **McKittrick E, Gafken PR, Ahmad K, Henikoff S.** 2004. Histone H3.3 is enriched in covalent modifications associated with active chromatin. Proc Natl Acad Sci U S A **101:**1525–1530. http://dx.doi.org/10.1073/pnas.0308092100.
8. **Santos-Rosa H, Schneider R, Bannister AJ, Sheriff J, Bernstein BE, Emre NC, Schreiber SL, Mellor J, Kouzarides T.** 2002. Active genes are tri-methylated at K4 of histone H3. Nature **419:**407–411. http://dx.doi.org/10.1038/nature01080.
9. **Knipe DM.** 2015. Nuclear sensing of viral DNA, epigenetic regulation of herpes simplex virus infection, and innate immunity. Virology **479:**153–159.
10. **Cereghini S, Yaniv M.** 1984. Assembly of transfected DNA into chromatin: structural changes in the origin-promoter-enhancer region upon replication. EMBO J **3:**1243–1253.
11. **Johnson KE, Bottero V, Flaherty S, Dutta S, Singh VV, Chandran B.** 2014. IFI16 restricts HSV-1 replication by accumulating on the hsv-1 genome, repressing HSV-1 gene expression, and directly or indirectly modulating histone modifications. PLoS Pathog **10**(11):e1004503. http://dx.doi.org/10.1371/journal.ppat.1004503.
12. **Orzalli MH, Knipe DM.** 2014. Cellular sensing of viral DNA and viral evasion mechanisms. Annu Rev Microbiol **68:**477–492. http://dx.doi.org/10.1146/annurev-micro-091313-103409.
13. **Riu E, Chen Z-Y, Xu H, He C-Y, Kay M.** 2007. Histone modifications are associated with the persistence or silencing of vector-mediated transgene expression in vivo. Mol Ther **15:**1348–1355. http://dx.doi.org/10.1038/sj.mt.6300177.
14. **Knipe DM, Cliffe A.** 2008. Chromatin control of herpes simplex virus lytic and latent infection. Nat Rev Microbiol **6:**211–221. http://dx.doi.org/10.1038/nrmicro1794.
15. **Knipe DM, Lieberman PM, Jung JU, McBride AA, Morris KV, Ott M, Margolis D, Nieto A, Nevels M, Parks RJ, Kristie TM.** 2013. Snapshots: chromatin control of viral infection. Virology **435:**141–156. http://dx.doi.org/10.1016/j.virol.2012.09.023.
16. **Van Opdenbosch N, Favoreel H, Van de Walle GR.** 2012. Histone modifications in herpesvirus infections. Biol Cell **104:**139–164. http://dx.doi.org/10.1111/boc.201100067.
17. **Milavetz B, Kallestad L, Gefroh A, Adams N, Woods E, Balakirshnan L.** 2012. Virion-mediated transfer of SV40 epigenetic information. Epigenetics **7:**528–534. http://dx.doi.org/10.4161/epi.20057.
18. **Fang CY, Shen CH, Wang M, Chen PL, Chan MW, Hsu PH, Chang D.** 2015. Global profiling of histone modifications in the polyomavirus BK virion minichromosome. Virology **483:**1–12. http://dx.doi.org/10.1016/j.virol.2015.04.009.
19. **Giberson AN, Davidson AR, Parks RJ.** 2012. Chromatin structure of adenovirus DNA throughout infection. Nucleic Acids Res **40:**2369–2376. http://dx.doi.org/10.1093/nar/gkr1076.
20. **Saffert RT, Kalejta RF.** 2006. Inactivating a cellular intrinsic immune defense mediated by Daxx is the mechanism through which the human cytomegalovirus pp71 protein stimulates viral immediate-early gene expression. J Virol **80:**3863–3871. http://dx.doi.org/10.1128/JVI.80.8.3863-3871.2006.
21. **Nevels M, Paulus C, Shenk T.** 2004. Human cytomegalovirus immediate-early 1 protein facilitates viral replication by antagonizing histone deacetylation. Proc Natl Acad Sci U S A **101:**17234–17239. http://dx.doi.org/10.1073/pnas.0407933101.
22. **Berns K, Parrish CR.** 2007. Parvoviridae, p 2437–2477. *In* Knipe DM, Howley PM, Griffin DE, Lamb RA, Martin MA, Roizman B, Straus SE (ed), Fields virology, 5th ed. Lippincott Williams & Wilkins, Philadelphia, PA.
23. **Reed AP, Jones EV, Miller TJ.** 1988. Nucleotide sequence and genome organization of canine parvovirus. J Virol **62:**266–276.
24. **Cotmore SF, Tattersall P.** 1998. High-mobility group 1/2 proteins are

essential for initiating rolling-circle-type DNA replication at a parvovirus hairpin origin. J Virol **72:**8477–8484.
25. **Cziepluch C, Lampel S, Grewenig A, Grund C, Lichter P, Rommelaere J.** 2000. H-1 parvovirus-associated replication bodies: a distinct virus-induced nuclear structure. J Virol **74:**4807–4815. http://dx.doi.org/10.1128/JVI.74.10.4807-4815.2000.
26. **Ihalainen TO, Willman SF, Niskanen EA, Paloheimo O, Smolander H, Laurila JP, Kaikkonen MU, Vihinen-Ranta M.** 2012. Distribution and dynamics of transcription-associated proteins during parvovirus infection. J Virol **86:**13779–13784. http://dx.doi.org/10.1128/JVI.01625-12.
27. **Parrish CR.** 1991. Mapping specific functions in the capsid structure of canine parvovirus and feline panleukopenia virus using infectious plasmid clones. Virology **183:**195–205. http://dx.doi.org/10.1016/0042-6822(91)90132-U.
28. **Suikkanen S, Sääjärvi K, Hirsimäki J, Välilehto O, Reunanen H, Vihinen-Ranta M, Vuento M.** 2002. Role of recycling endosomes and lysosomes in dynein-dependent entry of canine parvovirus. J Virol **76:**4401–4411. http://dx.doi.org/10.1128/JVI.76.9.4401-4411.2002.
29. **Yeung DE, Brown GW, Tam P, Russnak RH, Wilson G, Clark-Lewis I, Astell CR.** 1991. Monoclonal antibodies to the major nonstructural nuclear protein of minute virus of mice. Virology **181:**35–45. http://dx.doi.org/10.1016/0042-6822(91)90467-P.
30. **Abràmoff MD, Magalhães PJ, Ram SJ.** 2004. Image processing with ImageJ. Biophotonics Int **11:**36–41.
31. **Bolte S, Cordelieres FP.** 2006. A guided tour into subcellular colocalisation analysis in light microscopy. J Microsc **224:**13–232.
32. **Söderberg O, Gullberg M, Jarvius M, Ridderstråle K, Leuchowius K-J, Jarvius J, Wester K, Hydbring P, Bahram F, Larsson LG, Landegren U.** 2006. Direct observation of individual endogenous protein complexes in situ by proximity ligation. Nat Methods **3:**995–1000. http://dx.doi.org/10.1038/nmeth947.
33. **Martin M.** 2011. Cutadapt removes adapter sequences from high-throughput sequencing reads. EMBnet J **17:**10. http://dx.doi.org/10.14806/ej.17.1.200.
34. **Langmead B, Salzberg SL.** 2012. Fast gapped-read alignment with Bowtie 2. Nat Methods **9:**357–359. http://dx.doi.org/10.1038/nmeth.1923.
35. **Li H, Handsaker B, Wysoker A, Fennell T, Ruan J, Homer N, Marth G, Abecasis G, Durbin R.** 2009. The Sequence Alignment/Map format and SAMtools. Bioinformatics **25:**2078–2079. http://dx.doi.org/10.1093/bioinformatics/btp352.
36. **Ramírez F, Dündar F, Diehl S, Grüning BA, Manke T.** 2014. deepTools: a flexible platform for exploring deep-sequencing data. Nucleic Acids Res **42:**W187–W191. http://dx.doi.org/10.1093/nar/gku365.
37. **Robinson JT, Thorvaldsdóttir H, Winckler W, Guttman M, Lander ES, Getz G, Mesirov JP.** 2011. Integrative genomics viewer. Nat Biotechnol **29:**24–26. http://dx.doi.org/10.1038/nbt.1754.
38. **Christensen J, Storgaard T, Viuff B, Aasted B, Alexandersen S.** 1993. Comparison of promoter activity in Aleutian mink disease parvovirus, minute virus of mice, and canine parvovirus: possible role of weak promoters in the pathogenesis of Aleutian mink disease parvovirus infection. J Virol **67:**1877–1886.
39. **Cotmore SF, Tattersall P.** 1987. The autonomously replicating parvoviruses of vertebrates. Adv Virus Res **33:**91–174. http://dx.doi.org/10.1016/S0065-3527(08)60317-6.
40. **Hancock MH, Cliffe AR, Knipe DM, Smiley JR.** 2010. Herpes simplex virus VP16, but not ICP0, is required to reduce histone occupancy and enhance histone acetylation on viral genomes in U2OS osteosarcoma cells. J Virol **84:**1366–1375. http://dx.doi.org/10.1128/JVI.01727-09.
41. **Kalamvoki M, Roizman B.** 2010. Circadian CLOCK histone acetyl transferase localizes at ND10 nuclear bodies and enables herpes simplex virus gene expression. Proc Natl Acad Sci U S A **107:**17721–17726. http://dx.doi.org/10.1073/pnas.1012991107.
42. **Huang J, Kent JR, Placek B, Whelan KA, Hollow CM, Zeng P-Y, Fraser NW, Berger SL.** 2006. Trimethylation of histone H3 lysine 4 by Set1 in the lytic infection of human herpes simplex virus 1. J Virol **80:**5740–5746. http://dx.doi.org/10.1128/JVI.00169-06.
43. **Ioudinkova E, Arcangeletti MC, Rynditch A, De Conto F, Motta F, Covan S, Pinardi F, Razin SV, Chezzi C.** 2006. Control of human cytomegalovirus gene expression by differential histone modifications during lytic and latent infection of a monocytic cell line. Gene **384:**120–128. http://dx.doi.org/10.1016/j.gene.2006.07.021.
44. **Nitzsche A, Paulus C, Nevels M.** 2008. Temporal dynamics of cytomegalovirus chromatin assembly in productively infected human cells. J Virol **82:**11167–11180. http://dx.doi.org/10.1128/JVI.01218-08.
45. **Chen J, Morral N, Engel DA.** 2007. Transcription releases protein VII from adenovirus chromatin. Virology **369:**411–422. http://dx.doi.org/10.1016/j.virol.2007.08.012.
46. **Komatsu T, Haruki H, Nagata K.** 2011. Cellular and viral chromatin proteins are positive factors in the regulation of adenovirus gene expression. Nucleic Acids Res **39:**889–901. http://dx.doi.org/10.1093/nar/gkq783.
47. **Komatsu T, Nagata K.** 2012. Replication-uncoupled histone deposition during adenovirus DNA replication. J Virol **86:**6701–6711. http://dx.doi.org/10.1128/JVI.00380-12.
48. **Ben-Asher E, Bratosin S, Aloni Y.** 1982. Intracellular DNA of the parvovirus minute virus of mice is organized in a minichromosome structure. J Virol **41:**1044–1054.
49. **Marcus-Sekura CJ, Carter BJ.** 1983. Chromatin-like structure of adeno-associated virus DNA in infected cells. J Virol **48:**79–87.
50. **Doerig C, McMaster G, Sogo J, Bruggmann H, Beard P.** 1986. Nucleoprotein complexes of minute virus of mice have a distinct structure different from that of chromatin. J Virol **58:**817–824.
51. **Penaud-Budloo M, Le Guiner C, Nowrouzi A, Toromanoff A, Chérel Y, Chenuaud P, Scmidt M, von Kalle C, Rolling F, Moullier P, Snyder RO.** 2008. Adeno-associated virus vector genomes persist as episomal chromatin in primate muscle. J Virol **82:**7875–7885. http://dx.doi.org/10.1128/JVI.00649-08.
52. **Cotmore SF, Gottlieb RL, Tattersall P.** 2007. Replication initiator protein NS1 of the parvovirus minute virus of mice binds to modular divergent sites distributed throughout duplex viral DNA. J Virol **81:**13015–11327. http://dx.doi.org/10.1128/JVI.01703-07.
53. **Niskanen EA, Ihalainen TO, Kalliolinna O, Häkkinen MM, Vihinen-Ranta M.** 2010. Effect of ATP binding and hydrolysis on dynamics of canine parvovirus NS1. J Virol **84:**5391–5403. http://dx.doi.org/10.1128/JVI.02221-09.
54. **Niskanen EA, Kalliolinna O, Ihalainen TO, Häkkinen M, Vihinen-Ranta M.** 2013. Mutations in DNA binding and transactivation domains affect the dynamics of parvovirus NS1 protein. J Virol **87:**11762–11774. http://dx.doi.org/10.1128/JVI.01678-13.
55. **Iseki H, Shimizukawa R, Sugiyama F, Kunita S, Iwama A, Onodera M, Nakauchi H, Yagami K.** 2005. Parvovirus nonstructural proteins induce an epigenetic modification through histone acetylation in host genes and revert tumor malignancy to benignancy. J Virol **79:**8886–8893. http://dx.doi.org/10.1128/JVI.79.14.8886-8893.2005.
56. **Ohshima T, Yoshida E, Nakajima T, Yagami K, Fukamizu A.** 2001. Effects of interaction between parvovirus minute virus of mice NS1 and coactivator CBP on NS1- and p53-transactivation. Int J Mol Med **7:**49–54.
57. **Ihalainen TO, Niskanen EA, Jylhävä J, Turpeinen T, Rinne J, Timonen J, Vihinen-Ranta M.** 2007. Dynamics and interactions of parvoviral NS1 protein in the nucleus. Cell Microbiol **9:**1946–1959. http://dx.doi.org/10.1111/j.1462-5822.2007.00926.x.
58. **Clemens KE, Pintel DJ.** 1988. The two transcription units of the autonomous parvovirus minute virus of mice are transcribed in a temporal order. J Virol **62:**1448–1451.
59. **Schoborg RV, Pintel DJ.** 1991. Accumulation of MVM gene products is differentially regulated by transcription initiation, RNA processing and protein stability. Virology **181:**22–34. http://dx.doi.org/10.1016/0042-6822(91)90466-O.
60. **Tullis G, Schoborg RV, Pintel DJ.** 1994. Characterization of the temporal accumulation of minute virus of mice replicative intermediates. J Gen Virol **75:**1633–1646. http://dx.doi.org/10.1099/0022-1317-75-7-1633.
61. **Lieberman PM.** 2006. Chromatin regulation of virus infection. Trends Microbiol **14:**132–140. http://dx.doi.org/10.1016/j.tim.2006.01.001.

III

REORGANIZATION OF NUCLEAR PORE COMPLEXES AND THE LAMINA IN LATE-STAGE PARVOVIRUS INFECTION

by

Elina Mäntylä, Einari A. Niskanen, Teemu O. Ihalainen & Maija Vihinen-Ranta
2016

J Virol 89: 11706-11710

JVI Journals.ASM.org

Reorganization of Nuclear Pore Complexes and the Lamina in Late-Stage Parvovirus Infection

Elina Mäntylä,[a] Einari A. Niskanen,[b] Teemu O. Ihalainen,[c] Maija Vihinen-Ranta[a]

Department of Biological and Environmental Science and Nanoscience Center, University of Jyväskylä, Jyväskylä, Finland[a]; Institute of Biomedicine, University of Eastern Finland, Kuopio, Finland[b]; NeuroGroup, BioMediTech, University of Tampere, Tampere, Finland[c]

Canine parvovirus (CPV) infection induces reorganization of nuclear structures. Our studies indicated that late-stage infection induces accumulation of nuclear pore complexes (NPCs) and lamin B1 concomitantly with a decrease of lamin A/C levels on the apical side of the nucleus. Newly formed CPV capsids are located in close proximity to NPCs on the apical side. These results suggest that parvoviruses cause apical enrichment of NPCs and reorganization of nuclear lamina, presumably to facilitate the late-stage infection.

The nuclear lamina is a protein-rich structural scaffold, the main components of which are the dynamic type V intermediate filament proteins called lamins. Lamin proteins comprise two subtypes, type A (lamin A, A10, C, and C2) and type B (B1, B2, and B3). The former are alternative splice products of the *LMNA* gene, and the latter are encoded by *LMNB1* (B1) and *LMNB2* (B2 and germ line-specific B3) genes (1). In structure, the lamins of both subtypes contain a central α-helical rod with globular head (N) and tail (C) domains. *In vitro*, the lamins dimerize in a parallel fashion followed by filament assembly (2, 3). The lamina is connected to the cytoskeleton via the nuclear envelope (NE)-spanning linker of nucleoskeleton and cytoskeleton (LINC) complex (4). Lamina also interacts with nuclear pore complexes (NPCs) consisting of ~30 nucleoporins (Nups) and regulating bidirectional transport of molecules over the NE (5). Together, the NPCs and lamina define a dynamic barrier that mediates signals in response to cellular stress conditions such as virus infections and limits release of viral progeny after nuclear assembly (6–9). To overcome this barrier, viruses are known to alter the architecture of all aforementioned subnuclear structures, which in turn contribute to the function of the nucleus (10). Nuclear egress of parvovirus (PV) capsids has been suggested to occur by active export via the NPC pathway prior to cell lysis (11–13). However, the influence of parvovirus egress on the organization of NPCs and nuclear lamina is unknown. Here, we examined the distribution and organization of NPCs as well as A and B type lamins in canine parvovirus (CPV)-infected cells in late infection in comparison with those in noninfected S- and G-phase (G_1/G_2) cells.

The NPCs are dynamic structures capable of assembly, disassembly, and redistribution during the cell cycle (14, 15). The nucleus has a spatially polarized architecture (16); however, the NPC distributions between the apical and basal sides of the nucleus have not been comparatively determined. Here, we examined the spatial distributions of NPCs at the apical and basal sides of nuclei in CPV-infected (multiplicity of infection [MOI] of 1 at 24 h postinfection [p.i.]) and mock-infected S- or G_1/G_2-phase Norden laboratory feline kidney (NLFK) cells. The NPCs were immunostained with a nucleoporin 153 (Nup153) antibody (Ab) (ab24700; Abcam, Cambridge, United Kingdom) also recognizing Nup62. A proliferating cell nuclear antigen (PCNA) Ab (ab18197; Abcam, Cambridge, United Kingdom) was used as a marker for cell cycle phases and the presence of parvoviral replication bodies (17, 18) (Fig. 1A). In confocal microscopy, *z* stacks consisting of an average of 30 *z* planes spaced by 0.15 μm were collected with the *z* axis corresponding to the apical-basal axis of the cell nucleus. Nuclei were scanned over a range of 4 to 6 μm. The middle *z* plane was applied to define the positions of the basal and apical surfaces. Confocal microscopy of infected cells showed unequal distributions of NPCs on the apical and the basal sides of NE. First, the number of NPCs at the apical side was ~31% higher than that at the basal side (Fig. 1B). In G_1/G_2 cells, the distribution of NPCs was also asymmetric, with ~20% more NPCs at the apical than the basal side. In the S phase, NPCs were more equally distributed, with only ~10% more NPCs localized to the apical side. Second, the overall NPC densities on both the apical and basal sides were significantly decreased in infection (Fig. 1C). In the infected cells, the apical NPC density (number ± standard deviation [SD], 3.6 ± 0.51 NPC/μm^2, $n = 22$) was lower than in the S-phase cells (4.0 ± 0.42 NPC/μm^2, $n = 21$, Student's *t* test $P < 0.05$) or the G-phase control cells (4.12 ± 0.48 NPC/μm^2, $n = 22$, $P < 0.01$) (Fig. 1A and C). An even more prominent decrease was seen at the basal side of infected-cell nuclei, where the NPC density (2.51 ± 0.65 NPC/μm^2, $n = 22$) was ~25% lower than in the mock-infected G-phase (G_1/G_2) cells and ~30% lower than in the S-phase cells (3.36 ± 0.88 NPC/μm^2 [$n = 21$, $P < 0.01$] and 3.57 ± 0.31 NPC/μm^2 [$n = 22$, $P < 0.01$], respectively) (Fig. 1A and C). Our results showed that infection was accompanied by a profound modification of the NPC network, including a significant reduction in the density of NPCs at the basal side, resembling the overall NPC distribution in G_1/G_2 cells. Earlier studies showed that cell cycle-dependent increases in the amount of NPCs and the nuclear volume occur simultaneously but do so with different regulation mechanisms (15, 19). The frequency of NPC biogenesis fluctuates

Received 22 June 2015 **Accepted** 21 August 2015
Accepted manuscript posted online 26 August 2015
Citation Mäntylä E, Niskanen EA, Ihalainen TO, Vihinen-Ranta M. 2015. Reorganization of nuclear pore complexes and the lamina in late-stage parvovirus infection. J Virol 89:11706–11710. doi:10.1128/JVI.01608-15.
Editor: G. McFadden
Address correspondence to Maija Vihinen-Ranta, maija.vihinen-ranta@jyu.fi.

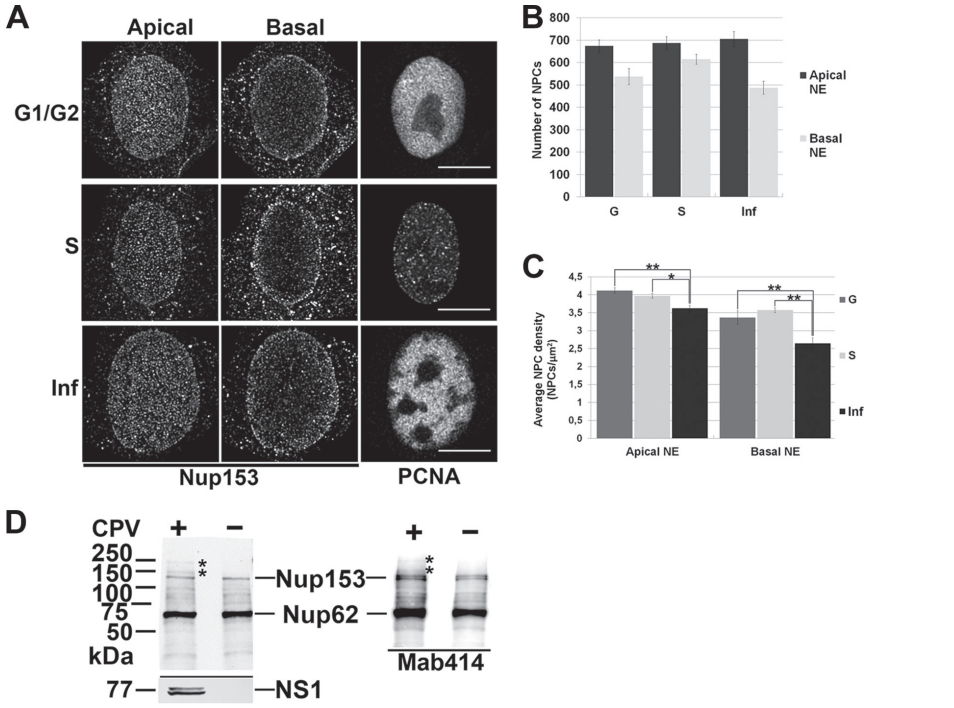

FIG 1 Infection- and cell cycle-dependent distribution of nuclear pore complexes. (A) Confocal microscopy images of the infected cells (Inf) at 24 h p.i. and the mock-infected cells in S and G_1/G_2 phases. NPCs and PCNA were visualized with Nup153 (left and middle panels) and PCNA (right panel) antibodies. (B) The amount of NPCs calculated from the apical and basal sides of NE. (C) Average density of NPCs in apical and basal side of NE. The average values of the results of triplicate experiments ± SDs are shown. (D) Western blot analysis of Nup153 and Nup62 proteins harvested from the infected and mock-infected cells and their structural integrity. Nups were detected with Nup153-specific antibody and Mab414 antibody recognizing FG-repeated Nup62 and Nup153 in feline cells. Statistical significance in comparison to the mock-infected cells is shown (Student's *t* test *P* values: *, $P < 0.05$; **, $P < 0.01$). Bars, 10 μm. Error bars represent the 95% confidence interval.

during cell cycle progression, being highest in the S and G_2 phases (19–21). CPV infection is accompanied by cell cycle arrest in the S phase (22–24). Notably, in contrast with the high density of NPCs seen in S-phase cells, we observed significantly decreased density in infected cells. To exclude the possibility that the decrease in NPC density was due to infection-induced degradation, the structural integrity of Nup153 in the infected cells at 24 h p.i. was analyzed by Western blotting (4.2×10^4 cells per well). The analysis of FG-repeated Nup153 and Nup62 (Nup153 Ab, monoclonal antibody 414 [Mab414], and ab24609; Abcam) in infected and mock-infected cells showed no major differences in abundance or integrity (Fig. 1D). For comparison, actinomycin D (Act D)-treated (0.5 to 1 μg/ml, 24 h) apoptotic cells showed cleavage of Nup153 (data not shown). However, in the infected cells, two additional bands with lower electrophoretic mobility were seen. The change may have reflected a posttranslational modification of Nup153, such as increased phosphorylation. With many viruses, Nup153 undergoes structural modification to support viral replication and spread. As an example, viruses use phosphorylation of Nups to alter the nucleocytoplasmic transport of the host (25). Furthermore, phosphorylation of Nups can occur in response to DNA damage, commonly detected in parvovirus infections (26, 27), and can indicate an infection-induced functional change of Nup153 (28, 29). Our analyses do not exclude the possibility of Nup153 becoming detached from the NPCs in infection. However, the amount of homogenously distributed Nup153 in the cytoplasm seemed to remain unaltered as judged by confocal microscopy (Fig. 1A). Taken together, these results demonstrated that CPV infection is accompanied by accumulation of NPCs at the apical side of the nucleus along with a decrease in their overall density concomitantly with structural modification of Nup153.

NPCs are anchored into the nuclear lamina (30, 31). B-type lamins concentrate in pore-rich regions, whereas A-type lamins are found in pore-free islands (32). Accordingly, changes in the distribution of NPCs correlate with nuclear lamina reorganization (19, 33). As CPV infection was accompanied by significant changes in the distribution of NPCs, we next analyzed the distributions of lamins at the apical and basal sides of the nucleus. Immunofluorescence analysis was carried out with antibodies recognizing lamins A/C and B1 (NCL-LAM-A/C [monoclonal; Leica

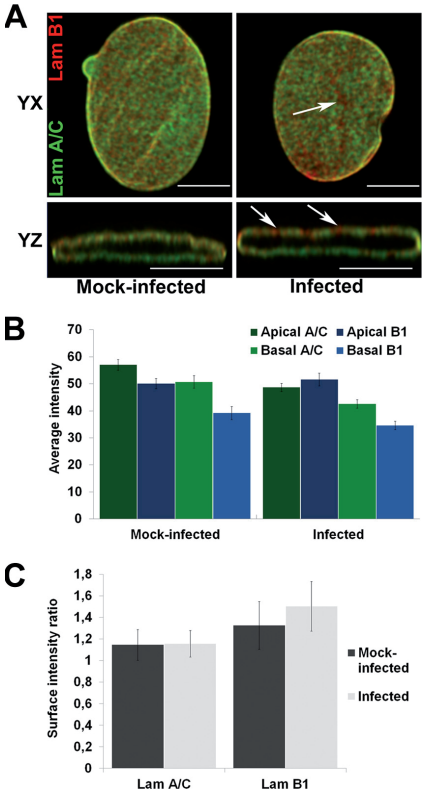

FIG 2 Distributions of lamin A/C and lamin B1. (A) Confocal *yx* and *yz* cross sections taken through the nucleus show localization of lamin A/C (Lam A/C) (green) and lamin B1 (Lam B1) (red) Abs in mock-infected (left) and infected (right) cells. Arrowheads show lamin B1-enriched areas. (B) Average intensities of lamin A/C and B in apical and basal sides of NE. (C) Surface intensity ratio between the apical and basal sides for both lamins individually per ImageJ analysis. Error bars represent the 95% confidence intervals. Bars, 10 μm.

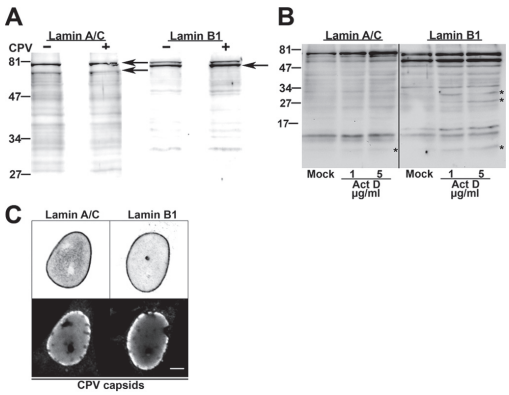

FIG 3 Structural integrity of lamins. (A and B) Western blot analysis of structural integrity of lamins A/C and B1 in infected, mock-infected cells (A) and actinomycin D (1 to 5 μg/ml)-treated cells (B). Asterisks indicate disintegration products of lamins. (C) Confocal microscopy sections of infected cells showing distributions of lamin A/C and lamin B1 and accumulation of viral capsids at the nuclear periphery at 24 h p.i. Bar, 5 μm.

Biosystems, Newcastle, United Kingdom] and ab16048 [polyclonal; Abcam, Cambridge, United Kingdom]). In virus-infected cells, similarly to NPCs, lamin B1 was enriched in clusters along the apical side of the NE (Fig. 2A), whereas in mock-infected cells, lamin B1 was distributed more equally between the two sides. These data suggested that infection affected the composition of the lamina or the lamin epitope. To study the distributions of lamins A/C and B1 in more detail, we first compared their intensities at the apical and basal sides ($n = 24$) (Fig. 2B) and then determined the surface intensity ratios (apical intensity divided by basal intensity) for both lamins ($n = 24$) (Fig. 2C). At the apical side of mock-infected cells, the intensity of lamin AC was ~16% higher than that of lamin B1. In infection, the intensity of lamin A/C at the apical side was significantly ($P < 0.05$) decreased and was ~6% lower than that of lamin B1 (Fig. 2B). At the basal side, the average intensities of both lamins were significantly ($P < 0.05$) decreased in infection in comparison with those in mock-infected cells. Determination of surface intensity ratios showed that, in general, lamin intensities were higher at the apical side than at the basal side (Fig. 2C) as reported earlier (16). In infection, the surface intensity ratio of lamin B1 was slightly increased whereas that of lamin A/C was similar to that in the mock-infected cells (Fig. 2C). These results showed that infection was accompanied by a decrease in the abundance of lamin A/C in the lamina concomitantly with enrichment of lamin B1 at the apical side. We then analyzed whether the infection-induced changes in distributions of lamins were due to their degradation. Western blot analysis (4.2×10^4 cells per well) indicated that lamins A/C and B1 (ab8984 and ab16048; Abcam, Cambridge, United Kingdom) remained intact in infection (Fig. 3A) but disintegrated in Act D-induced (1 and 5 μg/ml, 24 h) apoptotic cells (Fig. 3B). This agrees with earlier data showing that parvoviral nuclear egress does not induce degradation of lamins (34). Importantly, the expression levels of lamin A/C and B1 in the infected and mock-infected cells were comparable (Fig. 3A). In parallel, confocal imaging showed no marked discontinuity in lamin A/C or B1 staining in the infected cells; i.e., the lamin A/C and lamin B1 layers remained continuous even when viral capsids accumulated in the nuclear periphery at late-stage infection (Fig. 3C). Finally, the apical distributions of lamin B1, Nup153, and newly formed CPV capsids in infection were compared using deconvoluted confocal *yz* cross sections and analyzed with the program ImageJ. The apical distribution of lamin B1 was found to be similar to those of Nup153 (Fig. 4A, B, and C) and virus capsids (Fig. 4D, E, and F). Importantly, virus capsids were concentrated beneath apical NPCs (Fig. 4G, H, and I). In summary, our results indicated that, in CPV infection, lamin B1 was enriched in the apical side concomitantly with an overall decrease of lamin A/C levels. Instead of inducing degradation, parvovirus infection might influence the organizational and/or functional status of nuclear lamins.

To conclude, we observed that, in late-stage parvovirus infec-

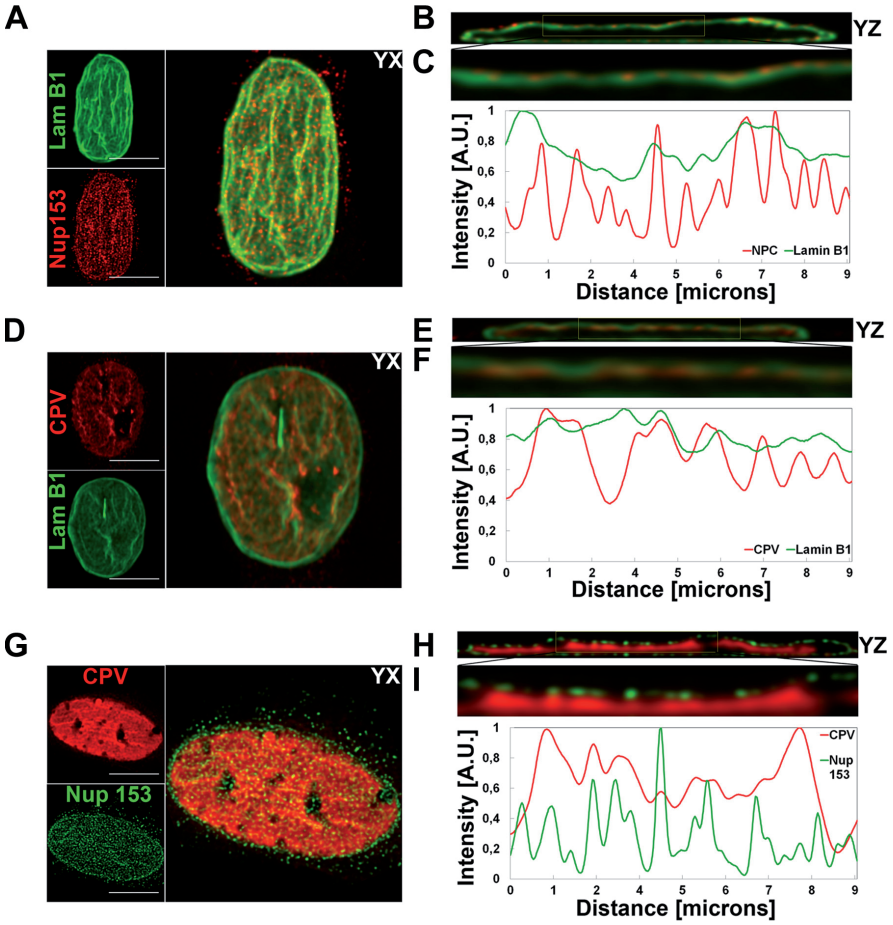

FIG 4 Intranuclear localization of lamin B1, NPCs, and viral capsids. Confocal microscopy-derived apical maximum-intensity projections are visualized with *yz* cross sections showing intranuclear distribution of NPCs (red) and lamin B1 (green) (A and B), virus capsids (red) and lamin B1 (green) (D and F), and virus capsids (red) and NPCs (green) (G and H). Capsids, NPC, and lamin B1 were visualized with capsid protein, Nup153, and lamin B1 antibodies. (C, F, and I) Normalized correlative intensity profiles from *yz* cross-section closeups are shown. Results of fluorescence line profile analysis of the intensity of capsids (red), NPCs (red/green), and lamin B1 (green) in a single optical section through the center of each nucleus are shown beside each image. Analysis was performed with ImageJ and the Plot RGB Profile plugin. A.U., arbitrary units. Bars, 10 μm.

tion, significant relocation of NPCs and reorganization of nuclear lamina occurred at the apical side of the nucleus. These changes were associated with the location of viral capsids in close proximity to apical NPCs. These results suggest that reorganization of the nuclear envelope might be important for viral egress. This report extends knowledge on parvovirus nuclear egress and the accompanying virus-induced changes in organization of the NPCs and the nuclear lamina.

ACKNOWLEDGMENTS

We thank Colin Parrish for the infectious CPV clone and CPV antibodies. We are grateful to Klaus Hedman for comments on the manuscript.

This work was financed by the Academy of Finland under the award numbers 135609 (E.A.N.), 267471 (T.O.I.), and 138388 (M.V.-R.).

REFERENCES

1. **Dittmer TA, Misteli T.** 2011. The lamin protein family. Genome Biol **12**:222–222. http://dx.doi.org/10.1186/gb-2011-12-5-222.
2. **Gruenbaum Y, Medalia O.** 2015. Lamins: the structure and protein complexes. Curr Opin Cell Biol **32**:7–12. http://dx.doi.org/10.1016/j.ceb.2014.09.009.
3. **Köster S, Weitz DA, Goldman RD, Aebi U, Herrmann H.** 2015. Intermediate filament mechanics in vitro and in the cell: from coiled coils to filaments, fibers and networks. Curr Opin Cell Biol **32**:82–91. http://dx.doi.org/10.1016/j.ceb.2015.01.001.

4. **Ho CY, Lammerding J.** 2012. Lamins at a glance. J Cell Sci **125:**2087–2093. http://dx.doi.org/10.1242/jcs.087288.
5. **Fahrenkrog B, Köser J, Aebi U.** 2004. The nuclear pore complex: a jack of all trades? Trends Biochem Sci **29:**175–182. http://dx.doi.org/10.1016/j.tibs.2004.02.006.
6. **Osmanagic-Myers S, Dechat T, Foisner R.** 2015. Lamins at the crossroads of mechanosignaling. Genes Dev **29:**225–237. http://dx.doi.org/10.1101/gad.255968.114.
7. **Pascual-Garcia P, Capelson M.** 2014. Nuclear pores as versatile platforms for gene regulation. Curr Opin Genet Dev **25:**110–117. http://dx.doi.org/10.1016/j.gde.2013.12.009.
8. **Cibulka J, Fraiberk M, Forstova J.** 2012. Nuclear actin and lamins in viral infections. Viruses **4:**325–347. http://dx.doi.org/10.3390/v4030325.
9. **Malhas AN, Lee CF, Vaux DJ.** 2009. Lamin B1 controls oxidative stress responses via Oct-1. J Cell Biol **184:**45–55. http://dx.doi.org/10.1083/jcb.200804155.
10. **Zakaryan H, Stamminger T.** 2011. Nuclear remodelling during viral infections. Cell Microbiol **13:**806–813. http://dx.doi.org/10.1111/j.1462-5822.2011.01596.x.
11. **Cotmore SF, Tattersall P.** 2014. Parvoviruses: small does not mean simple. Annu Rev Virol **1:**517–537. http://dx.doi.org/10.1146/annurev-virology-031413-085444.
12. **Engelsma DN, Valle N, Fish A, Salomé N, Almendral JM, Fornerod M.** 2008. A supraphysiological nuclear export signal is required for parvovirus nuclear export. Mol Biol Cell **19:**2544–2552. http://dx.doi.org/10.1091/mbc.E08-01-0009.
13. **Maroto B, Valle N, Saffrich R, Almendral JM.** 2004. Nuclear export of the nonenveloped parvovirus virion is directed by an unordered protein signal exposed on the capsid surface. J Virol **78:**10685–10694. http://dx.doi.org/10.1128/JVI.78.19.10685-10694.2004.
14. **Imamoto N, Funakoshi T.** 2012. Nuclear pore dynamics during the cell cycle. Curr Opin Cell Biol **24:**453–459. http://dx.doi.org/10.1016/j.ceb.2012.06.004.
15. **Dultz E, Ellenberg J.** 2010. Live imaging of single nuclear pores reveals unique assembly kinetics and mechanism in interphase. J Cell Biol **191:**15–22. http://dx.doi.org/10.1083/jcb.201007076.
16. **Kim D, Wirtz D.** 2015. Cytoskeletal tension induces the polarized architecture of the nucleus. Biomaterials **48:**161–172. http://dx.doi.org/10.1016/j.biomaterials.2015.01.023.
17. **Essers J, Theil AF, Baldeyron C, van Cappellen WA, Houtsmuller AB, Kanaar R, Vermeulen W.** 2005. Nuclear dynamics of PCNA in DNA replication and repair. Mol Cell Biol **25:**9350–9359. http://dx.doi.org/10.1128/MCB.25.21.9350-9359.2005.
18. **Ihalainen TO, Niskanen EA, Jylhävä J, Paloheimo O, Dross N, Smolander H, Langowski J, Timonen J, Vihinen-Ranta M.** 2009. Parvovirus induced alterations in nuclear architecture and dynamics. PLoS One **4:**e5948. http://dx.doi.org/10.1371/journal.pone.0005948.
19. **Maeshima K, Iino H, Hihara S, Funakoshi T, Watanabe A, Nishimura M, Nakatomi R, Yahata K, Imamoto F, Hashikawa T, Yokota H, Imamoto N.** 2010. Nuclear pore formation but not nuclear growth is governed by cyclin-dependent kinases (Cdks) during interphase. Nat Struct Mol Biol **17:**1065–1071. http://dx.doi.org/10.1038/nsmb.1878.
20. **Maul GG, Maul HM, Scogna JE, Lieberman MW, Stein GS, Hsu BY, Borun TW.** 1972. Time sequence of nuclear pore formation in phytohemagglutinin-stimulated lymphocytes and in HeLa cells during the cell cycle. J Cell Biol **55:**433–447. http://dx.doi.org/10.1083/jcb.55.2.433.
21. **Winey M, Yarar D, Giddings TH, Mastronarde DN.** 1997. Nuclear pore complex number and distribution throughout the Saccharomyces cerevisiae cell cycle by three-dimensional reconstruction from electron micrographs of nuclear envelopes. Mol Biol Cell **8:**2119–2132. http://dx.doi.org/10.1091/mbc.8.11.2119.
22. **Nykky J, Tuusa JE, Kirjavainen S, Vuento M, Gilbert L.** 2010. Mechanisms of cell death in canine parvovirus-infected cells provide intuitive insights to developing nanotools for medicine. Int J Nanomedicine **5:**417–428.
23. **Rothballer A, Kutay U.** 2013. Poring over pores: nuclear pore complex insertion into the nuclear envelope. Trends Biochem Sci **38:**292–301. http://dx.doi.org/10.1016/j.tibs.2013.04.001.
24. **Antonin W, Ellenberg J, Dultz E.** 2008. Nuclear pore complex assembly through the cell cycle: Regulation and membrane organization. FEBS Lett **582:**2004–2016. http://dx.doi.org/10.1016/j.febslet.2008.02.067.
25. **Porter FW, Palmenberg AC.** 2009. Leader-induced phosphorylation of nucleoporins correlates with nuclear trafficking inhibition by cardioviruses. J Virol **83:**1941–1951. http://dx.doi.org/10.1128/JVI.01752-08.
26. **Cotmore SF, Tattersall P.** 2013. Parvovirus diversity and DNA damage responses. Cold Spring Harb Perspect Biol **5:**a012989. http://dx.doi.org/10.1101/cshperspect.a012989.
27. **Luo Y, Qiu J.** 2013. Parvovirus infection-induced DNA damage response. Future Virol **8:**245–257. http://dx.doi.org/10.2217/fvl.13.5.
28. **Güttinger S, Laurell E, Kutay U.** 2009. Orchestrating nuclear envelope disassembly and reassembly during mitosis. Nat Rev Mol Cell Biol **10:**178–191. http://dx.doi.org/10.1038/nrm2641.
29. **Wan G, Zhang X, Langley RR, Liu Y, Hu X, Han C, Peng G, Ellis LM, Jones SN, Lu X.** 2013. DNA damage-induced nuclear export of precursor microRNAs is regulated by the ATM-AKT pathway. Cell Rep **3:**2100–2112. http://dx.doi.org/10.1016/j.celrep.2013.05.038.
30. **Hutchison CJ.** 2002. Lamins: building blocks or regulators of gene expression? Nat Rev Mol Cell Biol **3:**848–858. http://dx.doi.org/10.1038/nrm950.
31. **Guo Y, Kim Y, Shimi T, Goldman RD, Zheng Y.** 2014. Concentration-dependent lamin assembly and its roles in the localization of other nuclear proteins. Mol Biol Cell **25:**1287–1297. http://dx.doi.org/10.1091/mbc.E13-11-0644.
32. **Maeshima K, Yahata K, Sasaki Y, Nakatomi R, Tachibana T, Hashikawa T, Imamoto F, Imamoto N.** 2006. Cell-cycle-dependent dynamics of nuclear pores: pore-free islands and lamins. J Cell Sci **119:**4442–4451. http://dx.doi.org/10.1242/jcs.03207.
33. **Fiserova J, Goldberg M.** 2010. Relationships at the nuclear envelope: lamins and nuclear pore complexes in animals and plants. Biochem Soc Trans **38:**829. http://dx.doi.org/10.1042/BST0380829.
34. **Nüesch JPF, Lachmann S, Rommelaere J.** 2005. Selective alterations of the host cell architecture upon infection with parvovirus minute virus of mice. Virology **331:**159–174. http://dx.doi.org/10.1016/j.virol.2004.10.019.